
Article:
Daly, Kevin, Maisano Delser, Pierpaolo, Mullin, Victoria et al. (37 more authors) (2018) Ancient goat genomes reveal mosaic domestication in the Fertile Crescent. Science. pp. 85-88. ISSN 1095-9203

https://doi.org/10.1126/science.aas9411

Title: Ancient goat genomes reveal mosaic domestication in the Fertile Crescent.

One Sentence Summary:
Ancient goat genomes show a dispersed domestication process across the Near East and highlight genes under early selection.

Authors: Kevin G. Daly[1†], Pierpaolo Maisano Delser[1,2†], Victoria E. Mullin[1,27], Amelie Scheu[1,3], Valeria Mattiangeli[1], Matthew D. Teasdale[1,4], Andrew J. Hare[1], Joachim Burger[3], Marta Pereira Verdugo[1], Matthew J. Collins[4,5], Ron Kehati[6], Cevdet Merih Erek[7], Guy Bar-Oz[8], François Pompanon[9], Tristan Cumer[9], Canan Çakırlar[10], Azadeh Fatemeh Mohaseb[11,12], Delphine Decruyenaere[11], Hossein Davoudi[13,14], Özlem Çevik[15], Gary Rollefson[16], Jean-Denis Vigne[11], Roya Khazaeli[12], Homa Fathi[12], Sanaz Beizaee Doost[12], Roghayeh Rahimi Sorkhani[17], Ali Akbar Vahdati[18], Eberhard W. Sauer[19], Hossein Azizi Kharanaghi[20], Sepideh Maziar[21], Boris Gasparian[22], Ron Pinhasi[23], Louise Martin[24], David Orton[4], Benjamin S. Arbuckle[25], Norbert Benecke[26], Andrea Manica[2], Liora Kolska Horwitz[6], Marjan Mashkour[11,12,14], Daniel G. Bradley[1 *]

Affiliations:
[1] Smurfit Institute of Genetics, Trinity College Dublin, Dublin, Dublin 2, Ireland
[2] Department of Zoology, University of Cambridge, Downing Street, Cambridge CB2 3EJ, UK
[3] Palaeogenetics Group, Institute of Organismic and Molecular Evolution (iOME), Johannes Gutenberg-University Mainz, 55099 Mainz, Germany
[4] BioArCh, University of York, York YO10 5DD, UK
[5] Museum of Natural History, University of Copenhagen, Copenhagen, Denmark
[6] National Natural History Collections, Faculty of Life Sciences, The Hebrew University, Jerusalem, Israel
[7] Gazi University, Ankara 06500, Turkey
[8] Zinman Institute of Archaeology, University of Haifa, Mount Carmel, Haifa, Israel
[9] Université Grenoble Alpes, Univ. Savoie Mont Blanc, CNRS, LECA, F-38000 Grenoble, France
[10] Groningen Institute of Archaeology, Groningen University, Groningen, the Netherlands
[11] Archéozoologie, Archéobotanique (UMR 7209), CNRS, MNHN, UPMC, Sorbonne Universités, Paris, France
[12] Archaeozoology section, Archaeometry Laboratory, University of Tehran, Tehran, Iran
[13] Department of Archaeology, Faculty of Humanities, Tarbiat Modares University, Tehran, Iran

[14] Osteology Department, National Museum of Iran, Tehran, Iran
[15] Trakya Universitesi, Edebiyat Fakültesi, Arkeoloi Bölümü, Edirne, Turkey
[16] Department of Anthropology, Whitman College, Walla Walla, WA 99362, USA
[17] Faculty of Cultural Heritage, Handicrafts and Tourism, University of Mazandaran, Noshahr, Iran
[18] Provincial Office of the Iranian Center for Cultural Heritage, Handicrafts and Tourism Organisation, North Khorassan, Bojnord, Iran
[19] School of History, Classics and Archaeology, University of Edinburgh, William Robertson Wing, Old Medical School, Teviot Place, Edinburgh EH8 9AG, UK
[20] Prehistory Department, National Museum of Iran, Tehran, Iran
[21] Institut für Archäologische Wissenschaften, Goethe Universität, Frankfurt am Main, Germany
[22] Institute of Archaeology and Ethnology, National Academy of Sciences of the Republic of Armenia, Yerevan 0025, Republic of Armenia
[23] Department of Anthropology, University of Vienna, Althanstrasse 14, 1090, Vienna
[24] Institute of Archeology, University College London, London, UK
[25] Department of Anthropology, University of North Carolina at Chapel Hill, Chapel Hill, North Carolina, USA
[26] German Archaeological Institute, Department of Natural Sciences, Berlin, 14195 Berlin, Germany
[27] Department of Earth Sciences, Natural History Museum, Cromwell Road, London SW7 5BD, UK
[*] Corresponding author: Daniel G. Bradley - dbradley@tcd.ie
[†] Equally contributed

Abstract:
Current genetic data are equivocal as to whether goat domestication occurred multiple times or was a singular process. We generated genomic data from 83 ancient goats (51 with genome-wide coverage), from Palaeolithic through to Medieval contexts throughout the Near East. Our results demonstrate that multiple divergent ancient wild goat sources were domesticated in a dispersed process, resulting in genetically and geographically-distinct Neolithic goat populations, echoing contemporaneous human divergence across the region. These early goat populations contributed differently to modern goats in Asia, Africa and Europe. We also detect early selection for pigmentation, stature, reproduction, milking and response to dietary change, providing 8,000 year old evidence for human agency in moulding genome variation within a partner species.

Main Text:

The Fertile Crescent of Southwest Asia and adjacent areas were the location of transformative prehistoric innovations including the domestication of sheep, goats, cattle and pigs (*1–3*). Archaeological evidence suggests local development of wild goat (bezoar) management strategies in different regions in the mid to late 11th millennium BP with domestic phenotypes emerging in the 10th millennium, first in the Anatolian region (*4–6*). A key question is whether these early patterns of exploitation are consistent with a geographically-focused singular domestication process or if domestic goats were recruited from separate populations, with parallel genetic consequences. Genetic evidence is inconclusive (*7*, *8*).

We generated ancient *Capra* genome data from Neolithic sites from western (Anatolia and the Balkans), eastern (Iran and Turkmenistan) and southern (Jordan and Israel) regions around the Fertile Crescent (tables S1-S3). To maximise yields we sampled mainly petrous bones and 51 produced nuclear genome coverage ranging 0.01-14.89X (median 1.05X) (tables S4-5). We enriched for mitochondrial DNA (mtDNA) in poorly preserved samples and obtained a total of 83 whole mitochondrial genomes (median 70.95X) (table S6, figs. S1-S2, (*9*)).

The majority of our ancient domestic mitochondrial sequences fall within modern haplogroups *A-D* and *G* (figs. 1a, S3-S6, tables S7-S9). The Paleolithic wild goat samples fall exclusively in more divergent clades *T* (similar to the related wild caprid, the West Caucasus Tur (*Capra caucasica*)) and *F* (previously reported in bezoar and a small number of Sicilian goats (*10*)). Here we found *F* in a >47,000 BP bezoar from Hovk-1 cave, Armenia, in pre-domestic goat from Direkli Cave, Turkey, as well as in Levantine goats at ‘Ain Ghazal, an early Neolithic village in Jordan, and Abu Ghosh, Israel (*9*).

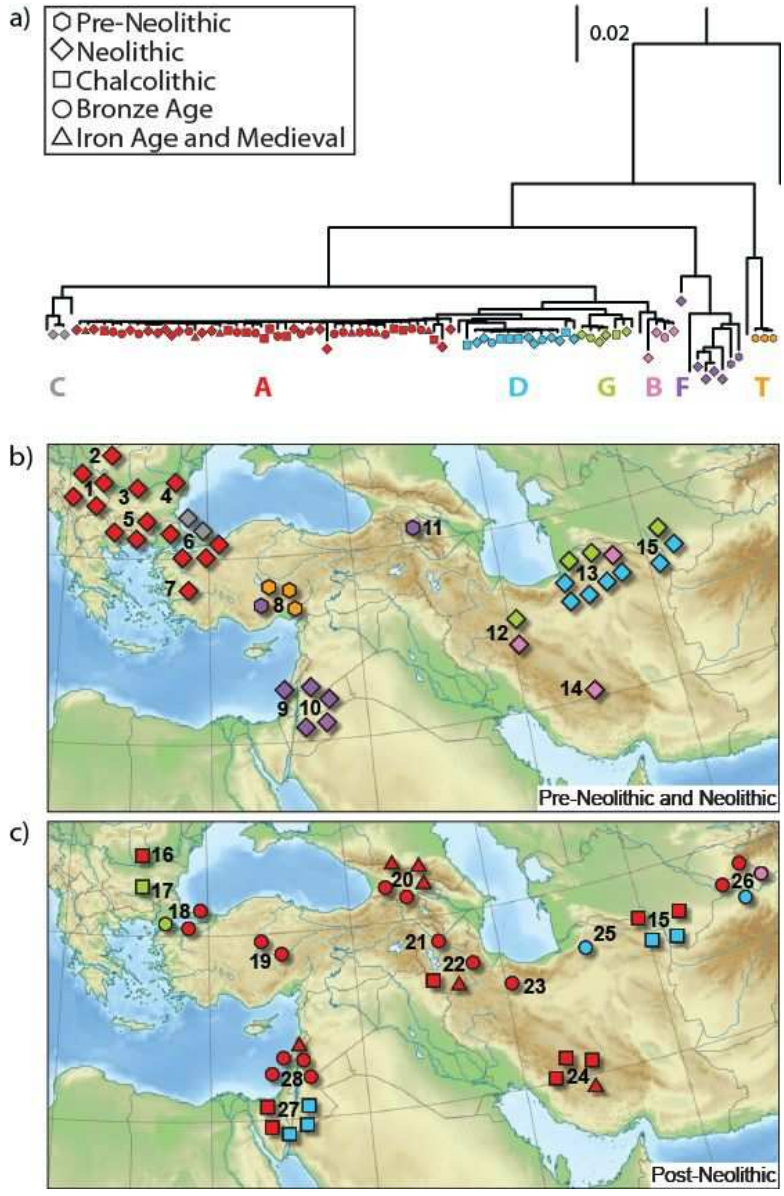

Fig. 1. Maximum likelihood phylogeny and geographical distributions of ancient mtDNA haplogroups. ***a.*** A phylogeny placing ancient whole mtDNA sequences in the context of known haplogroups; symbols denoting individuals are colored by clade membership and shape indicates archaeological period (see key). Unlabelled nodes are modern bezoar and outgroup sequence (Nubian Ibex) added for reference. Haplogroup T we define as the sister branch to the West Caucasian Tur (*9*). ***b.*** Geographical distributions of haplogroups are given and show early highly structured diversity in the Neolithic period followed by ***c.*** collapse of structure in succeeding periods. We delineate the tiled maps at 5300-5000 BC; a period bracketing both our earliest Chalcolithic sequence (24, Mianroud) and latest Neolithic (6, Aşağı Pınar). Numbered archaeological sites also include Direkli Cave (8), Abu Ghosh (9), 'Ain Ghazal (10) and Hovk-1 Cave (11) (table S1, (*9*)).

A geographic plot of Neolithic samples illustrates that early domestic goat haplogroups are highly structured (fig. 1b), with disjunct distributions in the western, eastern and southern (Levantine) regions of the Near East (tables S10-S11). In this early farming period partitioning is significant; AMOVA (*9*) estimates that 81% of the mtDNA diversity stems from differences between the three regions ($p=0.028$, permutation test) (tables S12-S13). When we use an approximate Bayesian computation (ABC) framework on this mtDNA

variation to investigate demographic history, a model suggesting a pre-domestic branching of the divergent Levant population (38,500-195,200 BP) is favored. This suggests multiple wild origins of Neolithic goat herds (tables S14-S19, (*9*)). In the later post-Neolithic samples this partitioning collapses to zero (fig. 1c) and the ubiquitous modern haplogroup, *A*, becomes widespread.

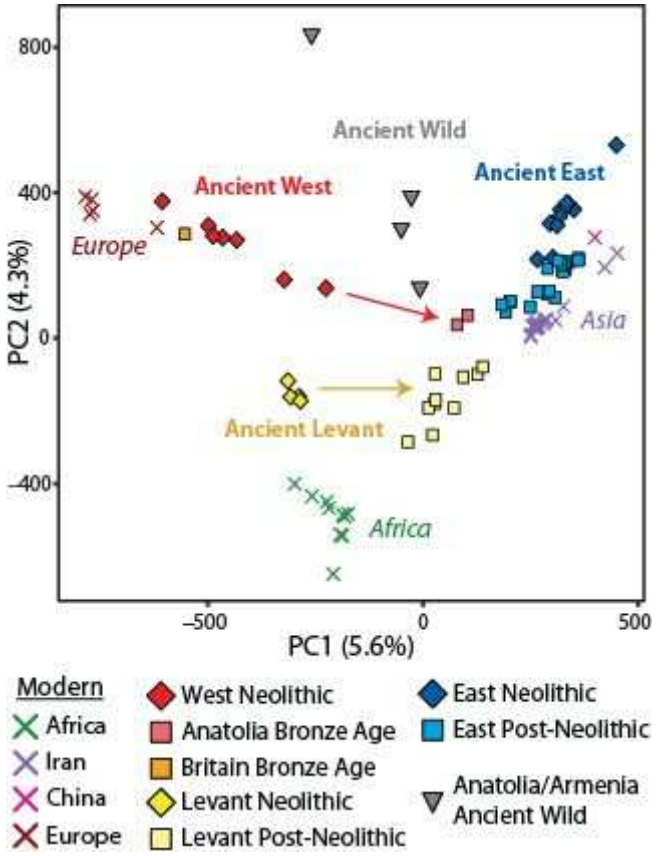

Fig. 2. Principal Components Analysis of ancient and modern goat genomes. Ancient goats cluster in three vertices: eastern (Iran, Uzbekistan, Turkmenistan, Georgia), western (Balkans, Anatolia) and southern or Levantine (Jordan, Israel) margins of the Near East. Modern European, Asian and, interestingly, African goat follow this pattern but Bronze Age Anatolian (red arrow) and Chalcolithic/Bronze Age Israeli (yellow arrow) samples show shifts compared to earlier genomes from those regions, suggesting post-Neolithic admixture within the primary regions.

Analyses of genome-wide variation also argue against a single common origin. Neolithic samples from the west, east and Levant each cluster separately in principal components analysis (PCA; fig. 2) and in phylogenetic reconstruction (figs. S7-S10). *D* statistics show that these clusters have significantly different levels of allele sharing with two regional samples of pre-domestic wild goat; a ~13,000 BP population from Direkli cave (Southeast Anatolia) and a >47,000 BP bezoar from Hovk-1 cave (Armenia) (fig. 3a, (*9*)). These differences are consistent with *qpGraph* estimation of relationships (fig 3b and S11, table S20 (*9*)) where a primary ancestral divide between western and eastern genomes occurred more

than 47,000 BP. The latter clade gave rise to the eastern Neolithic population. However the western and Levant Neolithic goat derive ~50% and ~70% of their ancestry from a divergent source in the western clade which had affinity to the Anatolian wild population, in line with f_4 ratios and Treemix graphs (table S21, fig. S12). These different proportions infer substantial local recruitment from different wild populations into early herds in regions proximal to each of the different vertices of the Fertile Crescent. ABC modelling of autosomal variation also rejects a single domestication origin scenario (tables S11, S22-25, figs. S13-15, (*9*)).

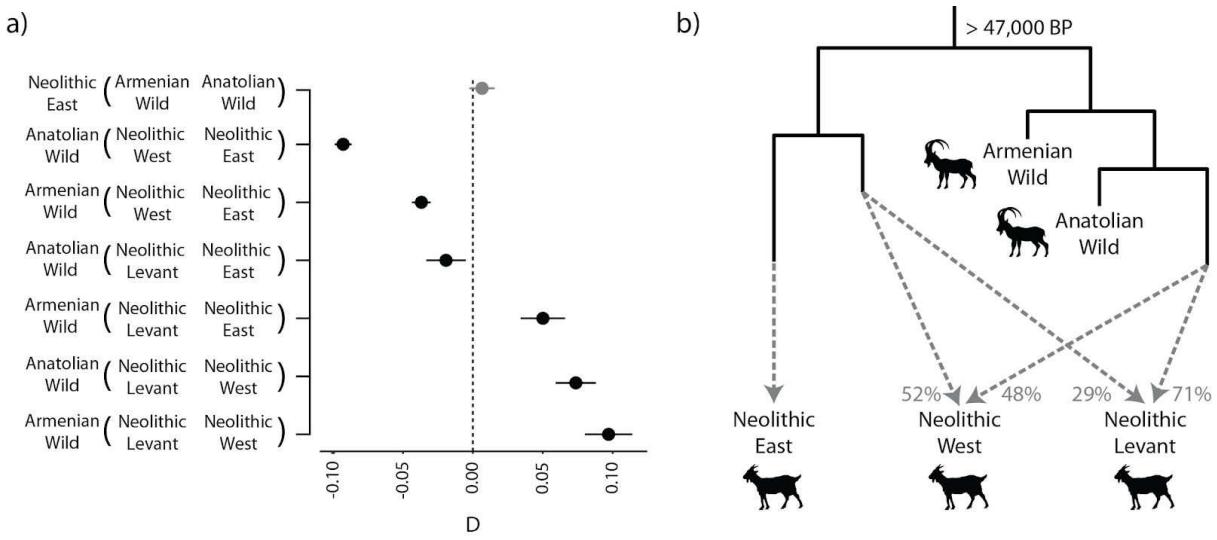

Fig. 3. *D* statistics and admixture graph of ancient and modern goat. ***a.*** In the test X(Y, Z) positive or negative *D* values indicate a greater number of derived alleles between X and Z or X and Y respectively; Yak is used as an outgroup. *D* values for each test are presented with error bars of 3 standard errors; non-significant tests are coloured grey. These show that regional pre-domestic wild goats relate asymmetrically to Neolithic domestic populations, ruling out a singular origin. ***b.*** Admixture graph reconstructing the population history of pre-Neolithic and Neolithic goat. Relative inputs from divergent sources into early domestic herds are are represented by grey dashed arrows (drawn from Figure S11f (*9*)).

Thus our data favor a process of Near Eastern animal domestication which is dispersed in space and time rather than a radiation from a central core (*3*, *11*). This resonates with archaeozoological evidence for disparate early management strategies from early Anatolian, Iranian and Levantine Neolithic sites (*12*, *13*). Interestingly, our finding of divergent goat genomes within the Neolithic echoes genetic investigation of early farmers. Northwestern Anatolian and Iranian human Neolithic genomes are also divergent (*14–16*) suggesting the sharing of techniques rather than large-scale migrations of populations across Southwest Asia in the period of early domestication. Several crop plants also show evidence of parallel domestication processes in the region (*17*).

PCA affinity (fig. 2), supported by *qpGraph* and outgroup f_3 analyses, suggests that modern European goat derive from a source close to the western Neolithic, Far Eastern goat derive from early eastern Neolithic domesticates and Africans have a contribution from the Levant,

but in this case with considerable admixture from the other sources (fig. S11, S16-17, tables S26-27). The latter may be in part a result of admixture that is discernible in the same analyses extended to ancient genomes within the Fertile Crescent after the Neolithic (fig. S18-19, tables S20, S27, S31) when the spread of metallurgy and other developments likely resulted in an expansion of inter-regional trade networks and livestock movement.

Animal domestication likely involved adaptive pressures due to infection, changes in diet, translocation beyond natural habitat and human selection (*18*). We thus took an outlier approach to identify loci that underwent selective sweeps in either six eastern Neolithic genomes or four western genome samples (minimum coverage 2X). We compared each population to 16 modern bezoar genomes (*19*) and identified 18 windows with both high divergence (highest 0.1% *Fst* values) and reduced diversity in Neolithic goats (lowest 5% θ ratio: Neolithic/wild; tables S28-S29, S32).

The pigmentation loci, *KIT* and *KITLG,* are the only shared signals in both Neolithic populations. Both are common signals in modern livestock analyses (*19*, *20*). We thus examined *Fst* values for previously reported coloration genes and identified *ASIP* and *MITF* as also showing high values (figs. 4a, b, S20 and table S30). Whereas modern breeds are defined in part by color pattern, the driver of the ~8,000 year old selection observed in the Neolithic for pigmentation may be less obvious. *KIT* is involved in the piebald trait in mammals (*21*) and may have been favored as a means of distinguishing individuals and maintaining ownership within shared herds as well as for aesthetic value. Pigmentation change has also been proposed as a pleiotropic effect of selection for tameness (*22*). Intriguingly, selective sweeps around the *KIT* locus were clearly independent in the eastern and western Neolithic goat sampled genomes as the resulting locus genotypes are distinct and contribute differently to modern eastern and western populations (fig. 4c).

Trait mapping in cattle, the most studied ungulate, offers interpretation of three other caprine signals identified here. *SIRT1* (identified in the western Neolithic) has variants affecting stature (*23*) and a reduction in size is a widespread signal of early domestication. *EPGN* (eastern Neolithic) is linked to calving interval; increase in reproductive frequency is another general feature of domestication. *STAT1* (eastern Neolithic) is involved in mammary gland development and has been linked to milk production (*24*). Interestingly, the second most extreme eastern signal maps to a homolog of human *CYP2C19* which (like other cytochrome P450 products) contributes to metabolism of xenobiotics including enniatin B, a toxic product of fungal strains that contaminate cereals and grains. Interestingly this selection signal has been hypothesized as a response to early agriculture in humans (*25*). Early recycling of agricultural by-products as animal fodder has been suggested as a motivation for the origins of husbandry (*3*) and fungal toxins may have been a challenge to early domestic goat as well as their agriculturist owners.

Our results imply a domestication process carried out by dispersed, divergent but communicating communities across the Fertile Crescent who selected animals in early millennia, including for pigmentation, the most visible of of domestic traits.

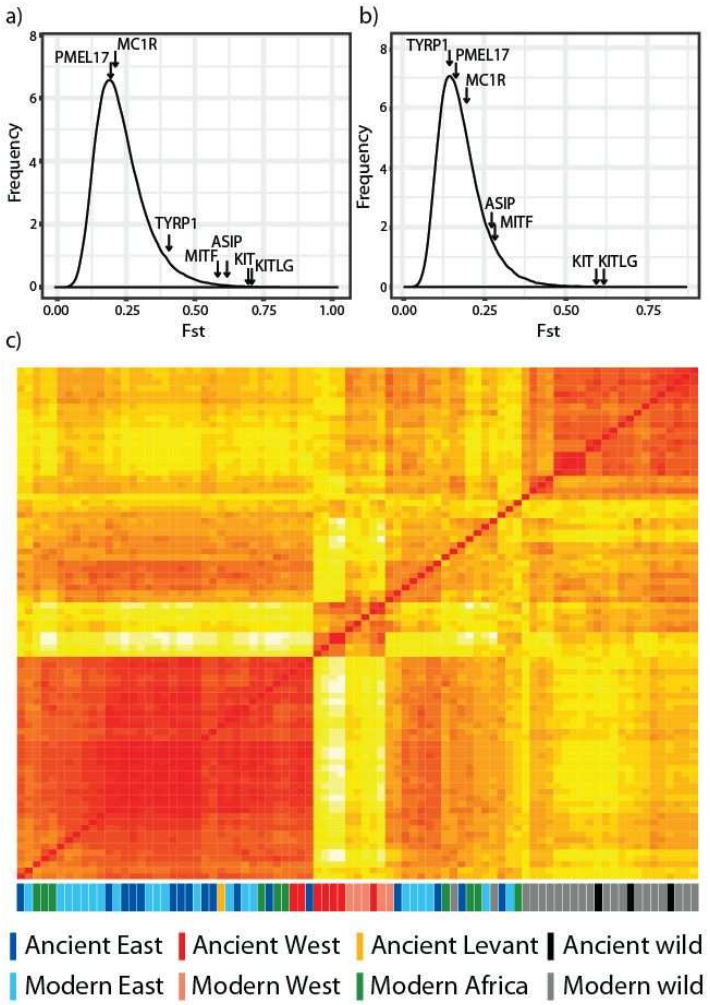

Fig. 4 *Fst* distributions between modern bezoar and Neolithic western and eastern populations, and a heatmap of identity by state between modern and domestic goat at the *KIT* locus. The highest *Fst* values for 50kb windows overlapping seven pigmentation loci showing evidence of selection in modern goat, sheep or cattle studies are indicated for **a.** western and **b**. eastern populations (table S30 and S32). ***c.*** The pigmentation locus, *KIT*, shows evidence of selection in both western and eastern Neolithic samples but allele sharing distances, illustrated using a heatmap, suggest that selection acted on divergent standing variation in parallel but separate processes. Five of the seven ancient west samples are from Neolithic contexts, and cluster with modern West haplogroups. The two remaining western ancients (red) falling in the eastern cluster (mainly blue) are Bronze Age Anatolian samples with indications of secondary admixture (fig. 2).

References

1. J. Peters, A. von den Driesch, D. Helmer, in *The First Steps of Animal Domestication. New Archaeological Approaches*, J. D. Vigne, J. Peters, D. Helmer, Eds. (Oxbow Books,

Oxford, 2005), pp. 96–123.

2. M. A. Zeder, The Domestication of Animals. *J. Anthropol. Res.* **68**, 161–190 (2012).

3. J.-D. Vigne, L. Gourichon, D. Helmer, L. Martin, J. Peters, in *Quaternary in the Levant*, Y. Enzel, O. Bar Yosef, Eds. (Cambridge Univ. Press, Cambridge, 2017), pp. 753–760.

4. M. A. Zeder, B. Hesse, The initial domestication of goats (Capra hircus) in the Zagros mountains 10,000 years ago. *Science*. **287**, 2254–2257 (2000).

5. D. Helmer, L. Gourichon, in *Archaeozoology of the Near East*, M. Mashkour, M. Beech, Eds. (Oxbow, Oxford, 2017), vol. 9, pp. 23–40.

6. B. Moradi *et al.*, in *The Neolithic of the Iranian Plateau. Recent Research and Prospects. Studies in Early Near Eastern Production, Subsistence, and Environment (SENEPSE series)*, K. Roustaei, M. Mashkour, Eds. (ex oriente, Berlin, 2016), pp. 1–14.

7. S. Naderi *et al.*, The goat domestication process inferred from large-scale mitochondrial DNA analysis of wild and domestic individuals. *Proc. Natl. Acad. Sci. U. S. A.* **105**, 17659–17664 (2008).

8. P. Gerbault *et al.*, in *Population dynamics in Pre- and Early History New Approaches by Stable Isotopes and Genetics*, E. Kaiser, W. Schier, J. Burger, Eds. (De Gruyter, Berlin, 2012), pp. 17–30.

9. See the supplementary materials.

10. M. T. Sardina *et al.*, Phylogenetic analysis of Sicilian goats reveals a new mtDNA lineage. *Anim. Genet.* **37**, 376–378 (2006).

11. M. A. Zeder, The Origins of Agriculture in the Near East. *Curr. Anthropol.* **52**, S221–S235 (2011).

12. L. K. Horwitz *et al.*, Animal domestication in the southern Levant. *Paléorient*. **25**, 63–80 (1999).

13. B. S. Arbuckle, L. Atici, Initial diversity in sheep and goat management in Neolithic south-western Asia. *Levantina*. **45**, 219–235 (2013).

14. F. Broushaki *et al.*, Early Neolithic genomes from the eastern Fertile Crescent. *Science*. **353**, 499–503 (2016).

15. I. Lazaridis *et al.*, Genomic insights into the origin of farming in the ancient Near East. *Nature*. **536**, 419–424 (2016).

16. M. Gallego-Llorente *et al.*, The genetics of an early Neolithic pastoralist from the Zagros, Iran. *Sci. Rep.* **6**, 31326 (2016).

17. D. Q. Fuller, G. Willcox, R. G. Allaby, Cultivation and domestication had multiple origins: arguments against the core area hypothesis for the origins of agriculture in the Near East. *World Archaeol.* **43**, 628–652 (2011).

18. M. A. Zeder, Domestication as a model system for the extended evolutionary synthesis. *Interface Focus*. **7**, 20160133 (2017).

19. F. J. Alberto *et al.*, Convergent genomic signatures of domestication in sheep and goats. *Nat. Commun.* **9**, 813 (2018).

20. J. W. Kijas *et al.*, Genome-wide analysis of the world's sheep breeds reveals high levels of historic mixture and strong recent selection. *PLoS Biol.* **10**, e1001258 (2012).

21. N. Reinsch *et al.*, A QTL for the degree of spotting in cattle shows synteny with the KIT locus on chromosome 6. *J. Hered.* **90**, 629–634 (1999).

22. L. Trut, I. Oskina, A. Kharlamova, Animal evolution during domestication: the domesticated fox as a model. *Bioessays*. **31**, 349–360 (2009).

23. M. Li *et al.*, SIRT1 gene polymorphisms are associated with growth traits in Nanyang cattle. *Mol. Cell. Probes*. **27**, 215–220 (2013).

24. O. Cobanoglu, I. Zaitoun, Y. M. Chang, G. E. Shook, H. Khatib, Effects of the signal transducer and activator of transcription 1 (STAT1) gene on milk production traits in Holstein dairy cattle. *J. Dairy Sci.* **89**, 4433–4437 (2006).

25. R. E. Janha *et al.*, Inactive alleles of cytochrome P450 2C19 may be positively selected in human evolution. *BMC Evol. Biol.* **14**, 71 (2014).

26. C. B. Ramsey, S. Lee, Recent and Planned Developments of the Program OxCal. *Radiocarbon*. **55**, 720–730 (2013).

27. C. Bronk Ramsey, Analysis of chronological information and radiocarbon calibration: the program OxCal. *Archaeological Computing Newsletter*. **41**, e16 (1994).

28. M. Niu, T. J. Heaton, P. G. Blackwell, C. E. Buck, The Bayesian Approach to Radiocarbon Calibration Curve Estimation: The IntCal13, Marine13, and SHCal13 Methodologies. *Radiocarbon*. **55**, 1905–1922 (2013).

29. Greenfield, H.J. Jongsma Greenfield, T., Subsistence and Settlement in the Early Neolithic of Temperate SE Europe: A View from Blagotin, Serbia. *Archaeologica Bulgarica*. **18**, 1–33 (2014).

30. Whittle, A. Bartosiewicz, L. Borić, D. Pettitt, P. Richards, M., In the beginning: New radiocarbon dates for the Early Neolithic in Northern Serbia and South-East Hungary. *Antaeus*. **25**, 63–117 (2002).

31. H. J. Greenfield, E. R. Arnold, "Go(a)t milk?" New perspectives on the zooarchaeological evidence for the earliest intensification of dairying in south eastern Europe. *World Archaeol.* **47**, 792–818 (2015).

32. W. Schier, F. Draşovean, Vorbericht über die rumänisch-deutschen Prospektionen und Ausgrabungen in der befestigten Tellsiedlung von Uivar, jud. Timiş, Rumänien (1998–2002). *Praehistorische Zeitschrift*. **79**, 147 (2004).

33. A. Scheu, C. Geörg, A. Schulz, J. Burger, N. Benecke, in *Population Dynamics in*

Prehistory and Early History. New Approaches by Using Stable Isotopes and Genetics, E. Kaiser, J. Burger, S. Wolfram, Eds. (De Gruyter, Berlin, Boston, 2012), pp. 45–54.

34. A. Scheu, *Palaeogenetische Studien zur Populationsgeschichte von Rind und Ziege mit einem Schwerpunkt auf dem Neolithikum in Südosteuropa* (Verlag Marie Leidorf, Rahden/Westf, 2012), vol. 4 of *Menschen-Kulturen-Traditionen*.

35. R. Dennell, *Early Farming in South Bulgaria from the VI to the III Millennia BC* (British Archaeological Reports Limited, Oxford, 1978), vol. 45.

36. N. Benecke, L. Ninov, in *Beiträge zu jungsteinzeitlichen Forschungen in Bulgarien. Saarbrücker Beiträge zur Altertumskunde*, M. Lichardus-Itten, J. Lichardus, V. Nikolov, Eds. (Habelt, Bonn, 2002), vol. 74, pp. 555–573.

37. R. Krauß, *Ovčarovo-Gorata. Eine frühneolithische Siedlung in Nordostbulgarien* (Habelt-Verlag, Bonn, 2014), vol. 29 of *Archaeologie in Euasien*.

38. M. Lichardus-Itten, J.-P. Demoule, L. Perničeva, M. Grebska-Kulova, I. Kulov, in *Beiträge zu jungsteinzeitlichen Forschungen in Bulgarien.*, J. L. M Lichardus-Itten, Ed. (Rudolf Habelt Verlag, Bonn, 2002), vol. 74 of *Saarbrücker Beiträge zur Altertumskunde*, pp. 99–158.

39. N. Karul, Z. Eres, M. Özdoğan, H. Parzinger., *Aşağı Pınar. 1. Einführung, Forschungsgeschichte, Stratigraphie und Architektur* (Institut, Eurasien-Abteilung Deutsches Archäologisches, Mainz, 2003), vol. 15 of *Archäologie in Eurasien*.

40. N. Benecke, in *Beiträge zur Archäozoologie und Prähistorischen Anthropologie*, E. May, N. Benecke, Eds. (Verlag Beier & Beran, Konstanz, 2001), vol. 3 of *Beiträge zur Archäozoologie und Prähistorischen Anthropologie*, pp. 31–40.

41. Ç. Çilingiroğlu, C. Çakırlar, Towards configuring the neolithisation of Aegean Turkey. *Documenta Praehistorica*. **40**, 21 (2013).

42. C. Çakırlar, Adaptation, identity, and innovation in Neolithic and Chalcolithic Western Anatolia (6800–3000 cal. BC): The evidence from aquatic mollusk shells. *Quat. Int.* **390**, 117–125 (2015).

43. C. M. Erek, A new Epi-paleolithic site in the Northeast Mediterranean region: Direkli Cave (Kahramanmaras, Turkey). *Adalya*. **13**, 1–17 (2010).

44. B. S. Arbuckle, C. M. Erek, Late Epipaleolithic hunters of the central Taurus: Faunal remains from Direkli Cave, Kahramanmaraş, Turkey. *Int. J. Osteoarchaeol.* **22**, 694–707 (2012).

45. J. Perrot, Le Néolithique d'Abou-Gosh. *Syria*. **29**, 119–145 (1952).

46. M. Lechevallier *et al.*, Abou Gosh et Beisamoun. Deux gisements du VII millénaire avant l'ère chrétienne en Israël. *Mémoires et Travaux du Centre de Recherches Préhistoriques Français de Jérusalem Jérusalem*. **2** (1978).

47. P. Ducos, L. K. Horwitz, in *The Neolithic Site of Abu Gosh. The 1995 Excavations.*, H.

Khalaily, O. Marder, Eds. (Israel Antiquities Authority Reports, 2003), vol. 19, pp. 103–120.

48. L. K. Horwitz, in *The Neolithic Site of Abu Gosh. The 1995 Excavations.*, H. Khalaily, O. Marder, Eds. (Israel Antiquities Authority Reports, Jerusalem, 2003), vol. 19, pp. 87–101.

49. G. Kahila Bar-Gal, H. Khalaily, O. Mader, P. Ducos, L. K. Horwitz, Ancient DNA Evidence for the Transition from Wild to Domestic Status in Neolithic Goats: A Case Study from the Site of Abu Gosh, Israel. *Anc. Biomol.* **4**, 9–17 (2002).

50. G. O. Rollefson, K. J. Pine, Measuring the impact of LPPNB immigration into highland Jordan. *Studies in the History and Archaeology of Jordan*. **10**, 473–482 (2009).

51. L. Martin, Y. Edwards, in *Origins and Spread of Domestic Animals in Southwest Asia and Europe*, S. Colledge, J. Conolly, K. Dobney, K. Manning, S. Shennan, Eds. (Left Coast Press, Walnut Creek, 2013), vol. 59, pp. 49–82.

52. A. Von den Driesch, U. Wodtke, in *The prehistory of Jordan, II: perspectives from 1997*, H. G. K. Gebel, Z. Kafafi, G. Rollefson, Eds. (Ex Oriente, Berlin, 1997), pp. 511–556.

53. A. Wasse, Final Results of an Analysis of the Sheep and Goat Bones from Ain Ghazal, Jordan. *Levantina*. **34**, 59–82 (2002).

54. R. Pinhasi *et al.*, Middle Palaeolithic human occupation of the high altitude region of Hovk-1, Armenia. *Quat. Sci. Rev.* **30**, 3846–3857 (2011).

55. J. Pullar, A. Hastings, R. Hubbard, G. Wilcox, *Tepe Abdul Hosein: a Neolithic site in Western Iran : excavations 1978* (B.A.R., Oxford, 1990).

56. A. Tsuneki, in *The First Farming Village in Northeast Iran and Turan: Tappeh Sang-e Chakhmaq and Beyond (Programs and Abstracts)*, A. Tsuneki, Ed. (University of Tsukuba, 2014), pp. 9–12.

57. K. Roustaei, M. Mashkour, M. Tengberg, Tappeh Sang-e Chakhmaq and the beginning of the Neolithic in north-east Iran. *Antiquity*. **89**, 573–595 (2015).

58. T. Nakamura, in *The First Farming Village in Northeast Iran and Turan: Tappeh Sang-e Chakhmaq and Beyond*, A. Tsuneki, Ed. (University of Tsukuba, Tsukuba, 2014), pp. 13–16.

59. M. Mashkour *et al.*, in *The first farming village in northeast Iran and Turan: Tappeh Sang-e Chakhmaq and beyond*, A. Tsuneki, Ed. (University of Tsukuba, Tsukuba, 2014), pp. 27–32.

60. H. Azizi Kharanaghi, thesis, University of Tehran (2014).

61. M. H. Tengberg, A. K. M, in *The Neolithic of the Iranian Plateau. Recent Research and Prospects. Studies in Early Near Eastern Production, Subsistence, and Environment (SENEPSE series)*, K. Roustaei, M. Mashkour, Eds. (Ex Oriente, Berlin, 2016), pp. 137–148.

62. S. Pollock *et al.*, Excavations at Monjukli Depe, Meana-Caaca Region, Turkmenistan, 2010. *Archäologische Mitteilungen aus Iran und Turan*. **43**, 169–237 (2011).

63. N. Benecke *et al.*, Pietrele in the Lower Danube region: integrating archaeological, faunal and environmental investigations. *Documenta Praehistorica*. **40**, 175 (2013).

64. M. Özdoğăn, H. Parzinger, J. W. E. Faßbinder, *Die frühbronzezeitliche Siedlung von Kanlıgeçit bei Kırklareli* (Verlag Philipp von Zabern, Darmstadt, 2012), vol. 27 of *Archäologie in Eurasien*.

65. B. S. Arbuckle, Zooarchaeology at Acemhöyük 2013. *Anadolu (Anatolia)*. **39**, 55–68 (2013).

66. N. Özgüc, New Light on the Dating of the Levels of the Karum of Kanish and of Acemhöyük near Aksaray. *Am. J. Archaeol.* **72**, 318–320 (1968).

67. B. S. Arbuckle, Pastoralism, Provisioning, and Power at Bronze Age Acemhöyük, Turkey. *Am. Anthropol.* **114**, 462–476 (2012).

68. I. Motzenbäcker, in *Aktuelle Forschungen in Eurasien*, S. Hansen, Ed. (Berlin, 2014), pp. 66–67.

69. H.-J. Gehrke, O. Dally, Eds., in *Deutsches Archäologisches Institut, Jahresbericht 2007* (Deutsches Archäologisches Institut, Zentrale, Podbielskiallee 69–71, Berlin, 2008), *Archäologischer Anzeiger 2008/1 Beiheft*, pp. 343–345.

70. M. Mashkour *et al.*, in *Sasanian Persia: Between Rome and the Steppes of Eurasia*, E. W. Sauer, Ed. (Edinburgh University Press, Edinburgh, 2017), pp. 74–95.

71. S. Maziar, Settlement dynamics of the Kura-Araxes culture: An overview of the Late Chalcolithic and Early Bronze Age in the Khoda Afarin Plain, North-western Iran. *Paléorient*. **41**, 25–36 (2015).

72. Davoudi H, Berthon R, Mohaseb A, Sheikhi S, Abedi A, Mashkour M., in *Iranian Plateau during the Third Millennium Urbanisation, Trade, Subsistence and Production*, J. W. Meyer, E. Vila, R. Vallet, M. Casanova, M. Mashkour, Eds. (Travaux de la Maison de l'Orient., Lyon, 2014).

73. R. H. Dyson, The Iron Age architecture at Hasanlu: an essay. *Expedition*. **31**, 107 (1989).

74. O. W. Muscarella, The Excavation of Hasanlu: An Archaeological Evaluation. *Bull. Am. Schools Orient. Res.*, 69–94 (2006).

75. M. D. Danti, *Hasanlu V: The Late Bronze and Iron I Periods* (University of Pennsylvania Press, Philadelphia, 2013).

76. M. D. Danti, M. M. Voigt, R. H. Dyson Jr, in *A View from the Highlands: Archaeological Studies in Honour of Charles Burney*, A. Sagona, Ed. (Peeters Publishers, Belgium, 2004), vol. 12 of *Ancient Near Eastern Studies Supplement*, pp. 583–616.

77. R. H. Dyson, O. W. Muscarella, Constructing the Chronology and Historical

Implications of Hasanlu IV. *Iran*. **27**, 1–27 (1989).

78. M. Danti, M. Cifarelli, Iron II Warrior Burials at Hasanlu Tepe, Iran. *Iranica Antiqua*. **50**, 61–157 (2015).

79. S. Kroll, Hasanlu Period III—annotations and corrections. *Iranica Antiqua*. **48**, 175–192 (2013).

80. R. H. Dyson, Digging in Iran: Hasanlu, 1958. *Expedition*. **1**, 4 (1959).

81. R. H. Dyson, The Achaemenid painted pottery of Hasanlu IIIA. *Anatolian studies*. **49**, 101–110 (1999).

82. H. Davoudi, thesis, Tarbiat Modares University (2017).

83. R. Rahimi Sorkhani, M. Eslami, Specialized pottery production in Dalma tradition; a statistical approach in pottery analysis from Soha Chay Tepe, Zanjan, Iran. *Journal of Archaeological Science: Reports*. **17**, 220–234 (2018).

84. C. Hamlin, Dalma Tepe. *Iran*. **13**, 111–127 (1975).

85. E. F. Henrickson, V. Vitali, The Dalma Tradition: Prehistoric Inter-Regional Cultural Integration In Highland Western Iran. *Paléorient*. **13**, 37–45 (1987).

86. I. Mostafapour, thesis, University of Tehran (2011).

87. A. M. Pollard, H. Davoudi, I. Mostafapour, H. R. Valipour, H. Fazeli Nashli, A New radiocarbon chronology for the late Neolithic to Iron age in the Qazvin plain, Iran. *International Journal of Humanities*. **19**, 110–151 (2012).

88. B. Hellwing, M. Seyedin, in *Beyond the Ubaid: Transformation and Integration in the Late Prehistoric Societies of the Middle East*, R. A. Carter, G. Philip, Eds. (The Oriental Institute of the University of Chicago, Chicago, 2010), vol. 63 of *Studies in Ancient Oriental Civilization*, pp. 277–394.

89. S. Ebrāhimi, A. Abolahrār, M. Zāre, in *The Neolithic of the Iranian Plateau. Recent Research and Prospects. Studies in Early Near Eastern Production, Subsistence, and Environment (SENEPSE series)*, K. Roustaei, M. Mashkour, Eds. (Ex Oriente, 2016), *SENEPSE*, pp. 49–74.

90. A. Vahdati *et al.*, in *Iranian Plateau during the Third Millennium Urbanisation, Trade, Subsistence and Production*, J. W. Meyer, E. Vila, R. Vallet, M. Casanova, M. Mashkour, Eds. (Maison de l'Orient, Lyon, 2014).

91. K. Kaniuth, in *Man and Environment in Prehistoric South Asia: New Perspectives*, V. Lefèvre, A. Didier, B. Mutin, Eds. (Brepols, Turnhout, Belgium, 2016), vol. 1 of *South Asian Archaeology and Art 2012*, pp. 117–127.

92. C. Grigson, in *Shiqmim: pastoralism and other aspects of animal management in the Chalcolithic of the northern Negev*, T. E. Levy, Ed. (B.A.R., Oxford, 1987), vol. 356 of *BAR International Series*.

93. S. E. Whitcher, thesis, University of Edinburgh (2000).

94. T. E. Levy, *Archaeology, Anthropology and Cult. The Sanctuary at Gilat* (Equinox, Sheffield, 2006), vol. 4 of *Approaches To Anthropological Archaeology*.

95. C. Grigson, in *Shiqmim: pastoralism and other aspects of animal management in the Chalcolithic of the northern Negev*, T. E. Levy, Ed. (B.A.R., Oxford, 1987), vol. 356 of *BAR International Series*, p. 319.

96. S. J. M. Davis, in *Rapport sur les trois premières campagnes de fouilles à Tel Yarmouth (Israël) (1980-1982)*, P. de Miroschedji, Ed. (Éditions Recherche sur les Civilisations, Paris, 1988), pp. 143–149.

97. L. K. Horwitz, E. Dahan, in *Yoqne'am I. The Late Periods.*, A. Ben-Tor, M. Avissar, Y. Portugali, Eds. (The Hebrew University, Jerusalem, 1996), vol. 3 of *Qedem Reports*, pp. 246–255.

98. L. K. Horwitz, N. Bar Giora, H. K. Mienis, O. Lernau, in *Yoqne'am III. The Middle and Late Bronze Ages. Final Report of the Archaeological Excavations (1977-1988)*, A. Ben-Tor, D. Ben-Ami, A. Livneh, Eds. (Institute of Archaeology, Hebrew University of Jerusalem, Jerusalem, 2005), vol. 7 of *Qedem Reports*, pp. 395–435.

99. M. Meiri *et al.*, Ancient DNA and population turnover in southern levantine pigs--signature of the sea peoples migration? *Sci. Rep.* **3**, 3035 (2013).

100. S. Frumin, A. M. Maeir, L. Kolska Horwitz, E. Weiss, Studying Ancient Anthropogenic Impacts on Current Floral Biodiversity in the Southern Levant as reflected by the Philistine Migration. *Sci. Rep.* **5**, 13308 (2015).

101. H. J. Greenfield, A. Brown, I. Shai, A. M. Maeir, in *Bones and Identity: Archaeozoological Approaches to Reconstructing Social and Cultural Landscapes in Southwest Asia*, N. Marom, R. Yeshurun, L. Weissbrod, G. Bar-Oz., Eds. (Oxbow, Oxford, 2016), pp. 170–192.

102. J. Lev-Tov, in *Tell es-Safi/Gath I: Report on the 1996–2005 Seasons.*, A. M. Maeir, Ed. (Harrassowitz, Wiesbaden, 2012), vol. 69 of *Ägypten und Altes Testament*, pp. 589–612.

103. Hitchcock LA, Horwitz LK, Boaretto E, Maeir AM, One Philistine's Trash is an Archaeologist's Treasure: Feasting at Iron Age I, Tell es-Safi/Gath. *Near Eastern Archaeology*. **78**, 12–25 (2015).

104. B. Hesse, Animal Use at Tel Miqne-Ekron in the Bronze Age and Iron Age. *Bull. Am. Schools Orient. Res.*, 17–27 (1986).

105. E. F. Maher, B. Hesse, in *Tel Miqne-Ekron Excavations 1985-1988, 1990, 1992-1995. Field IV Lower –The Elite Zone. Part 1. The Iron Age I Early Philistine City.*, T. Dothan, Y. Garfinkel, S. Gitin, Eds. (Eisenbrauns, Winona Lake, 2016), pp. 515–542.

106. E. F. Maher, thesis, University of Illinois at Chicago (2004).

107. J. S. E. Lev-Tov, thesis, University of Tennessee, Knoxville (2000).

108. A. J. Lawson, M. J. Allen, *Potterne 1982-5: Animal Husbandry in Later Prehistoric Wiltshire* (Trust for Wessex Archaeology, Salisbury, 2000).

109. S. Pääbo *et al.*, Genetic analyses from ancient DNA. *Annu. Rev. Genet.* **38**, 645–679 (2004).

110. A. Scheu *et al.*, The genetic prehistory of domesticated cattle from their origin to the spread across Europe. *BMC Genet.* **16**, 54 (2015).

111. D. Y. Yang, B. Eng, J. S. Waye, J. C. Dudar, S. R. Saunders, Technical note: improved DNA extraction from ancient bones using silica-based spin columns. *Am. J. Phys. Anthropol.* **105**, 539–543 (1998).

112. D. E. MacHugh, C. J. Edwards, J. F. Bailey, D. R. Bancroft, D. G. Bradley, The extraction and analysis of ancient DNA from bone and teeth: a survey of current methodologies. *Anc. Biomol.* **3**, 81–103 (2000).

113. C. Gamba *et al.*, Genome flux and stasis in a five millennium transect of European prehistory. *Nat. Commun.* **5**, 5257 (2014).

114. M. Meyer, M. Kircher, Illumina Sequencing Library Preparation for Highly Multiplexed Target Capture and Sequencing. *Cold Spring Harb. Protoc.* **2010**, db.prot5448–pdb.prot5448 (2010).

115. S. Andrews, *FastQC* (2010; available at http://www.bioinformatics.babraham.ac.uk/projects/fastqc/).

116. M. Martin, Cutadapt removes adapter sequences from high-throughput sequencing reads. *EMBnet.journal*. **17**, 10–12 (2011).

117. Y. Dong *et al.*, Sequencing and automated whole-genome optical mapping of the genome of a domestic goat (Capra hircus). *Nat. Biotechnol.* **31**, 135–141 (2013).

118. H. Li, R. Durbin, Fast and accurate short read alignment with Burrows-Wheeler transform. *Bioinformatics*. **25**, 1754–1760 (2009).

119. H. Li *et al.*, The Sequence Alignment/Map format and SAMtools. *Bioinformatics*. **25**, 2078–2079 (2009).

120. P. Brotherton *et al.*, Novel high-resolution characterization of ancient DNA reveals C > U-type base modification events as the sole cause of post mortem miscoding lesions. *Nucleic Acids Res.* **35**, 5717–5728 (2007).

121. J. Krause *et al.*, A complete mtDNA genome of an early modern human from Kostenki, Russia. *Curr. Biol.* **20**, 231–236 (2010).

122. S. Sawyer, J. Krause, K. Guschanski, V. Savolainen, S. Pääbo, Temporal patterns of nucleotide misincorporations and DNA fragmentation in ancient DNA. *PLoS One*. **7**, e34131 (2012).

123. H. Jónsson, A. Ginolhac, M. Schubert, P. L. F. Johnson, L. Orlando, mapDamage2.0: fast approximate Bayesian estimates of ancient DNA damage parameters. *Bioinformatics*. **29**, 1682–1684 (2013).

124. A. W. Briggs *et al.*, Removal of deaminated cytosines and detection of in vivo methylation in ancient DNA. *Nucleic Acids Res.* **38**, e87 (2010).

125. N. Rohland, E. Harney, S. Mallick, S. Nordenfelt, D. Reich, Partial uracil-DNA-glycosylase treatment for screening of ancient DNA. *Philos. Trans. R. Soc. Lond. B Biol. Sci.* **370**, 20130624 (2015).

126. A. Gnirke *et al.*, Solution hybrid selection with ultra-long oligonucleotides for massively parallel targeted sequencing. *Nat. Biotechnol.* **27**, 182–189 (2009).

127. T. Maricic, M. Whitten, S. Pääbo, Multiplexed DNA sequence capture of mitochondrial genomes using PCR products. *PLoS One*. **5**, e14004 (2010).

128. N. J. O'Sullivan *et al.*, A whole mitochondria analysis of the Tyrolean Iceman's leather provides insights into the animal sources of Copper Age clothing. *Sci. Rep.* **6**, 31279 (2016).

129. M. Schubert *et al.*, Improving ancient DNA read mapping against modern reference genomes. *BMC Genomics*. **13**, 178 (2012).

130. A. McKenna *et al.*, The Genome Analysis Toolkit: a MapReduce framework for analyzing next-generation DNA sequencing data. *Genome Res.* **20**, 1297–1303 (2010).

131. H. Li, Aligning sequence reads, clone sequences and assembly contigs with BWA-MEM. *arXiv [q-bio.GN]* (2013), (available at http://arxiv.org/abs/1303.3997).

132. A. Hassanin, C. Bonillo, B. X. Nguyen, C. Cruaud, Comparisons between mitochondrial genomes of domestic goat (Capra hircus) reveal the presence of numts and multiple sequencing errors. *Mitochondrial DNA*. **21**, 68–76 (2010).

133. T. S. Korneliussen, A. Albrechtsen, R. Nielsen, ANGSD: Analysis of Next Generation Sequencing Data. *BMC Bioinformatics*. **15**, 356 (2014).

134. L. Colli *et al.*, Whole mitochondrial genomes unveil the impact of domestication on goat matrilineal variability. *BMC Genomics*. **16**, 1115 (2015).

135. R. C. Edgar, MUSCLE: multiple sequence alignment with high accuracy and high throughput. *Nucleic Acids Res.* **32**, 1792–1797 (2004).

136. M. Gouy, S. Guindon, O. Gascuel, SeaView version 4: A multiplatform graphical user interface for sequence alignment and phylogenetic tree building. *Mol. Biol. Evol.* **27**, 221–224 (2010).

137. T. M. Keane, C. J. Creevey, M. M. Pentony, T. J. Naughton, J. O. Mclnerney, Assessment of methods for amino acid matrix selection and their use on empirical data shows that ad hoc assumptions for choice of matrix are not justified. *BMC Evol. Biol.* **6**, 29 (2006).

138. A. Rambaut, *FigTree v1. 3.1: Tree figure drawing tool* (2009) (available at http://tree.bio.ed.ac.uk/software/figtree/).

139. S. Naderi *et al.*, Large-scale mitochondrial DNA analysis of the domestic goat reveals six haplogroups with high diversity. *PLoS One*. **2**, e1012 (2007).

140. S. Naderi *et al.*, The goat domestication process inferred from large-scale mitochondrial DNA analysis of wild and domestic individuals. *Proc. Natl. Acad. Sci. U. S. A.* **105**, 17659–17664 (2008).

141. P. Weinberg, Capra caucasica. *The IUCN Red List of Threatened Species* (2008), , doi:10.2305/IUCN.UK.2008.RLTS.T3794A10088217.en.

142. A. J. Drummond, M. A. Suchard, D. Xie, A. Rambaut, Bayesian phylogenetics with BEAUti and the BEAST 1.7. *Mol. Biol. Evol.* **29**, 1969–1973 (2012).

143. R. Bouckaert *et al.*, BEAST 2: a software platform for Bayesian evolutionary analysis. *PLoS Comput. Biol.* **10**, e1003537 (2014).

144. R. Lanfear, B. Calcott, S. Y. W. Ho, S. Guindon, Partitionfinder: combined selection of partitioning schemes and substitution models for phylogenetic analyses. *Mol. Biol. Evol.* **29**, 1695–1701 (2012).

145. A. Rambaut, M. A. Suchard, D. Xie, D. A.j., *Tracer v1.6* (2014) (available at http://beast.bio.ed.ac.uk/Tracer.).

146. A. Hassanin *et al.*, Pattern and timing of diversification of Cetartiodactyla (Mammalia, Laurasiatheria), as revealed by a comprehensive analysis of mitochondrial genomes. *C. R. Biol.* **335**, 32–50 (2012).

147. D. Massilani *et al.*, Past climate changes, population dynamics and the origin of Bison in Europe. *BMC Biol.* **14**, 93 (2016).

148. L. Excoffier, H. E. L. Lischer, Arlequin suite ver 3.5: a new series of programs to perform population genetics analyses under Linux and Windows. *Mol. Ecol. Resour.* **10**, 564–567 (2010).

149. Smit, A.F.A., Hubley, R. & Green, P., RepeatMasker Web Server, (available at http://www.repeatmasker.org/cgi-bin/WEBRepeatMasker).

150. S. Purcell *et al.*, PLINK: a tool set for whole-genome association and population-based linkage analyses. *Am. J. Hum. Genet.* **81**, 559–575 (2007).

151. S. D. E. Park *et al.*, Genome sequencing of the extinct Eurasian wild aurochs, Bos primigenius, illuminates the phylogeography and evolution of cattle. *Genome Biol.* **16**, 234 (2015).

152. M. Lipatov, K. Sanjeev, R. Patro, K. Veeramah, Maximum Likelihood Estimation of Biological Relatedness from Low Coverage Sequencing Data. *bioRxiv* (2015), p. 023374.

153. R. E. Green *et al.*, A draft sequence of the Neandertal genome. *Science*. **328**, 710–722

(2010).

154. P. Skoglund, E. Ersmark, E. Palkopoulou, L. Dalén, Ancient wolf genome reveals an early divergence of domestic dog ancestors and admixture into high-latitude breeds. *Curr. Biol.* **25**, 1515–1519 (2015).

155. H. Li, R. Durbin, Inference of human population history from individual whole-genome sequences. *Nature*. **475**, 493–496 (2011).

156. R. R. Hudson, Generating samples under a Wright–Fisher neutral model of genetic variation. *Bioinformatics*. **8**, 337–338 (2002).

157. G. Hellenthal, M. Stephens, msHOT: modifying Hudson's ms simulator to incorporate crossover and gene conversion hotspots. *Bioinformatics*. **23**, 520–521 (2007).

158. H. Wickham, *Ggplot2: Elegant Graphics for Data Analysis* (Springer Publishing Company, Incorporated, ed. 2nd, 2009).

159. A. H. Freedman *et al.*, Genome sequencing highlights the dynamic early history of dogs. *PLoS Genet.* **10**, e1004016 (2014).

160. J. S. Pedersen *et al.*, Genome-wide nucleosome map and cytosine methylation levels of an ancient human genome. *Genome Res.* **24**, 454–466 (2014).

161. M. Bulmer, Neighboring base effects on substitution rates in pseudogenes. *Mol. Biol. Evol.* **3**, 322–329 (1986).

162. J. Sved, A. Bird, The expected equilibrium of the CpG dinucleotide in vertebrate genomes under a mutation model. *Proc. Natl. Acad. Sci. U. S. A.* **87**, 4692–4696 (1990).

163. C. Wang *et al.*, Ancestry estimation and control of population stratification for sequence-based association studies. *Nat. Genet.* **46**, 409–415 (2014).

164. O. M. Mine, K. Kedikilwe, R. T. Ndebele, S. J. Nsoso, Sheep-goat hybrid born under natural conditions. *Small Rumin. Res.* **37**, 141–145 (2000).

165. A. Pauciullo *et al.*, Characterization of a very rare case of living ewe-buck hybrid using classical and molecular cytogenetics. *Sci. Rep.* **6**, 34781 (2016).

166. E. Paradis, J. Claude, K. Strimmer, APE: Analyses of Phylogenetics and Evolution in R language. *Bioinformatics*. **20**, 289–290 (2004).

167. S. Soraggi, C. Wiuf, A. Albrechtsen, Powerful Inference with the D-statistic on Low-Coverage Whole-Genome Data. *bioRxiv* (2017), p. 127852.

168. J. K. Pickrell, J. K. Pritchard, Inference of population splits and mixtures from genome-wide allele frequency data. *PLoS Genet.* **8**, e1002967 (2012).

169. B. R. Baum, PHYLIP: Phylogeny Inference Package. Version 3.2. Joel Felsenstein. *Q. Rev. Biol.* **64**, 539–541 (1989).

170. L. Skotte, T. S. Korneliussen, A. Albrechtsen, Estimating individual admixture

proportions from next generation sequencing data. *Genetics*. **195**, 693–702 (2013).

171. D. Reich, K. Thangaraj, N. Patterson, A. L. Price, L. Singh, Reconstructing Indian population history. *Nature*. **461**, 489–494 (2009).

172. N. Patterson *et al.*, Ancient admixture in human history. *Genetics*. **192**, 1065–1093 (2012).

173. B. Виктор, *Relief Map of Middle East* (https://commons.wikimedia.org/wiki/File:Relief_Map_of_Middle_East.jpg).

174. L. M. Cassidy *et al.*, Capturing goats: documenting two hundred years of mitochondrial DNA diversity among goat populations from Britain and Ireland. *Biol. Lett.* **13** (2017).

175. L. Fontanesi *et al.*, Missense and nonsense mutations in melanocortin 1 receptor (MC1R) gene of different goat breeds: association with red and black coat colour phenotypes but with unexpected evidences. *BMC Genet.* **10**, 47 (2009).

176. E. Brunberg *et al.*, A missense mutation in PMEL17 is associated with the Silver coat color in the horse. *BMC Genet.* **7**, 46 (2006).

177. X. Zhang *et al.*, Alteration of sheep coat color pattern by disruption of ASIP gene via CRISPR Cas9. *Sci. Rep.* **7**, 8149 (2017).

178. D. Becker *et al.*, The brown coat colour of Coppernecked goats is associated with a non-synonymous variant at the TYRP1 locus on chromosome 8. *Anim. Genet.* **46**, 50–54 (2015).

179. R. Hauswirth *et al.*, Mutations in MITF and PAX3 cause “splashed white” and other white spotting phenotypes in horses. *PLoS Genet.* **8**, e1002653 (2012).

180. Gregory R. Warnes, Ben Bolker, Lodewijk Bonebakker, Robert Gentleman, Wolfgang Huber Andy Liaw, Thomas Lumley, Martin Maechler, Arni Magnusson, Steffen Moeller, Marc Schwartz and Bill Venables, *gplots: Various R Programming Tools for Plotting Data. R package version 3.0.1* (2016) (available at https://CRAN.R-project.org/package=gplots).

181. R. R. Hudson, M. Slatkin, W. P. Maddison, Estimation of levels of gene flow from DNA sequence data. *Genetics*. **132**, 583–589 (1992).

182. R Core Team, *R: A language and environment for statistical computing* (Vienna, Austria, 2015; https://www.R-project.org/).

183. M. A. Beaumont, W. Zhang, D. J. Balding, Approximate Bayesian computation in population genetics. *Genetics*. **162**, 2025–2035 (2002).

184. L. Excoffier, I. Dupanloup, E. Huerta-Sánchez, V. C. Sousa, M. Foll, Robust demographic inference from genomic and SNP data. *PLoS Genet.* **9**, e1003905 (2013).

185. D. E. Wilson, R. A. Mittermeier, Eds., *Handbook of the Mammals of the World. Vol*

2. Hoofed mammals (Lynx Edicions, Barcelona, 2011).

186. M. A. Beaumont, in *Simulation, genetics and human prehistory*, Matsumura, S., Forster, P. and Renfrew, C, Ed. (McDonald Institute, Cambridge, 2008), pp. 134–154.

187. K. Csilléry, O. François, M. Blum, abc: an R package for approximate Bayesian computation (ABC). *Methods Ecol. Evol.* (2012).

Acknowledgments: We thank L. Cassidy, E. Jones, L. Frantz, G. Larson and M. Zeder for critical reading of the text. We thank the Israel Antiquities Authority for permitting sampling of the Israeli sites (under permit); excavators, archaeozoologists and museums who permitted sampling from their excavations and collections without which this project would not have been possible including T. Levy, C. Grigson, A. Maeir, S. Gitin, P. de Miroschedji, S. Davis and A. Ben-Tor. We thank the Iranian Cultural Heritage Handicraft and Tourism organisation and the National Museum of Iran (NMI) and J.Nokandeh, director, and Dr F. Biglari, Cultural Deputy. We are grateful to Dr H. Laleh and Dr A. Aliyari, Directors of the Archaeometry Laboratory of the University of Tehran. The ATM Project of MNHN supported sampling of several sites as well as the LIA HAOMA CNRS project. We are grateful for assistance from J. Vuković, J. Bulatović, I. Stojanović, H. Greenfield, Wiltshire Museum and L. Brown. We would also like to acknowledge Science Foundation Ireland Award 12/ERC/B2227, Trinseq and the SFI/HEA Irish Centre for High-End Computing (ICHEC). **Funding:** This work was funded by ERC Investigator grant 295729-CodeX. This project has received additional support from the HERA Joint Research Programme “Uses of the Past” (CitiGen) and from the European Union's Horizon 2020 research and innovation programme under grant agreement No 649307. A.M. was supported by ERC Consolidator grant 647787-LocalAdaptation. **Author contributions:** D.G.B. conceived of the project and designed research, with input from J.B. and M.C.; C.C., R.P., L.M., D.O., B.S.A., N.B., L.K.H, M.M., R.Ke., C.M.E., G.B.O., F.P., T.C., J.D.V., A.F.M., D.D., H.D., Ö.C., R.Kh., H.F., S.B., R.R.S., A.A.V., E.W.S., H.A.K., and S.M. provided samples and data; K.G.D, V.E.M., V.M., A.S. and A.J.H. and M.D.T. performed genomics laboratory work; P.M.D. performed ABC analyses, with input from A.M., K.G.D. and D.G.B.; K.G.D. performed the computational analyses with input from D.G.B., V.E.M., M.P.V., and M.D.T.; D.G.B., K.G.D. wrote the paper, with input from all other coauthors; K.G.D and P.M.D. wrote the supplementary information, with input from all other authors. **Competing interests:** The authors declare that they have no competing interests. **Data and materials availability:** Raw reads and mitochondrial sequences have been deposited at the European Nucleotide Archive (ENA) with project number: PRJEB26011.

Supplementary materials:
Materials and Methods
Figs. S1 to S20
Tables S1 to S32

Supplementary Materials for

Ancient goat genomes reveal mosaic domestication in the Fertile Crescent

Kevin G. Daly†, Pierpaolo Maisano Delser†, Victoria E. Mullin, Amelie Scheu, Valeria Mattiangeli, Matthew D. Teasdale, Andrew J. Hare, Joachim Burger, Marta Pereira Verdugo, Matthew J. Collins, Ron Kehati, Cevdet Merih Erek, Guy Bar-Oz, François Pompanon, Tristan Cumer, Canan Çakırlar, Azadeh Fatemeh Mohaseb, Delphine Decruyenaere, Hossein Davoudi, Özlem Çevik, Gary Rollefson, Jean-Denis Vigne, Roya Khazaeli, Homa Fathi, Sanaz Beizaee Doost, Roghayeh Rahimi Sorkhani, Ali Akbar Vahdati, Eberhard W. Sauer, Hossein Azizi Kharanaghi, Sepideh Maziar, Boris Gasparian, Ron Pinhasi, Louise Martin, David Orton, Benjamin S. Arbuckle, Norbert Benecke, Andrea Manica, Liora Kolska Horwitz, Marjan Mashkour, Daniel G. Bradley*

† Equally contributed
* Corresponding author: Daniel G. Bradley - dbradley@tcd.ie

This PDF file includes:

Materials and Methods

Sample information and archaeological contexts

Ancient samples, molecular sex, mitochondrial haplogroup and the site-of-origin are displayed in Table S1. Radiocarbon dating information for dated samples is displayed in Table S3; 2 sigma calibration was performed using OxCal 4.3, (*26*, *27*) and IntCal 13 (*28*). Sites are numbered according to Figure 1. Geographically proximal sites were combined into a single numerical label in Figure 1, and are discussed separately here using the headings 1A, 1B etc. Following sites presented on Figure 1, an additional site (Potterne, Wiltshire, UK) is discussed. Sample IDs and archaeological identifiers are presented at the end of each section. Goat samples from sites outside the geographic distribution of bezoar (i.e. western coast of Anatolia; European continent) are assumed to be domestic specimen descending from goat populations introduced by Neolithic Anatolian farmers.

1. Blagotin-Poljna, Trstenik, Serbia

Blagotin is a small site in the Šumadija region of central Serbia, belonging to the Early Neolithic Starčevo-Körös-Criş complex of the central and northern Balkans, and more specifically to the proto-Starčevo phase. It was excavated between 1989 and 1995 by Svetozar Stanković. Typically for EN sites in the central Balkans, the site consists of a cluster of pits, some interpreted as pit-dwellings, and no apparent above-ground architecture. The pits have a uniform pattern of fill layers, each capped by a dense, artefact-rich deposit (*29*), indicating a consistent process of infilling within the period of the site's use, rather than later accumulations. Three of the samples described here derive from the fill of the large central pit-feature, *Zemunica 7*, and the fourth to the nearby and similar *Zemunica 6*. Zemunica 7 has been AMS radiocarbon dated to the late 7th millennium BC using three bone samples (*30*), making it the earliest-dated published Neolithic feature north of Macedonia at time of writing. One of these (a red deer antler) derives from the basal fill of an internal feature (Pit 2) and two from higher within the sequence, including an *in situ* infant human burial directly above Pit 2 and providing a secure *terminus ante quem* for it. Two of the Zemunica 7 goat samples described here derive from Pit 2, the third from higher in the fill. No dates were obtained from Zemunica 6, but based on stratigraphy, artefactual dating, and similarity of the features themselves it is likely to be very close in date to Zemunica 7.

Date ref.	Date BP (uncal.)	±	Context	Species
OxA-8760	7230	50	Zemunica 7	Un-ID animal(*30*)
OxA-8609	7270	50	Zemunica 7, infant burial	*H. sapiens(30)*
OxA-8608	7480	55	Zemunica 7, pit 2	*C. elaphus(30)*

Animal bones from Blagotin were studied by Greenfield and Jongsma Greenfield (*29*). Caprines make up c.60% of the identified bones, with a goat:sheep ratio of roughly 1:3.7. The age profiles of domestic species and goat in particular at Blagotin and other sites in the region have been discussed by Greenfield and Arnold (*31*), who note a paucity of very young specimens. Samples dated from this site (Table S3) are in line with previously reported dates presented above.

Blagotin1	Zemunica 7, pit 2, BLFj
Blagotin2	Zemunica 7, pit 2, BLFIII=1

Blagotin3	Zemunica 6, BLJhIII
Blagotin16	Zemunica 7, BLFr16

2. Uivar, Romania

The settlement hill of Uivar is located about 40 km southwest of Timişoara in Romania. Finds from the hill date back to the late Neolithic Vinča culture and the early Copper Age (Tiszapolgár culture). The majority of the previously excavated settlement strata belongs to Vinča C. with the most recent late Neolithic horizon dating between 4940-4800 cal BC (*32*). The goat bone analyzed here stems from a Neolithic context, approximately 5250-5050 cal BC and had 130 bp mtDNA sequence previously reported (*33*, *34*).

Uiv17	Schnitt I, #012424, Befund 5180, 2008

3. Čavdar, Bulgaria

Čavdar is a Neolithic mound in the Sofia district of Bulgaria. The sample comes from a feature dating to the Early Neolithic Karanovo I period (*35*). From the around 400 animal bones described from Čavdar, the majority (three-fourths) come from cattle, sheep and goat, with a slight dominance of ovicaprids (*36*).The analyzed sample dates to app. 6000-5500 cal BC. It had previous successful amplification of a 130 bp mtDNA fragment (*33*, *34*).

Cav8	N.A.

4. Ovčarovo-gorata, Bulgaria

Ovčarovo-gorata is an Early Neolithic settlement in the Tărgovište district of Bulgaria (*37*). The vast majority of animal remains from this site are domesticates, dominated by cows (72%), with ovicaprids constituting only 21% of the assemblage (*36*). The analyzed sample comes from a context dating to Ovčarovo-Samovodene-Culture (parallelized with Karanovo II) and dates to app. 5700-5500 cal BC. Reporting of mtDNA 130 bp data is given in (*33*, *34*).

Ovc11	Horizont 1, Tiefe 0, 10 m, Quadr 7

5. Kovačevo, Bulgaria

Kovačevo is a Neolithic settlement located in the Struma Valley in the Blagoevgrad district of Bulgaria (*38*). Animal remains from this site are dominated by domestics, in particular by ovicaprids (65%). The samples analyzed here are from Early Neolithic contexts dating to app. 6200-5600 cal BC. Reporting of mtDNA 130 bp data is given in (*33*, *34*).

Kov27	Sektor K, 48877
Kov57	Sektor M, 43651
Kov60	Sektor I, 34589

6. Aşağı Pınar, Turkey

Aşağı Pınar is a Neolithic mound found near Kırklareli, Thrace, Western Turkey. The samples come from occupation layers dating to the Middle and Late Neolithic (c. 5500-5000 cal BC) from excavations in 1993-1998 (*39*). Domestic animals are dominating the faunal assemblage with the

majority being ovicaprids in the older layers (around 50-60%) (*40*). Summary of dates and reporting of mtDNA 130 bp data is given in (*33*, *34*).

AP38	Ap 5, 13H/260
AP44	105/35
AP45	Ap 4/5, 13M/105
AP46	Ap 4/5, 151/206
AP50	Ap 2/3, 8N/7

7. Ulucak Höyük, Western Turkey

Ulucak Höyük is a settlement mound located in western Anatolia, close to the eastern Aegean coast, and contains a long Neolithic sequence spanning from the early 7th to early 6th millennium BC. The site has been central in investigating the relationship between the Fertile Crescent and Europe during the dispersals of animal husbandry. It is the type site of the so-called Mediterranean or maritime route. Interestingly, the earliest occupational layer at Ulucak VI lacks pottery, but contains morphologically domestic sheep, goat, cattle and pig (*41*, *42*). The goat specimen included in this study was found in a stratified context dated to 6200-6100 cal BC and is previously analysed (130 bp mtDNA) in (*33*, *34*).

Ulu38	Vb EPJ, 897

8. Direkli Cave, Turkey

Direkli Cave is located in the central Taurus mountains of southern Turkey at elevation of 1100 meters asl in the province of Kahramanmaras. Excavated by Dr. C. M. Erek since 2007, the site has revealed a prehistoric sequence dating to Epipaleolithic period (*43*). Radiocarbon dates for the Epipaleolithic levels place the occupation at the Terminal Pleistocene between 12,000-9000 cal BC. These dates are supported by a lithic assemblage dominated of microliths with parallels to the Natufian industry of the Levant. The remains of hearth features, round structures, baked clay figurines, as well as a human burial have been uncovered in these levels.

Based on analysis of the faunal remains the cave was used as a seasonal (summer/fall) campsite associated with hunter-gatherers in the region exploiting upland resources including primarily wild goats and secondarily deer and also tortoise (*44*). Direct dating of two samples (Direkli2 and Direkli4, presented in Table S3) indicate that they derive from the 13th-12th millennium cal BC.

Direkli1	DM2546
Direkli2	DM3110
Direkli4	DM3723
Direkli5	DM4072
Direkli6	DM4073

9. Abu Ghosh, Israel

The site of Abu Ghosh is situated in the Judean Hills, ca. 12 km west of the city of Jerusalem (UTM latitude 700711; longitude 35.21958). In proximity to the site are several freshwater springs as well as a small tributary of the Kesalon river. The site was first excavated in the 1950's by Jean Perrot (*45*) and again in 1967 by Monique Lechevallier (*46*), both of the Centre de Recherches

Français de Jerusalem. In 1995 a salvage excavation was undertaken by Hamoudi Khalaily and Ofer Marder for the Israel Antiquities Authority. All excavators reported finding mid-Pre-Pottery Neolithic B (9300-8500 uncal BP) layers as well as an ephemeral Pottery Neolithic layer. The mid-PPNB strata from which the samples examined in this study derive, yielded rectangular houses with plaster floors, installations, intra-mural human burials and large corpuses of lithic artifacts – produced both on and off-site (dominated by arrowheads and sickleblades), groundstone vessels and faunal remains.

The mid-PPNB fauna is dominated by goats followed by aurochs, wild boar, cervids, carnivores, small mammals birds, reptiles and amphibians.The goats have been identified as representing animals in the early (incipient) stages of domestication based on their biometric and morphological resemblance to wild goats (*Capra aegagrus*), predominance of males and some evidence for selective culling since only 30% of goats survived into adulthood (*47*, *48*). In addition, remains of ibex (*Capra ibex* sp.) have been identified in the assemblage based on aDNA analyses (*49*). This has been interpreted (*48*) as a reflection that local communities did not discriminate between the two wild goat taxa and attempted to domesticate both, or alternately, that the goat sample comprises hunted as well as incipient domesticates.

Ghosh5 2249 1429

10. ‘Ain Ghazal, Jordan

'Ain Ghazal is a large permanent Neolithic settlement on the NE outskirts of Amman, Jordan. The sampled excavation trenches are from a MPPNB "terrace" created by bulldozers to prevent erosion onto the (then) new highway between downtown Amman and Zarqa. The people living in the houses from the MPPNB in this part of the site had direct access to the Zarqa River, which was a permanent river ar this time. Also at this time 'Ain Ghazal was a sizeable village (estimated population of 550-650), but after ~7500 cal BC the size of the site and the population exploded in comparison to earlier times (*50*). The earlier phases at 'Ain Ghazal began as early as 8300 cal BC, and the MPPNB ended at c. 7500 cal BC. The Late PPNB emerged then and continued until c. 7000-6900 cal BC, followed by the PPNC, which lasted until c. 6500-6400 cal BC. Throughout its occupation, *Capra* made up a substantial proportion of faunal remains (*51*).

Original zooarchaeological studies of the ‘Ain Ghazal animal bones were undertaken by von den Driesch and Wodtke (*52*) and Wasse (*53*), based on separate collections. Martin and Edwards (*51*) undertook comparative osteometric analyses of the ‘Ain Ghazal goats and sheep only. The goat specimens sampled for the current study derive from Middle PPNB levels (see below). Von den Driesch and Wodtke interpret Middle PPNB goat bones as belonging to managed animals, with domesticated goats appearing by Late PPNB (c. 7,000 cal BC), on the basis of cull patterns and bone size. By contrast, Wasse and Martin & Edwards find the majority of the Ain Ghazal goats to be of small size by the Middle PPNB and likely domestic. All studies identified a small number of large size goats in Middle PPNB deposits, assumed to be wild local Capra aegagrus. Interpretation varies as to whether local wild goats were hunted prey, separate from imported domestic stock (*53*), or wild stock which was domesticated locally in the vicinity of ‘Ain Ghazal (*52*). Martin & Edwards (*51*) raise the possibility that imported domestic goats could have been crossed with local wild Capra aegagrus to explain osteometric size ranges. The wild/domestic/managed status of goats in Middle PPNB levels at ‘Ain Ghazal is unresolved, but their dominance (60-80% caprines,

mostly goats) supports an interpretation of management/domestication. Petrous bones (of medium ungulate size) were sampled from the ‘Ain Ghazal faunal assemblage housed at UCL (Institute of Archaeology) in May 2014 by Bradley, Mullin and Martin.

The following Yarmoukian Pottery Neolithic ("Late Neolithic") is very poorly dated anywhere but a general consensus appears to place it in the latter half of the 7th millennium BC and the earlier part of the 6th. Dates presented below refer to calibrated dates of the appropropriate Phase.

Ainghazal1	3077.261 (024) 111b AG83 PHASE IIIb (7804 ± 407 cal BC)
Ainghazal2	AG84 3080.133 (046) PHASE IVa, (7725 ± 407; 7728 ± 160; 7774 ± 128 cal BC)
Ainghazal3	3077.275 (037) 111b AG83 PHASE IIIb
Ainghazal4	AG84 3077 (024) PHASE IIIB

11. Hovk-1 Cave, Armenia

Hovk-1 cave (2040 m ASML Latitude 40° 49’21”N, Longitude 45° 0’ 18’’E) is in the north-easterly Tavush province of Armenia and has a rich and diverse large faunal assemblage. This has exceptional preservation that persists throughout stratigraphic units. Mammals consist mainly of ungulate and carnivore taxa; *C. aegagrus* constitutes over 70% of the former. The bone sampled was a petrous element excavated in 2006 from the Pleistocene colluvium of Unit 5a, the rear gallery of the cave. The sediments of the rear gallery were accumulated during the period at which the cave’s chimney was opened and their source was likely the plateau above the cave. The sediments consisted of various Pleistocene fauna, and a single limestone Levallois flake. This bone had a direct date estimated in this study but was outside the range of C14 and is therefore reported as >47,00 BP. This is in agreement with the dates reported for Hovk1 Cave as Unit 5 is >48,000 BP, Unit 6 is 54,600 +/- 7000 BP and Unit 8 is 104,000 +/- 9800 BP (*54*). The stratigraphic association of the 5a unit to the others is uncertain.

Hovk1	2006, Sq RP Unit 4, Level 92

12A. Kelek Asad Morad, Luristan, Zagros mountains, Iran

Kelek Asad-Morad is located at 47° 30 54’ longitude and 33° 09 55’ latitude in the western part of Pol e Dokhtar, in the southern foothills of the Maleh mountains in the province of Luristan. The site covers a two hectares area and is 800 m ASL. The site of Kalek Asad Morad is among the rare pre-pottery Neolithic sites recently investigated archaeologically in the Zagros (*6*). Because of the significant importance of this site and its progressive destruction due to continuous ploughing and illegal excavations a rescue short sounding season was undertaken in the site supported by a Fyssen Foundation Grant obtained by M. Tengberg & M. Mashkour. A very large lithic assemblage was found in Kelek Asad Morad among which several obsidian tools. The radiocarbon dates indicate a very short period of occupation of the site, ten thousand years ago (*6*). In comparison to the other early Neolithic sites of the Zagros it is slightly earlier than the earliest levels of Ganj Dareh and overlaps with some of the levels of Chogha Golan, Sheikhi Abad and Chia Sabz. The three dates (*6*) are consistent and range from 8500 to 8200 cal BC. The faunal remains were studied by M. Mashkour and F. A. Mohaseb. Only 300 remains could be identified out of which 95% belonged caprines while goat outnumbered sheep. Univariate metric analyses on second phalanges of the goat bones compared to other prehistoric sites in the Zagros as well as LSI

analyses shows the presence of both domestic and wild specimens in the site. The low number of teeth did not allow the analysis of the kill-off patterns.

Lur9 MM KAMCS12

12B. Tepe Abdul Hosein, Luristan, Zagros mountains, Iran

Tepe Abdul Hosein is a highland site located at 1860 m ASL in the Province of Luristan between Khorramabad and Malayer in the Zagros mountains of Iran. The site was excavated by Judith Pullar in 1978 and revealed to be unique for its preceramic occupation during the early Neolithic (*55*). Several new radiocarbon dates obtained on osteological material indicates dates around 8200 to 7800 cal BC. Recent genetic studies on the human remains of the site have shown the great potential of the site for the understanding of the Neolithic peopling of the Zagros and its spread to the East (*14*). The faunal remains of the site stored in the osteology department of the National Museum of Iran and currently under study by Marjan Mashkour and her team show a diversified subsistence economy with a prominent role of wild and domestic goats. For the distinction of wild or domestic goat skeletal elements, several cross-methodological approaches are used. The first indication is brought by morphology of horn cores. We use also univariate metric analyses on different skeletal parts (second phalanges, humerus etc…) and LSI analyses on the postcarnial bones with comparison to wild and domestic modern reference material or paleolithic /epipaleolithic assemblages. Additionally, kill off patterns were employed. The sample reported here dates to late 9th / early 8th millennium cal BC (Table S3).

Lur12 MM AH1

13. Sang-e Chakhmaq, Semnan, Northeast Iran

Tappeh Sang-e Chakhmaq is located at 1400m ASL, near Shahroud (36°29′59″N 55°00′02″E) in the Semnan province. It is a unique Neolithic site that provides the earliest evidence for agricultural and herding in the North East of Iran and the spread of the Neolithic way of life in Central Asia. During the early 70s a Japanese team supervised by Seichii Masuda exposed several trenches on the East and West mounds (*56*). Recent soundings on these mounds led by Kourosh Roustaei allowed a better contextualisation of the material culture and its chronological framework (*57*).The West mound is a pre-pottery site dating to late 8th to the beginning of 7th millennium cal BC, while the East mound has pottery levels occupied from the late 7th to mid 6th millennium cal BC (*57*, *58*). Goat remains were studied by M. Mashkour, J. D. Vigne and collaborators and sampled in Tsukuba, Japan. Wild species are very numerous in the faunal remains and the small herbivores (goat, sheep and gazelle) are the most exploited taxa. The presence of morphologically wild goat horn cores in addition to metric analysis reported for site 12 and kill-off patterns show that domestic goat is present from the earliest stages of the occupation (*57*, *59*). Samples reported here date (Table S3) to both the late 8th and 7th millennium cal BC, in line with dating of the West and East mounds.

Semnan1 MM TSC2
Semnan2 MM TSC3
Semnan3 MM TSC5
Semnan7 MM TSC9
Semnan8 MM TSC8

Semnan9	MM TSC10
Semnan10	MM TSC10
Semnan13	MM TSC10
Semnan17	MM TSC11

14. Rahmat Abad, Fars, Southwest Iran

Tepe Rahmat Abad is mound site (E 053° 3'27.89, N 30° 6'43.50"; 1774 amsl) located next to the village of Rahmat Abad, Fars province and south eastern of Zagros Mountain. The site covers an area just 0.5 ha and rises 5 m above the surrounding plain and is on edge of the fertile Kamin plain at the southerly end of the Bolaghi gorge. The Pulvar River runs 500 m to the east, and its bed cuts through the Bolaghi gorge, at the upper end of which lies Pasargadae, the royal capital of the founder of the Persian Empire, Cyrus the Great. Tepe Rahmat Abad was excavated during four seasons from 2005 to 2010 and nine meters of cultural deposits exposed a long sequence from the early Neolithic to the Antiquity. The Neolithic period can be divided in 2 phases, Pre-Pottery Neolithic (Rahmat Abad phase, 7450-7100 cal BC.) and Pottery Neolithic phase (7000-6028 cal BC). The Pottery Neolithic phase also divided to the 2 sub phases: Early Pottery Neolithic (Formative Mushki phase, 7100-6450 cal BC) and Middle Neolithic phase (Mushki phase, 6400-6100 cal BC) (*60*). Faunal remains of the site were studied by M. Mashkour, H. Davoudi and R. Khazaeili, using similar approaches as taken for Tepe Abdol Hossein, and were prepared for publication accompanied by analysis of botanical remains by M. Tengberg (*61*). The single sample dated from this site (Table S3) falls within the Pottery Neolithic Phase (7,047 - 6,772 cal BC).

Fars1	MM RA1
Fars2	MM RA4.1
Fars5	MM RA4.2

15. Monjukli Depe, Meana-Čaača Region, South Turkmenistan

Monjukli Depe is a tell site with layers of occupation dating to the Late Neolithic (c. 6400-5900 cal BC) and Early Copper Age (c. 5100-4500 cal BC). All samples are from features of the Early Copper Age (*62*). Zooarchaeological analysis was performed by Norbert Benecke. Domestic status of ovicaprid remains was assessed by metric analysis, primarily breadth measurements. Faunal evidence indicates a predominance of domesticates throughout the sequence, primarily sheep/goat (90% of identifiable bones). Based on forty seven mandible remains, a high proportion of sheep/goat were slaughtered at a young age, between five and eight months. This patterns is possibly an indication of autumnal/winter butchery, which may have been required to manage herd size during these months. Wild animals (goitered gazelle, half-ass, hare, fox etc) make up a small proportion of the assemblage.

Monjukli1	G, Locus 24, RN 7067, l
Monjukli2	C, Locus 295, RN 10550, r
Monjukli4	E, Locus 83, RN 4334, r
Monjukli6	D, Locus 208, RN 1347, B, r
Monjukli7	C, Locus 220, RN 6682, l
Monjukli8	C, Locus 169, RN 5765, A, l
Monjukli9	C, Locus 72, RN 5293, l

16. Pietrele, Romania

The settlement Magura Gorgana is a Chalcolithic mound from Gumelnița-Culture near Pietrele in the Giurgiu Province of Romania (*63*). The sample analyzed here dates to app. 4250-4450 cal BC. A report of 130 bp mtDNA sequence from this specimen is given in (*33*, *34*).

Pie17	P07 F415

17. Drama-Merdžumekja, Bulgaria

Merdžumekja is a mound located near Drama in the Jambol district of Bulgaria. The earlier phases can be parallelized with Karanovo IV-VI, while the sample analyzed here (c. 4500 cal BC) comes from a Chalcolithic layer belonging to Marica-Culture (Karanovo V). The faunal assemblage is dominated by domesticates with mostly cattle (around 60 %) and ovicaprines (around 30%) (*40*). A report of 130 bp mtDNA sequence from this specimen is given in (*33*, *34*).

Dra34	Haus 486, 98:0627

18. Kanlıgeçit, Turkey

Kanlıgeçit is a mound (*64*) located near Kırklareli, Thrace, in Western Turkey, with most finds dating to the Early Bronze Age (*64*). The samples analyzed here come from phases II and III (c. 2700-2200 cal BC). The faunal assemblage is dominated by cattle, ovicaprines are only constituting around 30% (*40*). Listing and sources of dates and summary of mtDNA 130 bp data are given in (*33*, *34*).

Kan19	KG97 29P/30
Kan23	KG05 32R/3
Kan25	KD94 31L/20

19. Acemhöyük, Turkey

Acemhöyük is a large mound site located on the Aksaray plain in central Turkey. The site has been excavated since 1962 by Dr. Nimet Özgüç and more recently Dr. Aliye Öztan of Ankara University (*65*, *66*). Acemhöyük's primary occupation sequence spans the Early and Middle Bronze Age periods (2800-1750 BC) when it represents a major urban settlement with a large city wall and central administrative complexes including palaces. In the Middle Bronze Age, the settlement, which may have been known as the kingdom of Purushattum, was heavily involved in international trade and political networks with evidence for intensive interaction with city states in northern Mesopotamia. Analysis of faunal remains indicates that goats were a central part of the animal economy at Bronze Age Acemhöyük with demographic evidence showing that young males were preferentially slaughtered in a management system likely focused on the production of a combination of meat, skins, fiber (goat hair) and milk (*67*). Acem1 is dated to the later half of the site's primary occupation (2346-2040 cal BC).

Acem1	AC13346
Acem2	AC14486

20A. Tachti Perda, Kakheti, Georgia

Tachti Perda is a mound of the Middle to Late Bronze and older Iron Ages located between the Greater and Lesser Caucasus Mountains in the Kakheti region of Georgia (*68*). Zooarchaeological analysis was performed by Norbert Benecke. Domestic status of ovicaprid remains was assessed by bone metric analysis, principally breadth measurements. The samples analyzed here come from Late Bronze Age (Tac1 and Tac3; c. 1400-1000 cal BC) and Iron Age (Tac2; c. 1000-700 cal BC). Preliminary analysis of the faunal remains indicate a preponderance of small and large domestic ruminants, supporting the hypothesis that inhabitants relied more heavily on animal farming during the Bronze and early Iron Age (*69*). A report of 130 bp mtDNA sequence and a summary of dating sources for these three specimens is given in (*33*, *34*).

Tac1	Ud2005, P268 / Bef 125
Tac2	Ud2005, P26A / Bef 102
Tac3	Ud2005, 025 / Bef 196

20B. Dariali Tamara Fort (Kazbegi), Georgia

In the border zone between Georgia and Russia in the Kazbegi region, Tamara Fort (Coordinates: UTM 38N 469400, 4731800) sits on top of a high flat outcrop on the west bank of the Tergi river with excellent views of the pass.The site is investigate within an ERC project "Persia and its Neighbors" directed by Eberhard Sauer (Edinburgh University).

Excavations at the site were indicate several occupations mainly between ca. 400 – 1000 AD which was first a military Fort from the Sasanian period. The site was re-occupied between the late 13th and early 15th centuries AD. Following this, there is no evidence for occupation until the 20th century (*70*).

A large number of animal bones (approximately half a tonne) have been studied during four seasons of excavation under the supervision of M. Mashkour. The domestic herbivores (sheep, goat and cattle) are dominant in the faunal remains. Very interestingly, specimen of Caucasian tur (*Capra caucasica*) were found among the remains (*70*).

Kazbeg1	MM CG5

21. Kohneh Tepesi, Western Azerbaijan, Iran

Kohneh Tepesi is a small site (*ca* 0.2 ha) located in the . The site was excavated by A. Zalaghi, B. Aghlari and S. Maziar as part of a Khoda-Afarin dam rescue project in 2006 and 2007. On the basis of the pottery and other material the site can be dated to the Kura-Araxes II or perhaps part of III (Early Bronze Age) (*71*). The faunal remains of the site are very abundant and were studied by S. Sheikhi, M. Mashkour and A. Mohaseb. Bone preservation in Kohneh Tepesi was satisfactory. The subsistence economy was based on domesticates (sheep, goat and cattle). However other resources such as red deer and suids (wild and domestic) contribute to the diet of the inhabitants (*72*).

Kohneh2	#202.2, 11027

22A. Tepe Hasanlu, Western Azerbaijan, Iran

Tepe Hasanlu is one of the key sites of northwestern Iran, due to its long-term occupation and well-defined stratigraphy. Hasanlu is located in the Solduz valley on the southern shore of Lake

Urmia at 1043 m ASL, (Latitude: 37° 0'16.15"N, Longitude: 45°27'31.74"E). Robert H. Dyson Jr. directed 10 seasons of excavations at Hasanlu from 1956 to 1977 (*73*, *74*). The site was occupied during 10 different cultural periods from the Late Neolithic (period X) to the Ilkhanid dynasty (period I) (*75*). Hasanlu Period VII can be linked to the Early Bronze Age from the first half of the third millennium to the late third millennium BC (3000-2100 cal BC) (*76*). The most represented periods in the site are the Late Bronze (period V) and Iron Age (period IV-III) (*77*, *78*). Hasanlu period IIIc and b, are attributed to Iron Age III (Urartian period) and period IIIa allocated to the Achaemenid Empire (550-530 cal BC), for which no substantial architectural remains have been found (*79*). Period II is also a debated issue but generally assigned to the Seleucid or Parthian period, post-Achaemenid (*80*, *81*). The samples were chosen from the fill of an oven from the late of Early Bronze Age (Campaign 1974, Op. W23, Stratum 20, Locus 23) and deposits of Achaemenid period (Campaign 1974, Op. W32, Stratum 4, Locus 1, Lot 17). Faunal remains of this site are very abundant and very well preserved (*82*). The assemblage was studied by H. Davoudi within a PhD Thesis under the supervision of M. Mashkour (*82*). The osteological material of this site had been used in several genetic studies (human, dog) (*14*).

Azer3	MM TH18
Azer4	MM TH21
Azer5	MM TH2

22B. Soha Chai Tepe, **Zanjan, Iran**

The site of Soha Chay Tepe is located on the Sojasrud Valley in western Iran in southwestern Zanjan province at 1712 m ASL, 36°19′06.25″ longitude, 48°22′47.50″ latitude. Soha Chay Tepe was excavated during summer and autumn of 2006, under the direction of A. Aali and R. Rahimi. It is a single-period site, with only 1.20 meters of cultural depositions (*83*). Excavations at this site exposed a small settlement of less than 1 hectare. The occupation comprises two architectural phases allocated to the Middle Chalcolithic (late 5th millennium cal BC) known as Dalma cultural tradition. The distinctive Dalma ceramic assemblage spread widely through the northern and central highland valleys of the Zagros Mountains in western Iran. Dalma is a widespread ceramic phenomenon throughout much of the rugged Zagros highlands of north and central western Iran (*84*, *85*), technically and stylistically homogeneous. Compared to the amount of archaeological research carried out in Dalma sites in west of Iran, there has not been much interdisciplinary work (*83*). Studied by Mashkour and Fathi, the bulk of the animal remains belong to small ruminants, with a predominance of sheep and goat.

Azer6	MM SCH1

23. Tepe Shizar, Qazvin Plain, Iran

Tepe Shizar is a 19 metres high mound with cultural deposits, which is located in the Takestan County, Qazvin Province. The site was excavated by opening two stratigraphic trenches in 2006 by H. Valipour. Tepe Shizar includes a cultural sequence from the Chalcolithic to the Iron Age (*86*). The goat sample from Tepe Shizar (Qazvin1, MM TCHZ2), belongs to the Middle Bronze Age and was occupied between 2400-1900 BC (*87*). The faunal remains of Tepe Shizar were studied were studied by H. Davoudi, and not yet published at the archaeozoology section of Archaeometry Laboratory (University of Tehran) to document the subsistence economy and herding strategies during the third millennium BC in the Qazvin Plain. The assemblage is composed by sheep, goat,

cattle and equids with the predominance of caprines. Remains of hunted animals are diverse, but rare. The most abundant game is gazelle, a steppe-adapted animal. Wild sheep and goat, deer and boar are among other identified hunted species. Despite this diversity that indicates a mosaic of environments around the site, the most exploited animals are the domesticates that grazed in the rich pastures in the junction of the hilly flanks of Alborz and Zagros mountains. No animal bones was directly dated and the chronology of the site is based on relative chronology.

Qazvin1 MM TCHZ2

24A. Darre-ye Bolāghi, Iran

Darre-ye Bolāghi is a valley with archaeological significance containing some 130 ancient settlements (*88*). It is located in the Fars Province of Iran, and is a small plain 1,800 m above sea level. This excavation dates to between the 5th and 4th Millenium BC, also known as Bakun period. There is evidence of a large-scale pottery production at several of the associated sites. Researchers are inconclusive as to whether the sites where inhabited seasonally or by a sedentary population. Zooarchaeological analysis was performed by Norbert Benecke. Domestic status of ovicaprid remains was assessed by bone metric analysis, principally breadth measurements. A single petrous bone here dates to the medieval period (Darre2, see Table S3).

Darre1 TB131, SU 623/04, S11, r
Darre2 TB91, SU 206/05, N14, r

24B. Rahmat Abad, Fars, Southwest Iran

See Site 14 above.

24C. Mianroud, Fars, Southwest Iran

Mianroud is located in the Marvdasht Plain in central Fars (UTM 39R 660495E 3339520 N) and is a 3.7 ha in area. The stratigraphic trench provided the complete cultural sequence of the site that spans from the Mianroud Neolithic Period (Late Neolithic) and continues with Bakun B1/Shamsabad and ends with Gap/Bakun B2. There are some similarities between the Neolithic pottery of Mianroud with Mushki and Jari traditions in Marvdasht (*89*). The archaeozoological analysis was performed by M. Mashkour, H. Fathi & F. A. Mohaseb and shows a very specialised subsistence economy relying on pastoralism and a significant contribution of sheep and goat herding. The single sample reported from Mianroud (Fars4) dates to mid/late 6th millennium cal BC (Table S3).

Fars4 MM MR4

25. Chalow, North Khorasan, Northeast Iran

The site of Tepe Chalow is situated in the easternmost part of the plain of Jajarm, 3 km. east of Sankhast and approximately 60 km west of Esfarayen. The site is located at the end of the ancient delta of Darband River at 56°53'7.01" E, 37° 6'12.78" N at an altitude of 980 m ASL. Recent excavations of the joint Irano-Italian team at Tepe Chalow in the plain of Jajarm have brought to light a necropolis in which not only the luxury objects but also the ordinary, household objects and the pottery are almost identical to the Greater Khorasan Complex ones. The pottery analysis as well as several radiocarbon dates show a sequence from late Chalcolithic to the Middle/Late

Bronze Age (end of the 4th millennium BC to 3rd millennium cal BC (*90*). Archaeozoological analyses by Mashkour, Fathi and Amiri show the importance of goat and sheep as well as cattle along with game species, hemione and gazelle. Of particular interest are the animal grave goods. In one case (Trench 29 Grave 2) a juvenile caprine was found adorned with bronze bracelets in forelegs.

Chalow1 #205, T10, G1 (8.7.2009, W, Basket 127006, 174.20-174.05)

26. Tilla Bulak, Surkhandarja Province, South Uzbekistan

Tilla Bulak is a Late Bronze Age settlement site dating to a period of less than 200 years at the beginning of the 2nd millennium BC. This was a small hamlet with a hilltop location with command of a perennial spring (*91*). Zooarchaeological analysis was performed by Norbert Benecke. Domestic status of ovicaprid remains was assessed by bone metric analysis, primarily breadth measurements. Based on preliminary analysis, sheep and goat makeup 79% of animal bones, followed by cattle (8%) and hunted species (9%).

Bulak1 TB, 08, KF291, r, A
Bulak2 TB, 08, KF291, r, B
Bulak3 TB, 08, KF291, r, D
Bulak4 TB, 08, KF291, l, A
Bulak5 TB, 08, KF291, l, B

27A. Shiqmim, Israel

Shiqmim is located ca. 18 km west of the town of Be'er Sheva, on the northern bank of Nahal Be'er Sheva in the northern Negev. The site represents a large Chalcolithic village and covers an area of about 9 hectares. Two excavation seasons were conducted at the site, in 1979, 1982-1984, 1989-1987 and 1993, under the direction of the late David Alon (Israel Department of Antiquities) and Tom Levy (University of California, San Diego). The excavations revealed evidence of social stratification, political connections, extensive trade relations, a local metal industry and other crafts.

Four strata of the Chalcolithic settlement were identified dating to 4500 to 3700 cal BC, with no earlier or later occupation. The faunal assemblages recovered from different seasons were examined by Grigson (*92*, *93*) and Whitcher (*92*, *93*). Remains are dominated by domestic sheep, goat and cattle, with paltry finds of gazelle, wild carnivores, dogs and equids, but lacking in pigs. It is suggested that the caprine cull pattern supports a specialized economy geared towards milk production. Overall, the subsistence economy of the site was based on mixed farming, along with agro-pastoralism. However, whether all or some of the Negev Chalcolithic communities were semi-nomadic or sedentary, continues to be debated.

Shiqmim1 1993; R13; 4241; A554
Shiqmim9 1993, 5004, C38

27B. Gilat, Israel

The “Ghassulian” Chalcolithic site of Gilat is located on the east bank of the Patish river, *ca.* 1km east of the town of Ofakim in the northern Negev (UTM latitude 31.328497; longitude 34.649997).

The first excavations at the site were undertaken in 1975-1977 by the late David Alon for the Israel Department of Antiquities, followed by more extensive excavations by Tom Levy (currently University of California, San Diego) and David Alon in 1987, 1990-1992 (*94*). Site size was estimated as ca. 12 hectares with several Chalcolithic occupation layers recognized. The occupation centers within three of four centuries around 4500 cal BC with the site abandoned during the Chalcolithic and not resettled.

Gilat has been interpreted as a permanent settlement, probably a ritual center (sanctuary) as attested to by the presence of a large structure interpreted as a temple comprising rooms, courtyards and special finds. Site subsistence was based on cereal cultivation, pastoralism (primarily of domestic caprines exploited for their secondary products) and trade. Grigson (*95*) who analysed the assemblage identified both domestic sheep and goats; the sheep have Ammon-type curved horns while the goats have twisted horns and represent animals of short stature. Remains of other species recovered include domestic pigs, cattle, equids, dogs and few game animals (e.g. hartebeest, gazelle, ostrich, carnivores).

Gilat2	1992; M2; 612; 5089
Gilat8	1992, 786, 5688
Gilat10	1992, M1-N1, 773, 5451

28A. Tel Yarmuth, Israel

Tel Yarmouth is located on the edge of the coastal plain of Israel, ca. 3 km south of the town of Bet Shemesh adjacent to freshwater springs and the Yarmouth River (UTM latitude 68.7148; longitude 35.09992). This large tel covers ca. 160 dunams with a 15 dunam acropolis. It was first excavated by Amnon Ben-Tor for the Hebrew University, and since the 1980's by Pierre de Miroschedji for the Centre de Recherches Français de Jerusalem from whose excavations the fauna examined in this study derive. Extensive remains belonging to both the Early Bronze Age III a and b (2300-2700 cal BC) have been found, including private houses, silos, a large public structure identified as a temple, fortifications and a city gate. Remains dating to the earlier Early Bronze Age II have also been found but only scanty finds dating to the Early Bronze Age I and overlying Iron Age and Roman deposits.

Domestic sheep and goat are the two most common species represented at Yarmouth and together comprise over 80% of the assemblages. Sheep outnumber goats. Only ca. 35% of the EB caprines were culled age less than two years suggesting exploitation of herds for their secondary products. After caprines, cattle are the third most common animal at the site and the bovine assemblage includes a few bones identified as aurochs. Remains of other animals are few: pigs, equid, hartebeest, cervids, gazelle, carnivores, fish and birds (*96*).

Yarmut1	14-82; 216; 6655
Yarmut7	28-87; 1109; 9542

28B. Tel Yoqne'am, Israel

Tel Yoqne'am, located ca. 30 km south-east of the city of Haifa (latitude 32.6641; longitude 35.1083), lies on important ancient trade routes that traversed northern Israel - the Via Maris which connected the Mediterranean coast from Tyre (Lebanon) and the route through Wadi Milek

to the Jordan Valley and beyond. Excavations at the site were conducted in 1977-1988 by Amon Ben Tor of The Hebrew University of Jerusalem. In 1993 Miriam Avissar of the Israel Antiquities Authority undertook a small excavation on the summit of the tel.

The tel is a multi-period settlement covering ca. 4 hectares, and comprises come 25 different occupation spanning from the Early Bronze Age (ca. 3150-2200 cal BC) to the Ottoman period. It was an important Canaanite city in the Middle Bronze and Late Bronze Ages, and was conquered in 1468 BC by Egyptian Pharaoh Thutmose IIIA. In the Bible, Yoqne'am appears on the list of Canaanite city-states conquered by Joshua. In the Iron Age it was an Israelite city. Excavations of the Bronze and Iron Age strata have revealed fortifications (city wall, glacis and defensive towers), storerooms, residential areas, a palace and an underground water reservoir. At this time the area around the tell was an additional residential area - the "lower" city.

Faunal remains from the Middle Bronze Age through the Ottoman period at the tel were analyzed by Horwitz and colleagues (*97*, *98*). In all periods the traditional triad of domestic species – sheep, goat, cattle – predominate, supplemented in some periods by swine. The relative proportions of these taxa shift over time with peak caprine frequencies –especially of sheep- recorded in the Late Bronze and Iron Age I. This was probably related to wool production in the Late Bronze Age, and is reflected in the cull patterns. Over time cattle numbers increased to peak in the Iron Age IIB a trend that may be associated with expansion of plough cultivation. There is a concomitant drop in pig numbers. Metric data shows no significant change in caprine sizes over time. Species derived from hunting and fishing occur in all periods but are not abundant, though some fluctuations are evident over time (*97*, *98*).

Yoqneam2 2343; 6107

28C. Tel es-Safi/Gath, Israel

Tel es-Safi/Gath is located ca. 53 km east of the city of Ashkelon in the central coastal plain (Shephelah) of Israel (UTM latitude 31.699722; UTM longitude 34.846944). Small scale excavations were first undertaken at the site in 1899 by Bliss and Macalister while extensive excavations have been directed at the site by Aren M. Maeir (Bar Ilan University) since 1996 and are ongoing. These investigations have yielded important archaeological data on the occupation of the tel spanning the Early Bronze Age to the Ottoman period.

The Early Bronze Age Canaanite deposits have revealed a series of occupation levels in a residential area as well as fortifications. To date, Middle Bronze Age occupation of the tel is attested to only the summit. Human activity at the site peaked during the Iron Age, when it was one of the main Philistine cities - the biblical "Gath of the Philistines". The excavations have shed light on the timing and origin of the Philistine culture, offering insights into its evolution and final disappearance. The advent of the Philistine occupation was accompanied by the introduction of a broad spectrum of plants from several regions as well as imported pigs from the Aegean (*99*, *100*). In the late Iron Age IIA (ca. late 9th century cal BC), the tel and the lower city at the foot of the tel were put under siege and conquered, apparently by King Hazael of Aram Damascus. This destruction layer has yielded a rich assortment of well-preserved finds including ritual, storage and domestic areas; hundreds of ceramic vessels; lithic and metal artefacts; ivory and bone decorations, ceramic figurines in addition to botanical and animal remains.

The archaeozoology of the Early Bronze Age layers is being studied by Greenfield and colleagues (*101*), while the Late Bronze and Iron Age faunal remains are studied by Lev-Tov (*102*) and Horwitz (*103*). In all periods and strata at the site, remains of sheep and goat are the most common but their frequencies changes over time relative to those of cattle and pigs. The latter are most common in layers associated with the Philistines and then decrease dramatically in the late Iron Age levels at the site. Adult goats are more common than sheep in the Early Bronze and Early Iron Ages, a finding interpreted as reflecting a management strategy focused on meat and milk production rather than wool. Additional domestic species found are equids, camels (in the late Iron Age) and dogs, while hunted taxa (e.g. gazelle, deer, wild carnivores) as well as fish occur in all periods (peak frequencies in the Bronze Age), but their contribution to the diet was negligible.

Safi2 8.7.2009, W, 1270007, 1270007, 174.20-174.05

28D. Tel Miqne-Ekron, Israel

The tel is located on the Israeli coastal plain (Shephelah) ca. 35 km south-west of Jerusalem (UTM latitude 31.77889; longitude 34.84992). It sits on trade routes going north-east from the coast into the hinterland. The site was excavated under the direction of Trude Dothan (Hebrew University) and Seymour Gitin (W.F. Albright Institute of Archaeological Research) beginning in 1981 through 1996. Tel Miqne-Ekron has been identified with biblical Ekron, one of the five Philistine cities that existed on the central Israeli coastal plain in the Late Bronze Age II through to the end of the Iron Age (ca. late 16^{th}-15^{th} centuries to 7^{th}/6^{th} centuries cal BC). Scanty earlier remains dating to the Chalcolithic and Early Bronze Age have been found at the site as well as fragmentary evidence for occupation in the Roman, Byzantine and Islamic periods.

Faunal assemblages from different parts of the tel have been studied by the late Brian Hesse, Justin Lev-Tov and Edward Maher (*104–107*). In almost all periods, domestic caprines formed the mainstay of the economy and were closely followed by cattle and, at the height of Philistine rule, also by pigs whose frequency drops off in the late Iron Age. Remains of domestic equids, dogs and wild animals are negligible in all periods but are often found in ritual contexts (*106*). Sheep-goat proportions change over time, with a predominance of sheep in the late Iron Age indicative of wool-production. Mortality patterns also change and are interpreted by Lev-Tov (*107*) as evidence for a shift from a local, household-oriented caprine production system focused on production for meat and secondary products, to a market-oriented system geared primarily toward secondary products in the late Iron Age.

Miqne5 4NW 24.118

29. Potterne, UK

The Late Bronze Age/Early Iron Age site of Potterne is situated in the village of Potterne in Wiltshire, UK. Excavation occurred between 1982 and 1985 led by Andrew Lawson (*108*). Dates for the site range from 3430+-110 to 2490 +-70 uncal BP; the majority of finds attributed to the Late Bronze Age and Early Iron Age. The site proved to contact a rich record of pottery, charred plants, and animal remains (134,000 specimen).

Zooarchaeological analyses have focused on Cutting 12, Zones 14-4, from which approximately 75,000 bone elements have been excavated. A small number of bones were specifically identified as goat, using metric data from metacarpals and metatarsals; 4,497 were classified as sheep/goat and 23,005 as small ungulate. Of the seventy-one horn cores recovered, just two could be attributed to goat; sheep are thought to have made up the majority of sheep/goat remains. Tibiae measurements of sheep/goat remains are comparable to other Late Bronze Age sites (Runnymeade and Barley). The sum total of the animal assemblage indicates a pastoral economy focused on cattle and sheep. Sheep/goat increase in frequency in more recent phases, likely reflecting greater reliance on sheep, ignoring differing yields.

The goat sample identified here (Potterne1) is from Phase 12 of Cutting 12. Radiocarbon dating of three charcoal remains from Phase 11 range from 2,040 cal BC to 990 cal BC (2 sigma calibration). As Potterne1 was recovered from beneath Phase 11, it should in the older end of this range, if not older; however slippage from a later Phase is possible.

Potterne1 1983.200 3120-3159 3125 Box 4110

Sample preparation and DNA extraction

Petrous bones morphologically identified as caprine were prepared in a dedicated ancient DNA facility at Trinity College Dublin, Ireland, following standard protocols (*109*). In addition, DNA from 21 samples for which mitochondrial fragments were previously reported (*33*, *34*) was extracted using an identical protocol. These samples were derived from various non-petrous bone elements, and were reduced to powder in dedicated ancient DNA facilities at Johannes Gutenberg-University Mainz, Germany as described in (*110*).

For each sample, 120mg of bone powder was subject to DNA extraction as described by (*111*) and later modified by (*112*) and (*113*). One further modification was introduced to the protocol: a total of three 24 hour proteinase K incubation digests were performed. At the end of each incubation step tubes were centrifuged at 13,000 rpm for 10 minutes. Supernatant was removed carefully to not disturb the undigested bone powder. 1ml lysis buffer was (1M Tris-HCl; 2% SDS; 0.5M EDTA; 100 µg/ml Proteinase K) was transferred into the tube containing the supernatant of the final (third) extraction, the tube vortexed, and re-incubated for 24 hours at 37℃. Controls were included for all amplifications.

Library preparation

Illumina sequencing libraries were constructed according to (*114*) with modifications (*113*). 16.25µl of purified DNA was used as the starting material. Control tubes (16.25µl H_2O x 2) were included.

For initial screening, 13 cycles of amplification were performed. 3µl library was amplified using 1µl of a unique index oligo (5 µM) and 21 µl of amplification master mix (20.5 µl AccuPrime Pfx Polymerase (Invitrogen), 0.5 µl primer IS4 (10 µM)). Blank PCR controls (3µl H_2O) were included. 12 cycles of amplification were performed for all samples and controls (95°C for 5 min; 12 x 95°C for 15 sec, 60°C for 30 sec, 68°C for 30 sec; 68°C for 5 min). Amplified product was

purified using Qiagen MinElute columns following manufacturer's instructions, eluting in 10 µl EB.

MiSeq Screening

10ng of each library was pooled and then sequenced on an Illumina MiSeq platform (Trinity Genome Sequencing Laboratory, Trinity College Dublin, Ireland), using 70bp single-end sequencing, and a PhiX control at 1X.

The quality of resulting fastq files was assessed using FastQC (*115*). Fastq files were then trimmed and filtered using cutadapt 1.1 (*116*) (cutadapt -a AGATCGGAAGAGCACACGTCTGAACTCCAGTCAC -O 1 -m 30). The trimmed reads of samples were aligned to CHIR_1.0 (*117*) using bwa (*118*) with seeding disabled (bwa aln -l 1024). Bam files were produced using Samtools 0.1.19 (*119*). Reads with a Mapping Quality <30 and duplicates were removed using Samtools. Endogenous DNA was calculated as number of unique reads aligned (following mapping quality filtering) divided by total reads following trimming step.

Damage patterns characteristic of ancient DNA (*120–122*) were assessed for all samples using mapDamage2.0 (*123*). All samples showed the short fragment length and 5' C-T / 3' G-A misincorporation, caused by cytosine deamination, typical of ancient DNA molecules (Figures S1-S2). For samples Direkli4, Direkli5 and Direkli6, no UDG-treated library was prepared due to scarcity of material. For samples previously reported by Amelie Scheu (*34*), no UDG-treated libraries were prepared as mitochondrial haplogroups assigned here were in concordance with previous work.

UDG Treatment of Ancient DNA

Treatment of ancient DNA with Uracil-DNA-glycosylase (UDG) has been demonstrated to remove misincorporation associated with ancient DNA (*124*, *125*). UDG-treated libraries were prepared identically as above, with an additional step prior to library construction: 5 µl USER (1,000U/ml; Uracil-Specific Excision Reagent, NEB) was added to 16.25 µl purified DNA and incubated for 3 hours at 37℃ prior to library construction. In the subsequent Blunt End Repair step, 5 µl less H2O was used (total reaction volume 70 µl).

Mitochondrial Capture

In general, samples with <5% endogenous DNA were selected for mitochondrial capture. An in-solution bait-and-capture approach (*126*, *127*) was taken, using custom RNA baits designed to target domesticate species (MYcroarray, 5692 Plymouth Road, Ann Arbor, MI 48105, USA). MYbaits v2.3.1 (Mycroarray) capture system was used according to the manufacturer's protocol (*128*).

Briefly, an additional five aliquots from selected libraries were PCR amplified, using unique indexes for each amplification and sample combination, according to the protocol described above. After MinElute purification and quantification, samples were pooled such that (i) each sample had an equal amount of endogenous DNA and (ii) there was a total of 2,000 ng of DNA present. This

pool was desiccated for 8 hours and then re-suspended in 8.4 µl H_2O. RNA baits and blocks were added to the pool as manufacturer's instructions, with a single modification: Block #1 was replaced with an additional 2.5 µl of pooled DNA (total 8.4 µl). Baits and DNA were incubated for 40 hours at 65°C. Captured DNA was recovered using Dynabeads® MyOne™Strepavidin C1 magnetic beads (ThermoFisher Scientific), and resuspended in 30 µl H_2O.

15 µl of the captured DNA was amplified for 14 cycles using KAPA HiFi DNA Polymerase (Kapa Biosystems), according to the Mybaits protocol. Single-end, 70 bp sequencing was performed on an Illumina MiSeq platform (Trinity Genome Sequencing Laboratory, Trinity College Dublin, Ireland).

Next-Generation Sequencing

Samples with >5% endogenous DNA were selected for sequencing on either Illumina HiSeq 2000 or 2500 platforms. Samples which were below 5% endogenous but from a poorly sampled region or archaeological context were also sequenced on a HiSeq platform. USER-treated libraries were amplified as described above using unique index oligos for a total of 6 indexes per lane of sequencing. The number of amplification cycle for each sample was chosen in order to both minimize the number of cycles, and obtain the minimum amount of DNA (15 ng) required for sequencing. Amplified product was purified and quantified as described above. The purified product was pooled such that each index was present in equimolar amounts for each lane of sequencing. Pools were then sequenced using a HiSeq 2000 or 2500 platform, single end, read length 1x100bp (Macrogen Inc., 1002, 254 Beotkkot-ro, Geumcheon-gu, Seoul, 153-781, Republic of Korea). Additionally, two modern goat from Ireland and Togo (Table S26) were sequenced to approximately 35X mean coverage on an Illumina HiSeq 4000, pair end, read length 2x150bp.

Whole genome data processing

For ancient samples, read quality was assessed using FastQC as described above. Read trimming and length filtering was performed using cutadapt 1.1 (*116*) (cutadapt -a AGATCGGAAGAGCACACGTCTGAACTCCAGTCAC -O 1 -m 30).

For samples selected for whole genome sequencing, alignment to CHIR_1.0 (*117*) was performed using bwa aln (*118*), with seeding disabled (bwa aln -l 1024) (*129*). Bam files were produced with samtools 0.1.19 (*119*), with read groups assigned to each unique PCR reaction. Clonal PCR products (PCR duplicates) were removed using samtools rmdup, following which reads with mapping quality less than 30 were removed. Reads from the same sample were merged using the MergeSamFiles option of picard (https://github.com/broadinstitute/picard), and duplicates removed again. Indel realignment was performed for samples aligned to CHIR_1.0 using GATK (*130*).

Damage patterns were assessed using mapDamage2 (*123*), and were substantially reduced compared to libraries constructed without USER-treatment (Figure S1). Mean C>T rates at the 3' end of USER-treated libraries ranged from 1.8% at base position 1, to 0.9% at base position 4. To combat the remaining damage, bam files were rescaled using mapDamage2, reducing the base qualities of sites likely to be affected by deamination. As a final precaution against damage, bam files were softclipped by 4bp at the end of each read.

Modern goat samples (Table S26) were aligned to reference genome CHIR_1.0 (*117*) using bwa mem (*131*), with mate information of paired end reads filled in using samtools fixmate (*119*). Duplicates were marked and removed using MarkDuplicates function of Picard Tools (https://broadinstitute.github.io/picard/). Indel realigned was performed using GATK (*130*). Reads with mapping quality less than 30 were then removed.

Mitochondrial alignment and sequence generation

All samples, those selected for whole genome sequencing and those subject to targeted capture, were aligned to a circularized version of the revised mitochondrial reference NC_005044.2 (*132*) using bwa aln. Bwa aln seeding was disabled (-l 1024). The sequence was circularized by concatenating 15bp from either end to the opposite end of the mitogenome, repeating such that each end has been extended.

Consensus fasta sequences were generated using ANGSD (*133*) (angsd -doFasta 2 -doCounts 1 -setMinDepth 3 -minQ 20 -minMapQ 30). Sequences were then decircularized by removing 15bp from each end. Samples were assigned to haplogroups according to position within an initial phylogeny (described in the succeeding section), and then realigned to a circularized representative sequence (Table S7) from the appropriate haplogroup, using the pipeline described above, to generate final mitochondrial sequences for each sample.

For the mitochondrial modelling dataset, an additional filtering step was performed. The number of singleton mutations present in each sequence (relative to all modern and ancient sequences) was determined, and sequences with greater than 15 singletons excluded from the analysis. In addition, sequences with greater than 25% missing data were excluded. The D-loop (positions 15431-16643) was removed from all samples prior to mitochondrial modelling.

Mitochondrial ML Phylogeny

The mitochondrial sequences generated, a dataset of previously-published goat whole mitochondria (*134*), reference sequences and Nubian Ibex outgroup (Table S7), were aligned in a multiple sequence alignment using MUSCLE (*135*). The alignment was visualized using Seaview (*136*).

Modelgenerator v0.85 (*137*) was used to determine the most appropriate substitution model for the multiple sequence alignment. A Maximum Likelihood tree was generated using PhyML 3.1 (*136*) with 100 bootstrap replicates, using model parameters estimated using modelgenerator. The resulting phylogeny was visualized using Figtree v1.4.2 (*138*).

The overall structure of ML tree (Figure S3) is similar to that reported in (*134*). Ancient domestic sequences group with modern domestics, with modern bezoar as outgroup, with some exceptions. Sequences from Neolithic Levant (‘Ain Ghazal and Abu Ghosh), along with mitochondria from pre-domestic contexts in the Taurus Mountains (Direkli Cave) and Armenia (Hovk-1 Cave), form a clade with a bezoar *F* haplogroup sequence. The *F* haplogroup has been reported in a very small number of domestic goat (*10*, *139*), and is mostly found in bezoar (*140*).

Within the *G* haplogroup, an individual (Lur12) from Tepe Abdul Hosein, a Pre-Pottery Neolithic site in the Zagros mountains, forms a clade with the bezoar reference sequence. Of the five remaining ancient *G* haplogroup sequences, four form a clade that is an outgroup to *G* sequences, both wild and domestic. Three of the four are from Neolithic sites in eastern Iran (Tappeh Sang-e Chakhmaq, Semnan) and Turkmenistan (Monjukli Depe). However, the fourth is from a Bronze Age context in Western Anatolia (Kanligecit, Kirklareli Province of Turkey). This sample falls outside the habitat of bezoar and has been directly radiocarbon-dated to the mid 3rd millenium BC (Table S3).

In haplogroup *D*, two ancient sequences are outgroups to the modern bezoar and domestic sequences: one mitochondrion from Neolithic Iran (Tappeh Sang-e Chakhmaq - Semnan), and another from Chalcolithic Israel (Shiqmim). An additional sample from Shiqmim is an outgroup to previously published domestic *D* sequences.

Additionally, three sequences from the Epipaleolithic site of Direkli Cave form a sister group to the West Caucasian Tur (*Capra caucasica*) mitochondrion. This caprid species, along with its subspecies the East Caucasian Tur (*Capra caucasica cylindricornis*), is found today only in the Caucasus Mountains (*141*). Two of the three ancient samples from Direkli Cave with this "Tur-like" mitochondria are radiocarbon dated to a securely pre-domestic time period (Table S3); they have not been introduced from a later or modern context. For the purposes of this paper, we denote the "Tur-like" clade as haplogroup *T*.

The multiple sequence alignment and tree building step was repeated with a dataset using the ancient mitochondrion generated here, a single bezoar sequence for each haplogroup (when available), and nubian ibex as an outgroup (Figure 1a, Figure S4). We obtain the same overall structure to the tree without modern sequences.

Mitochondrial Bayesian analysis

A BEAST analysis was performed using BEAST 2.4.2 (*142*, *143*). To estimate the goat mitochondrial mutation rate and split times for mitochondrial lineages, a multiple sequence alignment of modern goat/bezoar and radiocarbon dated ancient sequences which fell within domestic goat lineages was prepared using MUSCLE (*135*) (Tables S3 and S7). Partitions were defined using the NCBI annotation for NC_005044.2: tRNA, rRNA, the first and second codon positions (C1+2), third codon positions (C3), D-loop, and the remainder of the molecule.

The appropriateness of these partitions was tested using PartitionFinder (*144*), testing all models, linking branch lengths, performing model selection using BIC and using a greedy search algorithm. The best models determined were HKY+I for C1+2, TRN for C3, HKY+I+G for the D-loop, and TRN+I for a combined partition of tRNA genes, rRNA genes, and the remainder of the mitogenome.

For the BEAST analysis, site and clock models for each partition were unlinked, with the the tree linked across partitions. To replicate the TRN model in BEAST, TN93 with estimated base frequencies was used instead. For HKY, base frequencies were also set to estimated. Clocks for

each partition were set to strict. Priors for sample age were set as Normal distributions, mean equal to the midpoint of the radiocarbon 95% CI, sigma equal to one quarter of the length of the 95% CI. Clock priors were set to Log Normal, M=-18.42068, S=1.5. Kappa priors were set to Log Normal, and gamma shape priors set to exponential. A Coalescent Bayesian Skyline model was used as the tree model.

Four independent runs of 100 million chains were performed, with 10% burn-in, and assessed using Tracer (*145*). As each run converged with with all ESS >3000, independent runs were merged. Final posterior estimates are shown in Table S8. A final Maximum Clade Credibility tree was constructed with median heights, using TreeAnnotator (*142*) (Figure S5).

To estimate a mutation rate for the mitogenome with the D-loop for the purpose of modelling, the above was repeated using the same settings except for the clock models, which were linked across the non D-loop partitions (Table S8).

To estimate the divergence time of the "Tur-like" mitochondria, BEAST was repeated using the same dataset plus the "Tur-like" mitochondria from Direkli Cave, the West Caucasus Tur (*Capra caucasica*) reference sequence, and the Markhor reference sequence; a previous study (*146*) had placed the Tur mitochondrion as an outgroup to Markhor (*Capra falconeri*), bezoar and domestic goat. PartitionFinder selected the same models and partitions as the previous analysis. The BEAST analysis was set up as described above, and ESS of the final combined log file was satisfactory (all ESS >3000), and the Maximum Clade Credibility tree shown in Figure S6.

Mutation rates estimated here were calculated using different mitogenome partitions than (*134*), but our non D-loop rate 95% HPD overlaps with the rate reported there for the entire molecule (3.95×10^{-8} substitutions per nucleotide per year). Coding partition rate HPDs estimated here overlap with those reported for wisent using ancient DNA (*147*). Partition mutation rates determined using the addition of Tur, "Tur-like", and Markhor sequences overlapped did not substantially change compared to when calculated without.

The Maximum Clade Credibility tree, without Tur/Markhor (Figure S5) and with Tur/Markhor (Figure S6) are in broad agreement with the Maximum Likelihood phylogeny produced using all sequences (Figure 1a, Figure S3), with the same sequence of branching events. The ages of splitting events of the goat/bezoar mitochondrial phylogeny estimated here (Table S9) are more recent than those ML estimates using the synonymous substitution rate in (*134*). The TMRCA (Time to Most Recent Common Ancestor) 95% HPD of domestic sequences within each haplogroups all overlap with or are very close to the approximate time of domestication (10,000 years Before Present), and themselves overlap. As such, determining whether the radiation time of different haplogroups can be associated with their appearance in the domestic gene pool (i.e. domestication time) is difficult using sequence data alone.

As reported in (*146*), the Tur reference sequences, along with the "Tur-like" Direkli Cave sequences, are outgroups to bezoar/domestic goat and markhor. We estimate the time of the Tur/"Tur-like" mitochondrial split from other caprids to be 315,976 BP (95% HPD: 268,736-368,761 BP) and the "Tur-like" split from the West Caucasus Tur to be 167,548 BP (95% HPD: 137,231-201,478 BP) (Table S9). Though this "Tur-like" whole mitochondrial clade has not

been previously reported, there is a sparsity of whole mitochondrial sequences from bezoar and other wild caprids that limits what can be inferred. Additionally, whole genome sequences from these wild caprids are required to further investigate how *Capra* distributions may have changed through time, to avoid inference based solely on single locus data.

AMOVA

Partitioning of genetic diversity was calculated using Arlequin v3.5 (*148*). Populations and Groups were defined as in Table S12. Maximum missing data per site was set at 0.05. Significance of variance components and Fixation Indices were computed using 1000 permutations. Partitioning of variance are shown in Table S13.

Variant Calling

All modern goat samples, and ancient samples with average coverage >8X, were included in a "high confidence" variant call set. Samtools mpileup (*119*) was used to call variants (-C 50 -q 30 -Q 20 -s -O -u -t SP,AD,INFO/AD,ADF,ADR,DP,INFO/DPR) and bcftools (*119*) to generate vcf files (-v -mO z -f GQ,GP). Protein coding regions and repeat regions as defined by the Genbank annotation and RepeatMasker files (*149*) were not called. An additional 50kb was added to both sides of protein coding regions and not called. Indels and any variants within 3bp of them were removed using bcftools filter (*119*). Tri- and quad-allelic sites were removed. For each variants, individuals were marked as missing ("./.") if coverage at that site was below 2 or twice the mean coverage, or if SP (strand bias) was above 13. Heterozygous variants present in a single individual or more than 75% of individuals were removed. Variant positions with missing data in any individual were then removed, resulting in a dataset of 3,003,233 sites. Finally, LD pruning was performed using PLINK v1.07 (*150*) with the settings --indep-pairwise 50 5 0.2. The final number of SNPs in this call set was 726,401.

For all other ancient samples, the "high confidence" sites defined above were called. The same initial sites were called using samtools mpileup (*119*) with the same options, except without recalibration ("samtools mpileup -B") and without filtering for variant sites with bcftools (*119*). After indels and sites within 3bp of indels were removed, the 726,401 variant positions of the "high confidence" set were extracted. Tri- and quad- allelic sites were removed. For samples with >2X mean coverage, sites were set to missing as above (<2 reads, > twice mean coverage, >13 SP). For samples with less than 2X, no minimum coverage filter was imposed, and a maximum of 4 read coverage per site was permitted. Individuals were then pseudo-diploidized by randomly sampling a read at each site and setting that individual as homozygous for that allele. This call set was then merged with the "High Coverage Ancients and Moderns" set, to create a "Low Coverage Ancients and High Coverage" dataset.

For autosomal modelling, a call set using ancient individuals only was generated. Samples from Anatolia, the Balkans, Iran, and Georgia with coverage >2.5X were included. The same calling pipeline was used except that the samtools mpileup recalibration option was disabled (-B). Moreover, sites were also filtered for linkage disequilibrium and only variants at least 100kb apart were retained. The final call set was composed of 9,385 variants, which were pseudo-diploidized by random read sampling.

Molecular Sex Identification

Due to the absence of a complete Y chromosome in CHIR_1.0, molecular sex was determined using the relationship between the number of reads aligned to each chromosome versus the length of that chromosome (*151*). The ratio of reads aligned to the X chromosome and the length of that chromosome were then used to estimate the sex of each sample. The ratio for the X chromosome was then added to the plot, and examined to determine the molecular sex of the individual (Table S1).

Removal of individuals due to relatedness

Due to the complexity of zooarchaeology assemblages, samples were screened for relatedness or if they were the same individual. Samples which were from petrous bones of opposite orientations (left and right), and had the same mitochondrial sequence, and molecular sex were identified. All individuals were then assessed using lcMLkin (*152*) (Table S5). Four pairs of individuals had a pi-HAT >0.9 and met the other criteria: Direkli1 and Direkli2, Azer3 and Azer5, Semnan1 and Semnan2. These individuals were combined and considered a single individual. A fourth pair of samples, Bulak1 and Bulak3, met these criteria but were from petrous bones of the same orientation. One of these samples (Bulak3) was removed from subsequent analyses.

A final pair of samples were identified as having met the criteria above (Fars2 and Fars5), but due to low endogenous DNA did not have sufficient coverage to estimate pi-HAT. These samples were also combined into a single individual, Fars2-5.

Autosomal Mutation Rate Estimation

To estimate the goat autosomal mutation rate, we followed the "F(A|B)" method described in (*153*), (*154*). Briefly, heterozygous positions in modern individual "B" are identified, and the proportion of times the derived allele is randomly sampled in an ancient individual "A" at those positions is recorded, F(A|B). We selected the Neolithic Serbian Blagotin3 as the ancient individual "A" and the modern Old Irish Goat (IOG) as individual "B".

To control for genetic drift in the lineage specific to "B", a calibration curve was constructed using PSMC (*155*) to estimate past population demography. Sites in IOG were not considered if coverage was less than one third the mean coverage or more than twice the mean coverage. PSMC was performed on IOG using the following settings: -N25 -t15 -r5 -p '4+50*1+4+6'. msHOT-lite (*156*, *157*) was used to simulate 800mb of sequence data under the estimated demography, while varying the mutation rate and divergence time of A and B (measured in generations). The F(A|B) ratio for each simulation and blagotin3 was then estimated using POPSTATS (https://github.com/pontussk/popstats), and calibration curves were constructed using the ggplot2 function geom_smooth (*158*) (Figure S15). As the curve of $1.3x10^{-8}$ per site per generation ($5.2x10^{-9}$ per site per year using a generation time of 2.5 years) overlapped with the observed F(A|B) ratio at the radiocarbon age of Blagotin3 (Table S3), we used this as our mutation rate estimate. We note that this value is higher than the canine mutation rate estimated in (*154*). There are several possible explanations for this. The call set used here to estimate F(A|B) is non-coding

only, rather than coding and non-coding (*159*). The Freedman call set also removed CpG sites, which were not removed in our pipeline. As USER treatment does not reduce damage at methylated CpG sites (*160*), this, along with the inflated mutation rate at CpG sites (*161*, *162*), may partially explain the increased global mutation rate observed here.

LASER Principal Component Analysis (PCA)

To maximize the use of data generated from very low coverage samples (<0.01X), projection using Procrustes analysis was performed using LASER (*163*). PCA reference space and projection transformation were constructed using the High Coverage Ancients and Moderns dataset. All other samples were then projected onto the PCA space, and then filtered for individuals covered by less than 500 loci. To reduce the effect of simulation stochasticity, ten repetitions were performed, and the mean value of sample coordinates used in plotting. Other settings were left at default.

The plot of PC1 vs PC2 (Fig S7) shows that PC1 differentiates modern and ancient wild bezoar from modern and ancient domestics. Bezoar from Azerbaijan and Iranian Azerbaijan falling on the most extreme end of PC1. As these represent 10 of the 61 genomes used to compute the reference PCs, sampling bias may explain their plot location. Domesticates shows some small variation on PC1, with modern African and European samples falling somewhat apart from other samples. PC2 differentiates domestic east (Asian) and west (European) samples; bezoar from Hamedan, west Iran fall on one extreme of PC2, with modern Europeans falling on the other extreme. Within the domestic group, Neolithic West (western Anatolia and south east Europe) group apart from Neolithic East (Iran and Turkmenistan). A Bronze Age sample from Potterne, Britain, groups closely with a modern Irish Old Goat, and Neolithic samples from Blagotin, Serbia. Within the eastern group, a shift is observed following the Neolithic, with post-Neolithic ancients falling between modern sample from Iran. The reference individual from China, CHIR_1.0, clusters with this eastern group. Samples from Bronze Age Anatolia (Acemhöyük) and post-Neolithic Levant are found between Neolithic West/Levant and post-Neolithic/modern eastern samples. Modern samples from Morocco and Togo group between this post-Neolithic Levant/Bronze Age Anatolia cluster and the Neolithic West/Levant cluster. Other bezoar show some variation along this axis.

As certain bezoar populations appeared to dominate the Principal Components, LASER was repeated with modern bezoar removed, and PC1s and 2 plotted (Figure S8). A closer examination of domesticate structure is obtained when modern bezoar are removed from the analysis:

- Eastern and western Neolithics group at opposite ends of PC1.
- PC2 differentiates within East and West, and also African samples from East and West.
- Neolithic Levant falls between Neolithic West and modern Africans.
- Bronze Age Anatolia samples cluster beside the Post-Neolithic and modern East, with two Neolithic samples from western Anatolia (AP45 and AP49) being the closest Western samples.
- Post-Neolithic Levant samples fall between Eastern and African samples, close to Bronze Age Anatolia, showing a “Eastern” shift relative to Neolithic samples.
- Eastern Neolithic individuals fall away from post-Neolithic eastern, closer to Bronze Age Anatolian and western samples.

Ancient diploid Neolithic genomes used in the reference space calculation (Blagotin3, Semnan3, and Direkli1-2) occupy the extreme positions in the PCA. Neolithic samples from western Iran (Lur12 and Fars2-5) show greater affinity to post-Neolithic samples than those from Neolithic eastern Iran and Turkmenistan, but do not appear be admixed with a western source (Table S31).

As several low coverage samples were removed due to having an insufficient number of loci covered, we repeated the LASER process using the High Coverage Ancients and Moderns prior to LD pruning, using a minimum of 1,000 SNPs, using broad level grouping (Figure 2) and more granular groupings and individual labels (Figure S9; see Table S2 for ancient groupings). For samples with greater than one million SNPs covered, by default LASER randomly downsamples to one million SNPs, somewhat accounting for LD. The plot of PC1 vs PC2 for the modern-bezoar-removed pruned dataset was inspected (Figures S8) and were in close agreement. In particular, this recovered several additional samples from post-Neolithic Levant, which fell in the same region as the previous PCAs (between modern Africa, Neolithic Levant, Bronze Age Anatolia and eastern samples).

Population analyses using ANGSD

Due to the high proportion of low coverage (<8X mean coverage) genomes in our dataset, we used a genotype likelihood framework in ANGSD (*133*) to avoid explicit genotype calls. For all analyses using ANGSD, the following settings were used:
-minQ 20 -minMapQ 30 -skipTriallelic 1. This results in ANGSD ignoring bases with read quality less than 20, reads with mapping quality less than 30, and triallelic sites. Analyses were restricted to the autosomes. Yak was used to define the ancestral allele. For ANGSD analyses involving modern populations, these were subsampled randomly to ten individuals (see Table S26).

To generate the ancestral sequences, reads used to generate BosGru_v2.0 (available at https://www.ncbi.nlm.nih.gov/assembly/GCF_000298355.1) were aligned to CHIR_1.0 (*117*) as per for modern pair-end alignment pipeline. Consensus sequences were generated using the ANGSD (*133*) doFasta option, using the following options: -minQ 20 -minMapQ 30 -setMinDepth 6 -setMaxDepth 40. Yak was selected as the outgroup due to the possibility of hybridization and ancestral admixture between sheep and goat (*164*, *165*).

Identity By State (IBS)

As an alternative approach to visually assessing how ancient and modern domestic goat and bezoar relate to one another, we constructed an Identity-By-State matrix using ANGSD (*133*), using modern and ancient samples with >0.01X mean coverage. The maximum missing individuals per site was set as half the number of individuals in the analysis rounded up. The following settings were used in IBS calculation: -minFreq 0.05 -GL 1.

An unrooted neighbor-joining tree was constructed using the R package ape (*166*) (Figure S10). The tree were aesthetically modified using Figtree (*138*), branches coloured based on location and time period, and rooted on Yak.

The topology of this tree is described below:

- Bezoar, modern or ancients, are outgroups to domestic goat. Hovk1, an Armenian wild goat at least 47,000 years old (Table S3), is not an outgroup to all bezoar, suggesting structure within bezoar to be at least pre-Last Glacial Maximum.
- The major split within domestic goat is between Eastern (Iran, Turkmenistan, Uzbekistan, and Chinese) and Western/Levant/Africa (Europe, Anatolia, Israel, Jordan, Morocco, Togo). Modern Iranians are placed as an outgroup to all other domestics; however other analyses (PCA, Treemix) do not support this placement.
- Neolithic Iranian samples branch together, with the exception of Fars2-5 which groups with Chalcolithic and Bronze Age Iranian goat.

Though IBS analyses have limitations, the primary divisions and genetic affinities summarized by the IBS are supported by subsequent analyses.

D statistic (ABBA/BABA test)

To investigate population relatedness and to test for admixture between populations, the *D* statistic (*153*) was calculated at a group level (*167*) to better exploit low coverage data. Samples were grouped based on Table S2 for ancient individuals and Table S26 for modern. Transitions were ignored in the analysis, to reduce the effect of residual DNA damage on calculations. Results of tests performed are presented in Table S31. A Z score of 3 is taken to be significant. Positive *D*/Z scores indicates greater derived allele sharing with H2 and H3 than H1 and H3, using the test *D*(H1, H2, H3, Yak), while negative scores indicate the opposite.

To address admixture between eastern and western populations, we calculated *D*(H1, H2, H3, Yak), where H1 and H2 are either Neolithic West or Neolithic East, and Test is a Post-Neolithic population. We obtain a non-significant result (Z=1.3) for the test *D*(Neolithic East, Chalcolithic Iran, Neolithic West, Yak), and similarly for Chalcolithic Turkmenistan (Z=2.3). Significant results are obtained for Bronze Age Iran (Z=14.8), Bronze Age Uzbekistan (Z=10.4), Medieval Iran (Z=19.6) and modern Iran (Z=4.4). Goat from the Caucasus/North Iran region (Soha Chai, Azerbaijan) appear admixed as early as the Chalcolithic (Z=13.7), and remain so up until Iron Age and Medieval times (Z=28.9). Bronze Age Anatolia appear admixed with a Neolithic East-related population, based on the test *D*(Neolithic West, Bronze Age Anatolia, Neolithic East, Yak) (Z=26.4).

PCA analysis (Figure 1) suggest that goat from Levant undergo a change in genetic makeup following the Neolithic, showing greater affinity to Eastern populations. We test this in the form of *D*(Neolithic Levant, Test, Neolithic East, Yak). Chalcolithic Iran does not have a significant excess of Neolithic East derived alleles relative to Neolithic Levant (Z=0.3), but with a total of only ~650 ABBA/BABA sites we have little power using this combination of samples. The test *D*(Neolithic Levant, Bronze Age Levant, Neolithic East, Yak) gives a positive score (Z=31.6), indicating an increase in Iranian/Iranian-like ancestry in Levantine goat by the Bronze Age.

We also investigated if ancient wild goat from Anatolia contributed ancestry to any Neolithic population. The test *D*(Neolithic East, H2, Anatolian Ancient Wild, Yak) gives a significant positive result when H2 is either Neolithic West (Z=49.1) or Neolithic Levant (Z=4.1), indicating greater allele sharing between Anatolian Ancient Wilds with these two populations, compared to

eastern Neolithic genomes. This suggests differential input from wild bezoar populations into the ancestors of goat from different region; in this case from wild Anatolian goat into the ancestors of Neolithic goat in western Anatolia and South East Europe.

TreeMix

TreeMix (*168*) was used to construct a model of population splits and admixture events, based on the High Coverage Ancients and Moderns dataset, with CHIR_1.0 removed due it it being the reference individual. Samples were grouped based on Table S2 for ancient individuals and Table S26 for modern. Migration events were varied from 0 to 5. The following settings were used: -root Yak -k1000 --noss. Bootstrapping was performed using blocks of 1000 contiguous SNPs and repeated for 500 iterations, and a consensus tree generated using PHYLIP version 3.697 (*169*). The resulting consensus tree model and migration events are shown in Figure S12. Confidence of nodes is given as the proportion of bootstrap iterations supporting that grouping, when that proportion was not one.

Under a model of no migration edges, bezoar are modelled as an outgroup to all domestic goat. Within domestics, Neolithic East first branches out, followed by Bronze Age Anatolia and modern Iranian domestics as a clade. African goat form a sister clade to European modern and ancients. A model of a single migration edge is results in an admixture event from Ancient Anatolian Wilds to the common node of modern and ancient European goat, in line with *D* statistics. A second migration edge is modelled as an admixture event from Neolithic East into modern Iranian Domestics, suggesting that the bifurcating tree model is not sufficient to explain how the two populations relate to each other. When three migration events are modelled, an additional migration edge from Ancient Anatolian Wild to Neolithic West suggests that different modern and ancient goat populations have differing degrees of Ancient Anatolian Wild ancestry. The larger amount of shared ancestry observed in the Neolithic West population than the modern European goat population implies that the Neolithic West population (represented here by a single genome Blagotin3) alone is insufficient to explain modern European ancestry. Migration edges five and six are modelled as admixture within Africa, from Togolese goat to Moroccans, and between wild goat populations, from a population related to Hamedan bezoar to Qazvin bezoar, suggesting that genetic exchange between domestic populations, and between wild populations, has occurred in addition to wild-domestic admixture.

Model-based ancestry estimation using Genotype Likelihoods (NGSadmix)

NGSadmix (*170*) was used to estimate ancestry proportions using genotype likelihoods. NGSadmix is more accurate in estimation ancestral components from datasets containing both low coverage and variable coverage individuals. The analysis was repeated using two sets of samples:

a) all ancient samples with mean coverage ≥ 0.01X and modern genomes.
b) all ancient samples with mean coverage ≥ 0.01X.

The following settings were used for the analysis: -GL 1 -doGlf 2 -doMaf 1 -SNP_pval 1e-6, with -minInd set to half the number of individuals in the analysis, rounded up. A further filter of -minMaf 0.05 was used in the ancestral component estimation. K was set to 2 for all runs. Ancestry

estimation was repeated a total of fifty times, and the iteration with the highest best likelihood retained.

Estimation of ancestry proportions using dataset a) (Figure S19a) resulted in Iranian bezoar being modelled as a blue ancestral component, and modern domesticates modelled as a second red component. Some modern individuals (e.g. modern Europeans) are modelled as having a small proportion of "bezoar" ancestry. Ancient bezoar are modelled as being >50% of the red "bezoar" component. The remaining domestic goat are modelled as predominantly the red "domestic" component, with varying low levels of the "bezoar" which declines slightly through time.

Using dataset b), pre-domestic bezoar (excluding Hovk1), Neolithic goat from Serbia, western Anatolia and the Levant, and a goat from Bronze Age Britain are modelled as entirely a red component (Figure S19b). Hovk1, an Armenian sample at least 47,000 thousand years old, is described by predominantly the red "western" component, with some "eastern" component, and supports other analyses suggesting a greater affinity of this representative of a pre-Last Glacial Maximum population with Anatolian wild goat just prior to the Holocene. Eastern Neolithic samples and the majority of those from post-Neolithic contexts are modelled as a single blue component. A subset of post-Neolithic eastern samples are modelled as a mixture of both the blue "eastern" and red "western" components, including samples from the Caucasus region (Georgia, Iranian Azerbaijan), Bronze Age Tepe Chizar (Qazvin Province, Iran). In line with *D* statistics, the Chalcolithic samples from Iran and Turkmenistan do not appear admixed with the red "western" component. In contrast, Bronze Age goat from Tilla Bulak, Uzbekistan, also do not show admixture, in conflict with *D* statistic results (Table S31). Samples from 'Ain Ghazal (Neolithic Jordan) are modelled as entirely the red "western" component, while Chalcolithic and Bronze Age samples from several sites in Israel are modelled as a mixture of both, but primarily of the blue "eastern" component.

Outgroup f_3

To investigate shared drift between Neolithic populations and other domestic populations, outgroup f_3 statistics were calculated using ADMIXTOOLS (*171*, *172*). f_3 values were determined using the "Low Coverage Ancient and High Coverage" dataset, using individuals with greater than 0.01X mean coverage (Table S4) combined into populations, in the form of f_3(X, Neolithic; Qazvin Bezoar), where X is a population as defined in Table S2 for ancient individuals and Table S26 for modern. Qazvin Bezoar was selected as an outgroup due equal affinity between Neolithic East and Neolithic West, measured by the *D* statistic Qazvin Bezoar(Neolithic East, Neolithic West), Z=-0.8 (Table S31). Shared drift (Table S27) of each population was plotted on a map (modified from (*173*)) of the Near East (Figure S17).

Patterns of shared drift with Neolithic populations supported previous IBS (Figure S10) and PCA (Figure 2, S8, S9) analyses, which show a strong divide between eastern and western Neolithic populations, and a relationship between western and Levantine Neolithic goat. Shared drift with Neolithic West is highest with Bronze Age and modern European goat, and also high with Neolithic Levant and Modern Africa. Shared drift between Levantine goat and Neolithic West decreases with time, while drift with Iranian populations increases closer to the present day. Neolithic Levant shows similar patterns shared drift, with a greater amount shared with Modern

Africa. Neolithic Iran shows high levels of genetic affinity with post-Neolithic Iranian, Caucasus, and Central Asian populations. A change in shared drift with Neolithic Iran is observed in the Levant; low genetic affinity with Neolithic Levant is followed by greater affinity in Chalcolithic and Bronze Age Levantine goat, consistent with *D* statistics and NGSadmix results (Figure S19).

PCA, IBS and NGSadmix analyses suggest that Neolithic Levant and Neolithic West share some degree of common ancestry not shared with Neolithic East. The observed affinity of Neolithic Levant to modern African samples may therefore be confounded by Neolithic West-like ancestry in modern Africa. To investigate if the shared drift of Neolithic Levant and Modern Africa is independent to the drift shared between Neolithic West and Modern Africa, f_3 for all pairwise combinations of Neolithic population were then plotted with a linear regression and associated confidence interval using the ggplot (*158*) function geom_smooth (Figure S16). Three populations show an excess of Neolithic Levant shared drift relative to their drift with Neolithic West: Chalcolithic Israel, Modern Togo, and Modern Morocco, suggesting ancestry shared with Neolithic Levant, but not Neolithic West, is present in these populations.

In addition to Neolithic populations, shared drift between two modern genomes published here (IOG and Tog) was estimated (Table S27), representing feral Old Irish Goat and Togolese village goat respectively. Modern Togo shows highest shared drift with Modern Morocco, in line with their geographic proximity in Western Africa. Ancient Levantine and modern European populations show the next highest degree of shared drift with Modern Togo, suggesting that modern goat from western Africa share ancestry with a population related to European goat, Levantine goat, or a mixture of both. Lowest shared drift is observed with eastern populations (Iran, Turkmenistan, China). Interestingly, the highest shared drift between Modern Ireland is Bronze Age Britain (f_3=0.151, SE=0.002) rather than Modern France (f_3=0.139, SE=0.002). Though inference is limited by available modern European genomes, this suggests a degree of genetic continuity between ancient (Bronze Age) and modern British and Irish goat populations, supporting modern and historic mitochondrial evidence of an "insular" goat population across the isles (*174*). High drift is also observed with Neolithic West, Neolithic Levant and modern African populations, while low shared drift is observed with eastern populations.

f_4 ratio estimation

To estimate the contribution of Ancient Anatolian Wild bezoar to the genomes of Neolithic Levant and Neolithic West, f_4 ratios in the form (Yak, Direkli5+Dirkeli6; Neolithic X, Neolithic Iran)/(Yak, Direkli5+Dirkeli6; Direkli1-2, Neolithic Iran) were constructed using ADMIXTOOLS (*171*, *172*), where X is Neolithic Levant or Neolithic West. Ancient Anatolian Wild were divided into two haploid genomes (Direkli5 and Direkli6) and one diploid genome (Direkli1-2) in order to satisfy the requirements of the ratio. Results are displayed in Table S21. Both Neolithic West and Neolithic Levant show approximately 50% of their ancestry as deriving from the Ancient Anatolian Wild population, with Neolithic Levant showing a higher proportion (0.56) but a greater standard error (0.07).

Admixture Graph construction

To build a model of the population history of domestic goats, admixture graphs were fitted using *qpGraph* included in the ADMIXTOOLS package (*171*, *172*) which uses *f*-statistics based on allele frequency correlations between samples to assess whether a fitted admixture graph of population history is consistent with the data. We focused on fitting Neolithic populations, pre-domestic wild goat, and modern domesticates from the Europe, Africa and East Asia/China. Population groupings were as defined in Tables S2 and S26. As a base, we used the groups Ancient Anatolian Wilds, Neolithic West and Neolithic East, due to the quantity and quality of the samples in these groups. Yak was used as an outgroup. *qpGraph* was run using default settings with a Z score=3 as a cutoff for outlier *f*-statistics. The number of SNPs used in each graph is presented in Table S20.

Based on Treemix (Figure S12) and IBS (Figure S10) results, Ancient Anatolian Wild was placed as the outgroup to Neolithic East and Neolithic West (Figure S11a), but this model was rejected with 17 f_4 outliers with $|Z| \geq 3$. As Treemix and *D* statistics (Table S31) suggest that ancestors of Neolithic West to have admixed with Anatolian bezoar, we modelled Neolithic West as being a mixture of a population related to Ancient Anatolian Wilds and a population leading to Neolithic Eastern goat (Figure S11b). This model fits the data with no f_4 outliers.

We then added the Neolithic Levant population, comprising of three individuals of low coverage (average ~0.03X). Based on IBS results (Figure S10), we excluded Neolithic Levant as being an outgroup to all other populations modelled. We found that modelling Neolithic Levant as an outgroup to domestics (Neolithic East and West) was rejected with 42 f_4 outliers (Figure S11c). Based on f_3 outgroup (Figure S17) and ancestry estimation (Figure S19), Neolithic Levant and Neolithic West show relatively high affinity. We investigated topologies consistent with this and found that a graph in which Neolithic Levant and Neolithic West were composed of separate mixtures between an Anatolian-like population and a population sister to Neolithic East fits the data (Figure S11d). This topology was supported by IBS tree building (Figure S10), and the affinity of Neolithic Levant and Neolithic West in principal component analysis (Figure 2, Figures S7-9).

We then introduced a single genome, Hovk1, at least 47,000 years old (Table S3) and representing Ancient Armenian Wilds, to the graph. When placed as the root of sampled wild and domestic goat, the graph is rejected with 57 f_4 outliers. Modelling ancient Armenians as the sister clade of Ancient Anatolian Wild and related populations results in a graph that with no f_4 outliers, which we present in a Figure S14e and in a visually-modified form in Figure 3b. This graph topology is in line with PCA analyses (Figure 2, Figure S7-9) and IBS (Figure S10) which suggest an affinity of Ancient Armenian Wild and Ancient Anatolian Wild.

To investigate how these Neolithic populations contributed to modern goat populations, we sequentially added three modern populations (East Asian/China, Europe, and Africa) to the graph. We first removed Ancient Armenian Wild due to it being represented by a single pseudo-diploid sample, starting instead with the model depicted in Figure S11d. Modern East Asia required admixture between a population ancestral to Neolithic East, and Neolithic Levant, based on f_4 outliers such as:

(Neolithic West, Neolithic Levant; Neolithic East, Modern East Asia), Z=4.1

(Neolithic East, Modern East Asia; Ancient Anatolian, Neolithic Levant), Z=3

This affinity between Modern East Asia and Neolithic Levant was estimated as a contribution of ~2% from Neolithic Levant to the ancestor of Chinese goat. Additionally, fitting Modern East Asia required Neolithic East to be modelled as containing an additional source of wild ancestry. We note that the *D* statistic Neolithic Levant(Modern East Asia, Neolithic East) is not significant (Z=2.2), and that Neolithic Levant is represented by a small number of low coverage samples. Therefore, we cannot exclude that there might be additional unsampled populations which better represent ancestral populations which contributed to the genomes of modern Chinese goat, or that samples with greater sequencing depth would fit a different model of Chinese goat ancestry.

Modelling Modern Europe as descending from the same ancestral population to Neolithic West resulted in three f_4 outliers which did not clearly indicate a single unmodelled event. We hypothesised that the ancestors of modern European domestic goat may have undergone admixture with a European wild caprid population, and introduced an outgroup population to the model which mixed with the ancestors of modern Europe. The resulting model fit the data with no f_4 outliers. This admixture event is supported by the *D* statistic Neolithic East (Neolithic West, Modern Europe), Z=16.4 (Table S31), which can be interpreted as an increase of ancestral alleles in Modern Europe. Alternatively there may be unsampled structure in ancient European goat, despite the high affinity of Neolithic West with modern Europe (Table S27, Figure S17).

We then added Modern African to the model, which did not fit in a clade with either Neolithic Levant or Neolithic West despite IBS (Figure S10), Treemix (Figure S12), and outgroup f_3 values (Table S27, Figure S17) suggesting an affinity of Modern Africa with these populations. Modelling modern Africans as a threeway mixture between modern Europeans, Neolithic Levant, and a population basal to Neolithic West and Modern Europeans resulted in a model with two f_4 outliers. The larger of these outliers, (Neolithic West, Neolithic East; Neolithic Levant, Modern Africa), Z=3.4 suggested unmodelled shared drift between Neolithic West and Neolithic Levant or Neolithic East and Modern Africa. We then modelled an additional mixture event from a population ancestral to Neolithic East, to the ancestors of modern African goat, resulting in no f_4 outliers (Figure S11). We note that f_3 outgroup values (Table S27) suggests a greater affinity of Neolithic East with Modern Africa than with Modern Europe, as does the *D* statistic Neolithic Iran(Modern Africa, Modern Europe), Z=11.3 (Table S31).

Finally we attempted to fit the ancient Armenian sample Hovk1 into the graph with these modern populations fitted. Modelling Hovk1 as an a sister branch to Ancient Anatolian Wild was rejected with eight f_4 outliers, despite fitting in the case of Fig S14e. Several of these outlier statistics suggested unmodelled affinity between Hovk1 and Modern Africa, for example (Neolithic East, Ancient Armenian Wild; Modern Europe, Modern Africa), Z=4.1. Adding an additional admixture event from Hovk1 to the ancestors of Modern Africa resulted in three outlier Z values, all within the range of 3-3.2, and suggested a minor (2%) contribution to Modern Africa (Figure S11g). Additional admixture events or alterations to graph increased the number of *f*-statistic outliers. Given that Ancient Armenian Wild was represented by a single pseudo-diploid individual, and the uncertainty of modelling modern populations with ancient samples unevenly distributed across time and space, we did not further search the graph space to fit Ancient Armenian Wild.

We then investigated if other ancient goat populations could be modelled using Neolithic and Pre-Neolithic samples. Due to the quality and number of genomes for many time periods and regions, a skeleton graph of Neolithic East, Neolithic West and Ancient Anatolian Wild was used to fit single populations.

In fitting Bronze Age Levant, Neolithic Levant was included in order to investigate how local Neolithic ancestry contributed to later populations. Due to low coverage of Chalcolithic Levant samples, this population was not modelled. Bronze Age Levant could not be modelled as a sister clade to Neolithic Levant (55 f_4 outliers), with highest f_4 outlier (Neolithic West, Neolithic East; Neolithic Levant, Bronze Age Levant) (Z=11.95) implying unmodelled ancestry between Neolithic East and Bronze Age Levant. Similarly, Bronze Age Levant could not be modelled as a sister population to Neolithic East (24 f_4 outliers). Modelling Bronze Age Levant as a mixture of Neolithic Levant and Neolithic East-like ancestry results in a single outlier, with 24% and 76% ancestry contributions respectively (Figure S18a). The remaining f_4 outliers (Neolithic West, Neolithic Levant; Ancient Anatolia Wild, Bronze Age Levant), suggests additional affinity between the Levantine populations that is not explained by this model; modelling an additional contribution from a Anatolian-like population to the ancestors of Neolithic West did not resolve this outlier.

Bronze Age Anatolia could not be fit as a sister group to either Neolithic East or Neolithic West (38 and 54 outliers respectively), or as an outgroup to both (59 outliers). Fitting Bronze Age Anatolia as a mixture of Neolithic East and West resulted in 15 outliers, which strongly suggested an additional wild contribution to Neolithic East by the f_2 (Neolithic East, Ancient Anatolian Wild) producing a Z score of 7. Allowing this additional Anatolian Wild-like ancestry resulted in the model fitting the data with no outliers (Figure S18b), which describes Bronze Age Anatolia as approximately even mixes of Neolithic East and West-like ancestry (44% and 56%), with a 16% Anatolian Wild-like contribution to Neolithic East.

Fitting Bronze Age Britain as a sister group to Neolithic West resulted in two f_4 outliers, both suggestive of additional unmodelled ancestry present in Neolithic West but not Bronze Age Britain. Including this additional ancestry in Neolithic West results in no outlier statistics (Figure S18c). Interestingly, this result held when Neolithic West was represented only by high coverage individuals from Blagotin-Poljna, Serbia, suggesting that these early European goats have a population history that is distinct from the ancestors of Bronze Age British goat. This model was consistent with Treemix (Figure S12), which suggested additional Ancient Anatolian Wild ancestry in Neolithic West that was absent in modern European (French and Irish) goat.

To fit populations from the Caucasus region (Georgia and Iranian Azerbaijan), Chalcolithic, Bronze Age, and Iron Age/Medieval populations were sequentially added to the skeleton graph. Fitting all populations with no outliers (Figure S18d) suggested the Caucasus populations share the majority of ancestry with Neolithic East, with some admixture from Neolithic Western-like source that increases over time (23% for Chalcolithic and Bronze Age populations, and an additional influx of 11% to the ancestors of Iron Age/Medieval populations). Similar to previous models, this required a small (12%) wild input to the ancestors of Neolithic East.

To model the ancestry of Iranian, Turkmen, and Uzbeki goat, Chalcolithic Iran was first fit to the skeleton graph as a sister group to Neolithic East, which was rejected with 21 f_4 outliers. We added additional admixture from a Ancient Anatolian-like population to Neolithic East, and from a Neolithic West-like population to Chalcolithic Iran, which results in no outliers (Figure S18e). Notably, this model suggested a substantial contribution from the West to Chalcolithic Iran (33%) that is not detected in other analyses (NGSadmix, *D* statistics). To fit additional post-Neolithic eastern populations, Chalcolithic Iran was removed due to low SNP count (Table S20). The resulting graph, which fit with no outliers (Figure S18f), models these post-Neolithic populations (Chalcolithic Turkmenistan, Bronze Age Iran, Bronze Age Uzbekistan) as containing substantial Western-derived ancestry which increases through time. This is only partially consistent with other analyses; though a change in ancestry is observed in the PCA (Figure 1), *D* statistics (Table S31) and NGSadmix (Figure S19) detect a similar signal only in some populations. When adding Iron Age/Medieval Iran to this graph, a small number of f_4 outliers persisted which could not easily be resolved. As such we reduced the samples down to the skeleton graph and fit Iron Age/Medieval Iran as a mixture of Eastern (52%) and Western-like (48%) ancestries (Figure S18g).

Fst outlier scan

To investigate *Fst* outlier regions in Neolithic goat, *Fst* was calculated in ANGSD between modern bezoar and both Neolithic West and Neolithic East, as defined by the PCA groupings in Table S2. Modern bezoar were first screened based on PCA location, with the five bezoar closest to domestic goat removed prior to analysis (Table S26). Samples with mean coverage less than 2X were not included. *Fst* was computed in sliding 50kbp windows with 10kbp steps. For bezoar, the following settings were used to calculate the site frequency spectrum: -setMaxDepthInd 20 -HWE_pval 0.01 -minIndDepth 2 -minInd 2 -doMajorMinor 1 -C 50. For Neolithic goat, the following setting were used: -setMaxDepthInd 20 -minIndDepth 2 -minInd 2. Waterson's theta was then calculated in sliding 50kbp windows, 10kbp steps, for each of the three populations using the same filters as above. For each window in Neolithic populations, we expressed the observed diversity in terms of the diversity observed in same window in modern bezoar: log(theta_bezoar/theta_neolithic), so that Neolithic windows which show less diversity in than in bezoar will have a negative value. If a window had an observed theta of 0, it was replaced with a value of 0.000001 to avoid divisions by zero.

Outlier windows were selected by the following criteria:

1) Fst with bezoar in the top 0.1% quantile
2) log(theta_bezoar/theta_neolithic) in the bottom 5% quantile
3) theta_neolithic in the bottom 5% quantile

Outlier windows were then iteratively combined with adjacent windows with Fst in the top 1% quantile to form outlier regions. Gene overlapping outlier regions were determined using the GenBank annotation of CHIR_1.0 (*117*) (Table S28). For regions with no overlapping genes, the nearest genes were identified.

A total of 21 outlier regions were detected, 7 in the Neolithic West population and 14 in the Neolithic East (Table S28, S32). Of these, 2 pairs of regions were common/overlapping in both

populations; one overlapping the gene *KIT* and non-genic region for which the closest gene is *KITLG*. 16 of the regions overlapped at least one annotated gene.

The two genes identified in outlier regions in both samples are associated with pigmentation differences in domestic animals, *KIT* and *KITLG*, so we investigated where in the *Fst* distribution other pigmentation-associated genes fell. We selected five genes with prior evidence of selection signatures in modern studies - *MC1R* (*175*), *PMEL17* (*176*), *ASIP* (*177*), *TYRP1* (*178*), and *MITF* (*179*). For both the East and West Neolithic populations, we plotted the Fst distribution of all windows, and then plotted the highest *Fst* window for each gene or pigmentation-associated outlier region (Figure 4a), or the mean *Fst* of overlapping windows for each gene or pigmentation-associated outlier region (Figure S20, Table S30). For the Neolithic East population, both plots suggest that other pigmentation-related genes, specifically *ASIP*, and to a lesser degree *MITF* and *TYRP1*, were differentiated relative to wild goat.

To construct an allele sharing heatmap of the *KIT* region (figure 4b), ANGSD was used to construct an IBS matrix as described above, restricting the analysis to the union of the outlier regions detected around KIT (Table S28). This matrix was then visualized as a heatmap using the heatmap.2 function of gplots (*180*). Three main clusters are observed: a cluster containing mainly ancient and modern eastern goat, with several modern African, ancient Levantine and Bronze Age Anatolia individuals; a highly differentiated cluster composed of ancient (Neolithic Serbian) and modern European goat; and a cluster of ancient and modern wild individuals. A fourth rough grouping composed mainly of populations similar to cluster 1 also occurs, with an additional modern European individual. The strong structuring at the *KIT* locus, detected initially in distinct Neolithic populations, appears to persist into the present day. More modern genomes from a variety of breeds and geographic regions are required to comprehensively assess this observation.

Noting the relatively low coverage of the genomes used here and the paucity of genotype-phenotype relationships in goat compared to other domesticates, we investigated if the genes identified in or near the outlier regions contained non-synonymous variants at a high frequency in a Neolithic population and low in bezoar. 3'UTR and non-genic variants were not considered due to the difficulty in assessing phenotypic importance. To generate a preliminary list of genic variants, samtools mpileup (*119*) was used to call variants in the bezoar and two diploid Neolithic genomes included in the selection analysis, restricting to exons of the identified genes (Table S28), plus 2bp to detect possible splice site mutations. Sites within 3bp of indels were removed. Additionally, sheep and yak outgroups were also called to polarize variants as ancestral or derived. Sites that both outgroups shared fixed alleles were retained and the allele set as ancestral; sites that either outgroup was heterozygous or were not in consensus were discarded. Sites were then filtered for homozygous status in either Neolithic genome, a corresponding maximum frequency of 0.2 in bezoar. Synonymous and 3'UTR variants were removed, leaving a final nine nonsynonymous sites (Table S29). Allele frequencies of these sites in both Neolithic East and Neolithic West populations used in the selection analysis were estimated using ANGSD (*133*) using the following settings: -doMaf 1 -doMajorMinor 5 -GL 1 -trim 4.

The nine nonsynonymous variant sites were found across seven genes: *LOC102172205* (serotransferrin, two variants), *STAT1*, *MYOM3*, *KITLG*, *KIT*, *LOC102185708* (*CYP2C19*), *SIRT1* (two variants). One *LOC102172205* variant was identified in Neolithic East (frequency of 0.65),

while a second was identified in both East and West as being fixed for the ancestral allele. The *STAT1* variant matched the ancestral allele, and is at a high frequency in both East (0.91) and West (0.7) Neolithics. A *MYOM3* variant is fixed as derived in Neolithic East (in which population the gene was initially detected using the outlier approach) but is absent in Neolithic West. The *KITLG* nonsynonymous variant is fixed (1.0) in Neolithic East but common in Neolithic West (0.43). The *KIT* variant identified appears at a frequency of 0.75 in the Neolithic West but is absent in Neolithic East. Both *SIRT1* variants are a high frequency (≥0.75) in Neolithic West but low (~0.1) in Neolithic East; *SIRT1* was identified in an outlier region in Neolithic West (Table S28). *LOC102185708* (*CYP2C19*), identified originally in Neolithic East, is fixed for an ancestral allele in the same population, and fixed for the derived allele in Neolithic West.

Demographic modelling of population histories - whole mitochondria

Whole mitochondrial genomes from 23 samples were analysed and all sites were called as described above. Considering the heterogeneous level of missing data across samples (ranging from 0 to 23%, see Table S14), a dataset including only sites shared across all samples would have not had sufficient information. Therefore, each summary statistics was calculated using individual pairwise comparisons both within and between populations. Each within-population summary statistic has been calculated as average across all the individual pairwise comparisons between all samples belonging to that specific population. Each between-population summary statistic has been calculated as average across all individual pairwise comparisons between samples belonging to the two populations under study. Following this approach, both nucleotide diversity per population and Hudson's pairwise Fst (*181*) were calculated with an in-house R script v3.2.3 (*182*) (Table S15 and S16).

We developed an approximate Bayesian computation (ABC) (*183*) framework to estimate parameters and compare models. Two demographic models were designed to investigate the demographic histories of samples belonging to the Western, Eastern and Levantine populations: model SINGLE_MT and model MULTIPLE_MT (Figure S13a). Model SINGLE_MT represents a single domestication event shared for the three populations. An ancestral population (Nanc2) goes through a bottleneck from 11,000 to 10,500 years ago representing the domestication event before splitting in the three ancestral population which give rise to the Neolithic Western, Eastern and Levantine populations (represented by Nneow, Nneoe and Nneol respectively). Model MULTIPLE_MT describes a scenario with multiple domestication events. From an ancestral population (Nanc3), the Levantine branch splits before going through a bottleneck from 11,000 to 10,500 years ago and then exponentially expands from 10,500 to 8,000 years ago (Neolithic Levantine population). Subsequently, the ancestral population (Nanc2) splits into the ancestral population for the Western and Eastern samples (Nanc1w and Nanc1e respectively) before going through a bottleneck at 11,000 years ago and then exponentially expand up to 8,000 years ago (Neolithic Western and Eastern populations). Prior distributions for all parameters of the two models are reported in Table S17.

We built our simulations to have the same configuration as the observed data (to conform with sequence length and pattern of missing data). Specifically, we first recorded the exact position of each missing nucleotide across all sequences in the real dataset ("missing data layer"). Then, the maximum number of base pair (15,429) was simulated and subsequently the "missing data layer"

was applied to each simulated dataset. In this way we were able to recreate the exact pattern of missing data in terms of percentage and position observed in the real dataset in each simulated dataset.

We performed 100,000 simulations under each model using fastsimcoal 2 v.25221 (*184*). The mutation rate was calibrated as described above and a value of 1.411×10^{-7} per site per generation was used. Generation time was assumed at 2.5 years (*185*). The following summary statistics were used: nucleotide diversity per population (π_3E, π_3L) and pairwise Hudson's Fst for the following comparisons (Fst_3W_3E, Fst_3L_3W, Fst_3L_3E). Model posterior probabilities were calculated by a weighted multinomial logistic regression (*186*) for which we retained the best 25,000 and 50,000 simulations. Parameters under the most supported model were estimated from the 5,000 simulations closest to the observed dataset using the neuralnet algorithm (*187*). Analyses were performed in the R environment (*182*) with the library abc (*187*).

Model posterior probabilities suggest MULTIPLE_MT as the most supported model by the data using two thresholds of simulations retained (25,000 and 50,000) (Table S18). Parameters estimations was done under model MULTIPLE_MT for Tsplit and Tlevant. The mode for Tsplit is 12.1 KYA (95% credible interval 11.1-18.4 KYA) while the mode for Tlevant is 138 KYA (95% credible interval 38.5-195.2 KYA). This latter estimate, in particular, is clearly prior to the domestic period and supports the contribution of separate bezoar populations to different regional populations of early domesticates. Parameters estimates are shown in Table S19 and posterior distributions in Figure S15.

Demographic modelling of population histories - autosomes

Whole autosomal genomes from 9 Neolithic samples were analysed to investigate the relationship between Western and Eastern populations. Variant calling and filtering is described above, producing a final dataset of 9,385 variants which are at least 100 Kb apart to avoid the effect of linkage disequilibrium. We filtered for 0% missing data in the dataset to remove any additional source of uncertainty. Four samples belonged to the Neolithic West and five samples belonged to the Neolithic East (see Table S14). Both nucleotide diversity per population and Hudson's pairwise Fst (*181*) were calculated with in-house R script R v3.2.3 (*182*). Nucleotide diversity calculated on a pre-selected subset of variant sites does not correspond to the nucleotide diversity calculated across the whole genome. In order to take this bias into account, we generated simulated data in the same way that we preselected the variant sites in the real dataset. We subset the first 9,385 variant sites and calculated the nucleotide diversity per population on this subset. In this way, the nucleotide diversity calculated on both the simulated and real data are comparable.

We developed an Approximate Bayesian Computation (ABC) (*183*) framework to estimate parameters and compare models. Two demographic models were designed to investigate the demographic histories of samples belonging to the Western and Eastern populations: model SINGLE_AU and model BINARY_AU (Figure S13b). Model SINGLE_AU describes an ancestral population (Nanc2) that goes through a bottleneck (Nanc1) from 11,000 to 10,500 years ago representing the domestication event. After the bottleneck, Nanc1 branches into the ancestral populations (Nbotw and Nbtoe) of the Neolithic Western and Eastern samples respectively. Both populations exponentially increase in size from 10,500 to 8,000 years ago (Nneow and Nneoe).

Model BINARY_AU describes an ancestral population that at the time Tsplit branches into the two ancestral populations to the Western and Eastern samples (Nanc1w and Nanc1e respectively). Each of these two populations goes through a bottleneck from 11,000 to 10,500 years ago representing independent domestication events (Nbotw and Nbote). Afterwards, both populations exponentially increase in size from 10,500 to 8,000 years ago (Nneow and Nneoe). Prior distributions for all parameters of the two models are reported in Table S22.

We performed 50,000 simulations under each model using fastsimcoal 2 v.25221 (*184*). The mutation rate was calibrated as described above and a value of 1.3×10^{-8} per site per generation was used along with a generation time of 2.5 years (*185*). The following summary statistics were used: nucleotide diversity per population (π_3E, π_3W) and pairwise Hudson's Fst (Fst_3W_3E). Model posterior probabilities were calculated by a weighted multinomial logistic regression (*186*) for which we retained the best 25,000 and 50,000 simulations. Parameters under the most supported model were estimated from the 5,000 simulations closest to the observed dataset using the neuralnet algorithm (*187*). Analyses were performed in the R environment (*182*) with the library abc (*187*).

We calculated the nucleotide diversity for both the Western and Eastern Neolithic samples (π_3W, π_3E) which results in 0.15 and 0.16 per site respectively while the pairwise Hudson's Fst is 0.17. Model posterior probabilities suggest model BINARY_AU as the most supported model by the data using two thresholds of simulations retained (25,000 and 50,000) (Table S23). The preference of this model, which involves two separate domestications from bezoar for Eastern and Western goats over the single domestication model concurs with the evidence from other analyses.

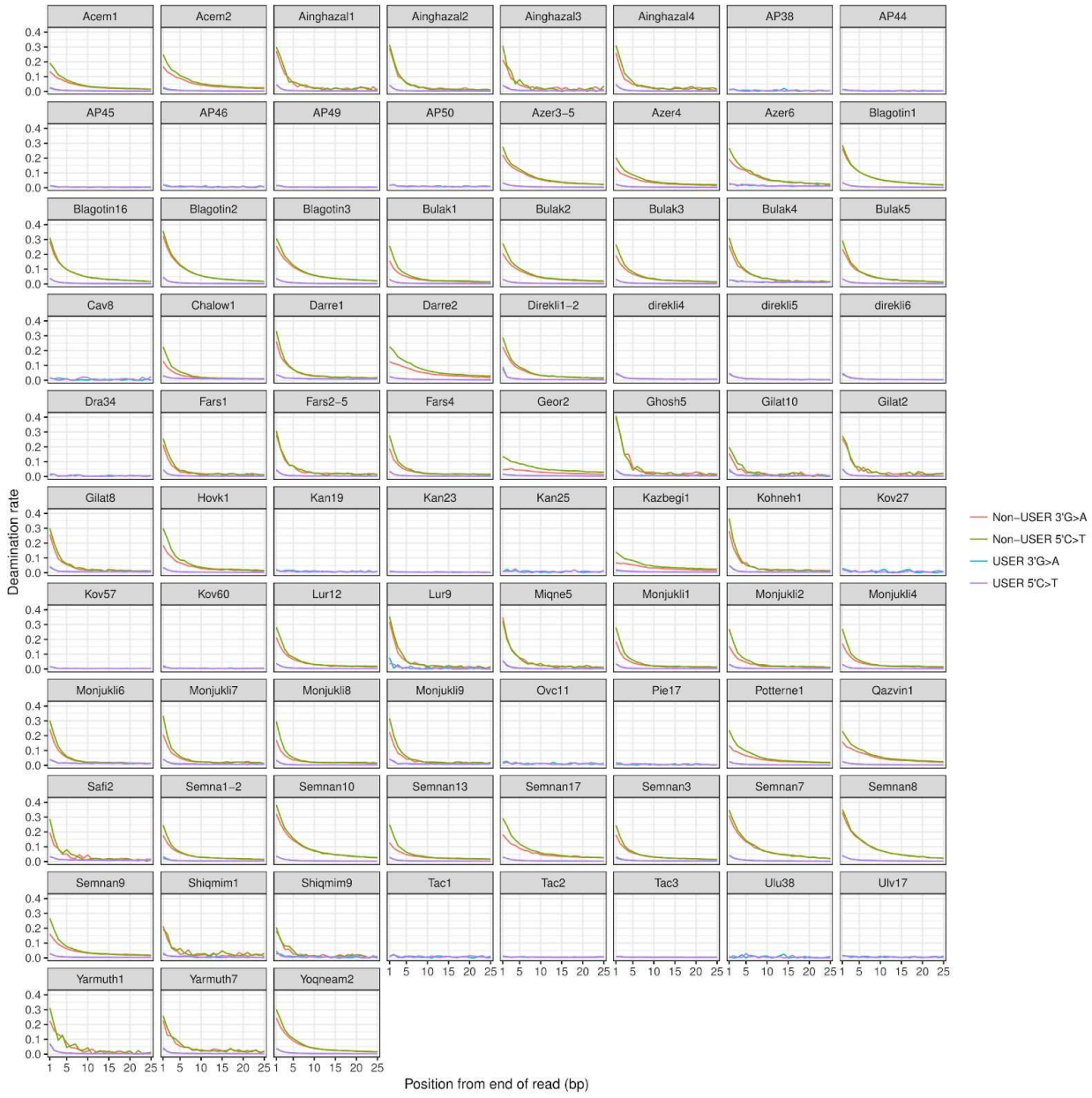

Fig. S1.

Damage patterns of non USER-treated and USER-treated libraries. Non-USER treated libraries were not constructed for Direkli4, Direkli5, and Direkli6 due to limited available DNA, and for those previously reported (*34*) due to prior authentication.

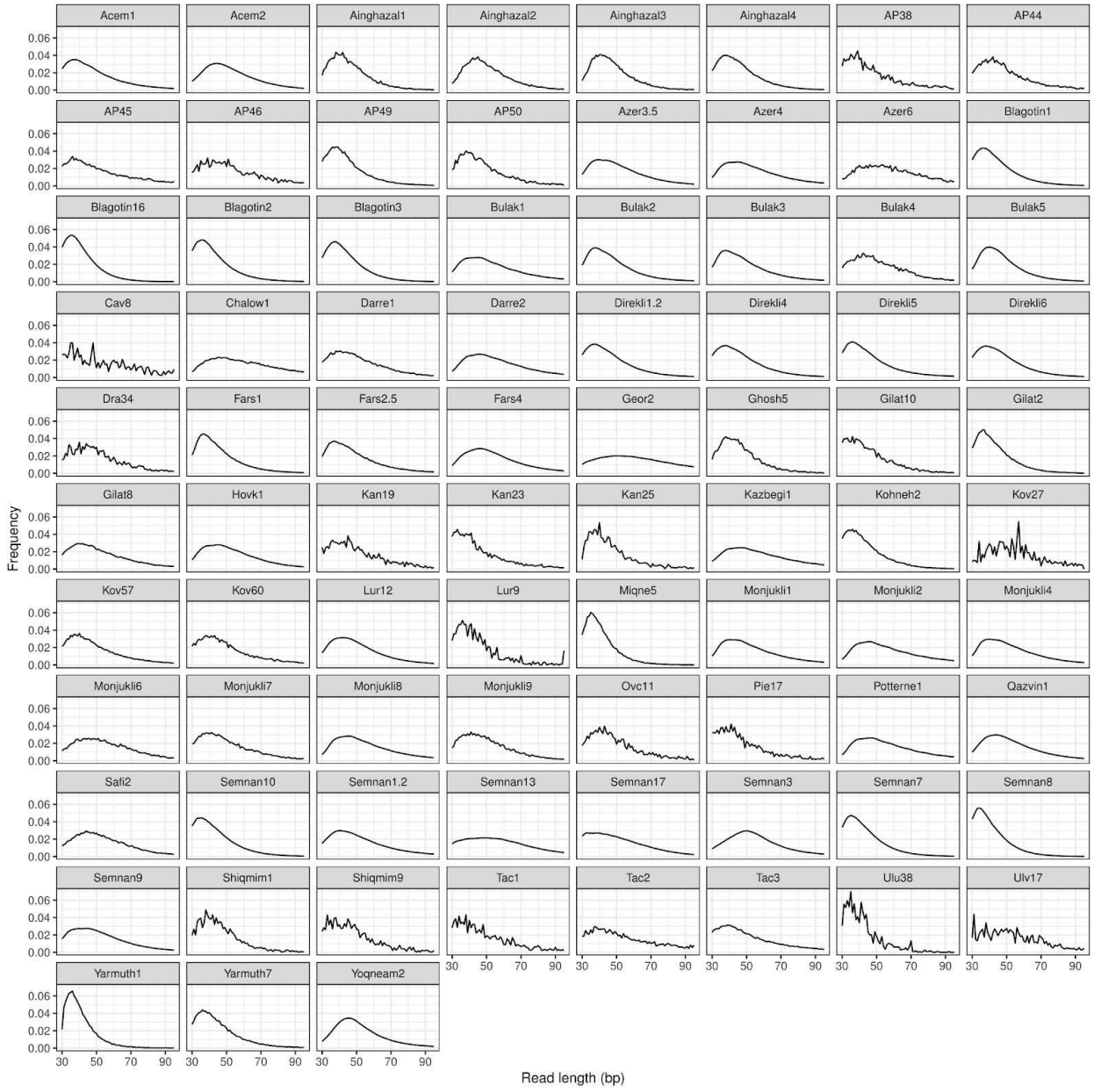

Fig. S2.
Read length distribution of sequenced libraries.

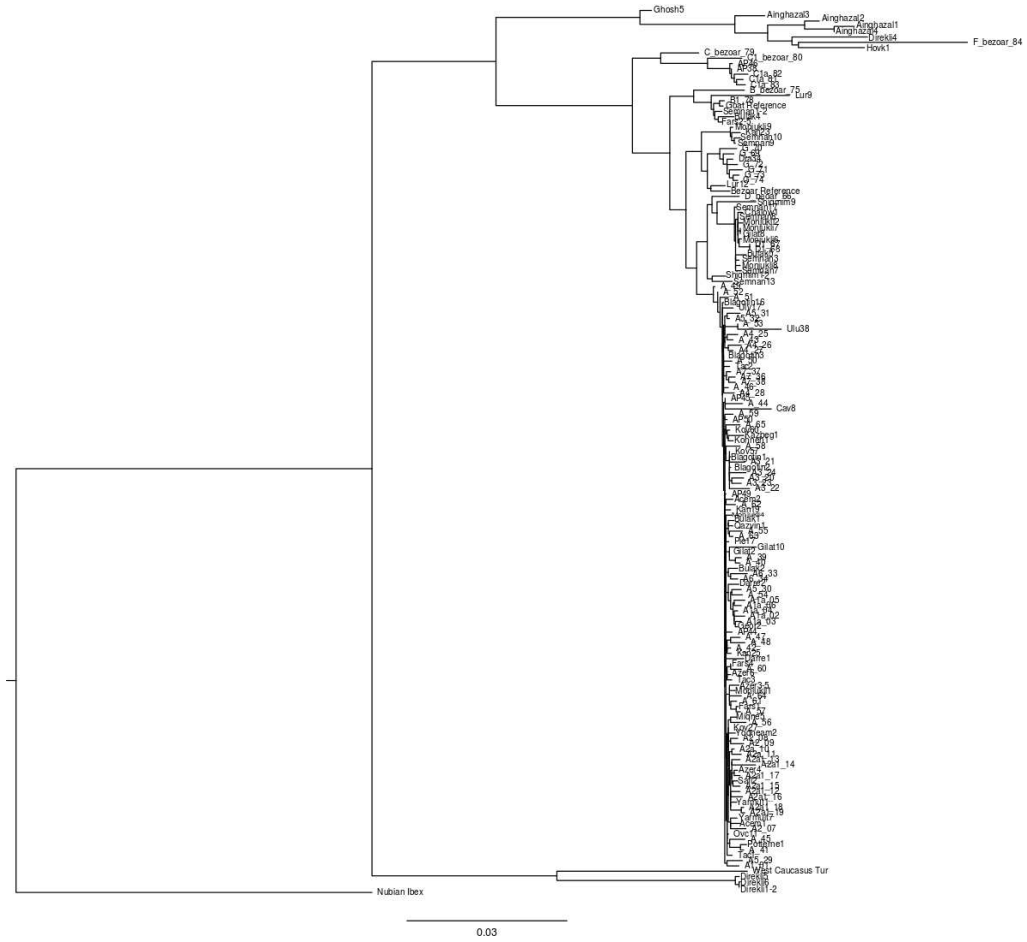

Fig. S3.

Maximum Likelihood phylogeny of ancient and modern goat/bezoar mitochondria. Nubian Ibex is included as an outgroup. High confidence bootstrap values for nodes (>0.6) are displayed. Most domestic samples fall in haplogroup A, the most common modern haplogroup. Neolithic goat from Iran and Turkmenistan, plus some later ancient domestics, show non-A haplogroups (D, G, B).

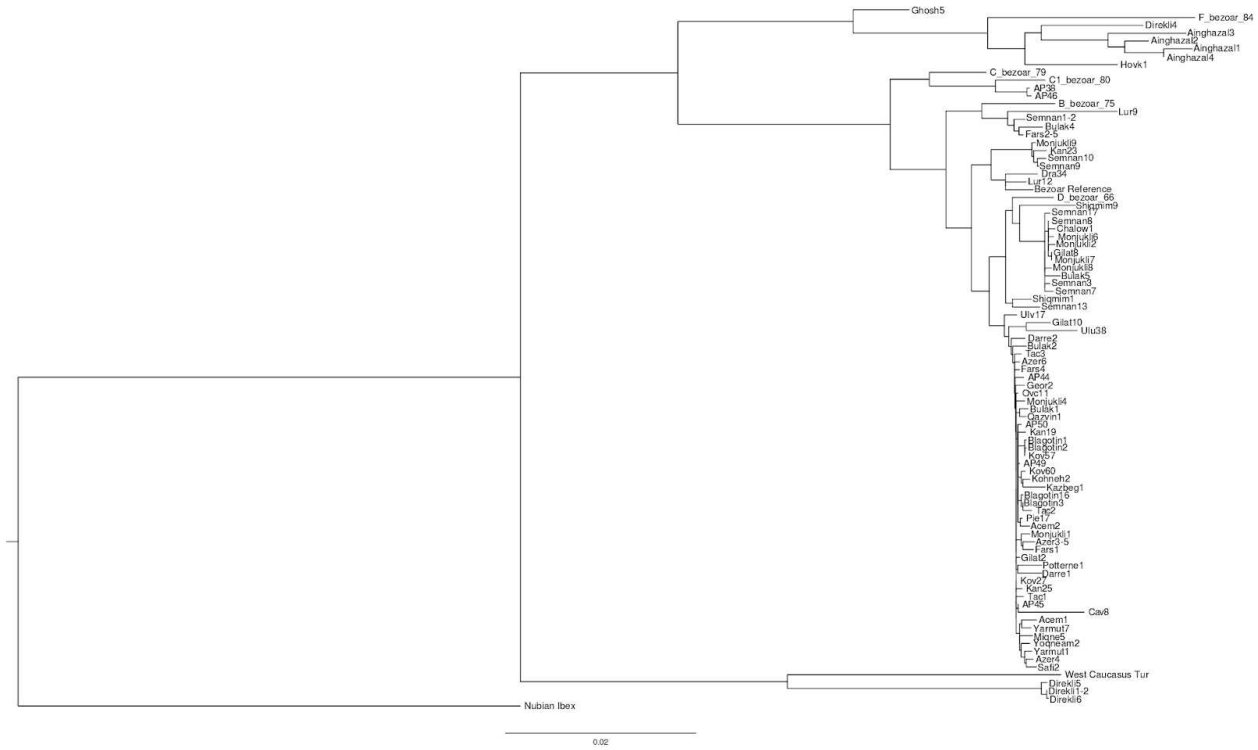

Fig. S4.

Maximum Likelihood phylogeny of ancient goat/bezoar mitochondria. Included is a representative modern bezoar sequence from each domestic haplogroup, the West Caucasian Tur, and the Nubian Ibex as an outgroup. High confidence bootstrap values for nodes (>0.6) are displayed.

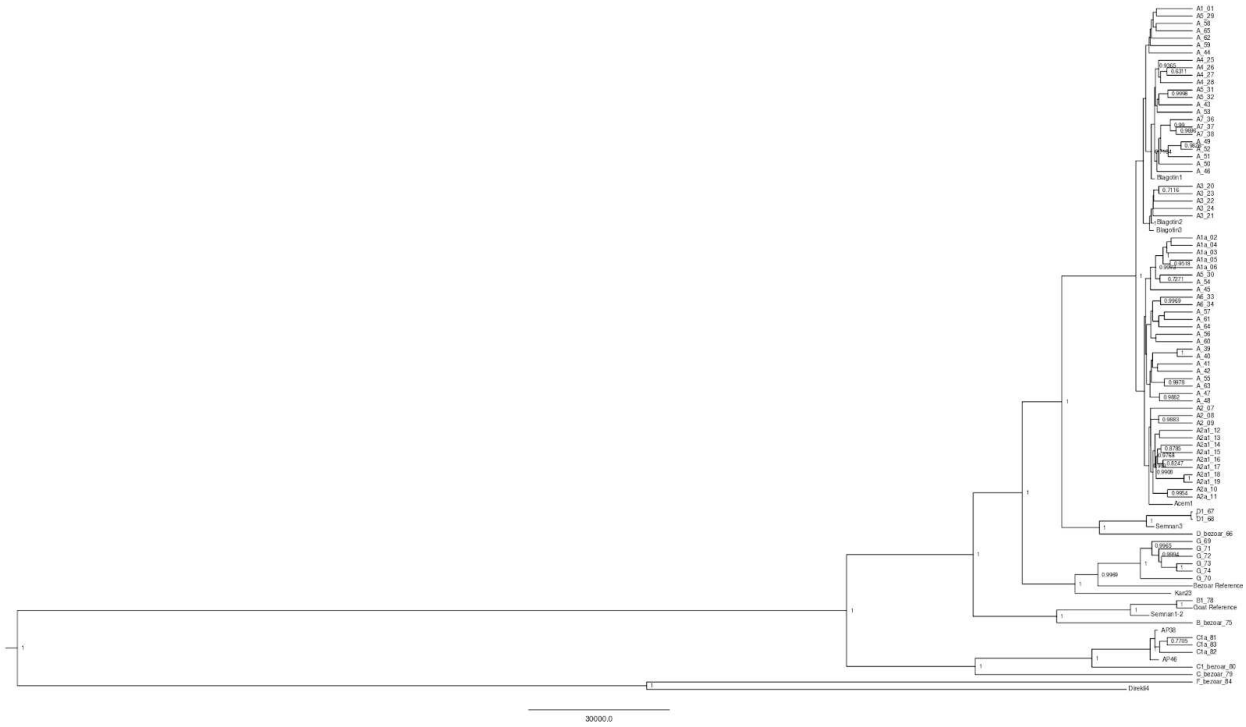

Fig. S5.

Mitochondrial Tree generated by BEAST, including wild and domestic sequences. High confidence posterior values for nodes (>0.6) are displayed.

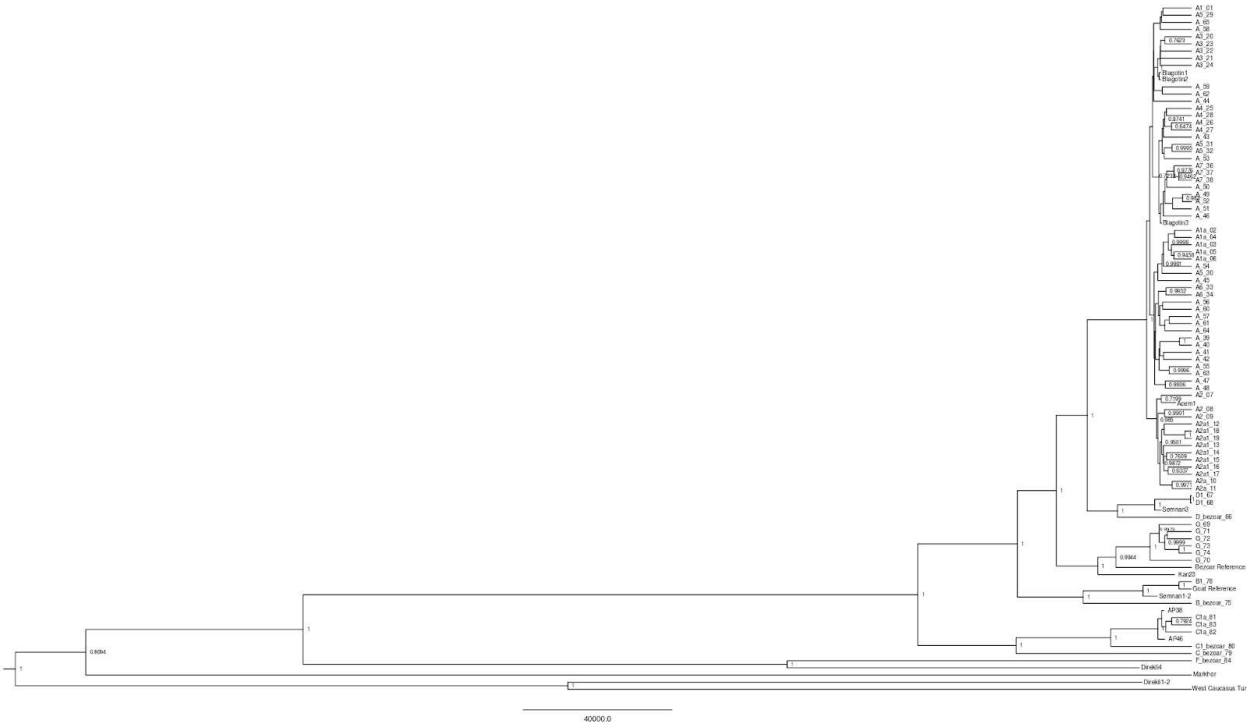

Fig. S6.

Mitochondrial Tree generated by BEAST, including wild and domestic goat, Tur and Markhor sequences. High confidence posterior values for nodes (>0.6) are displayed.

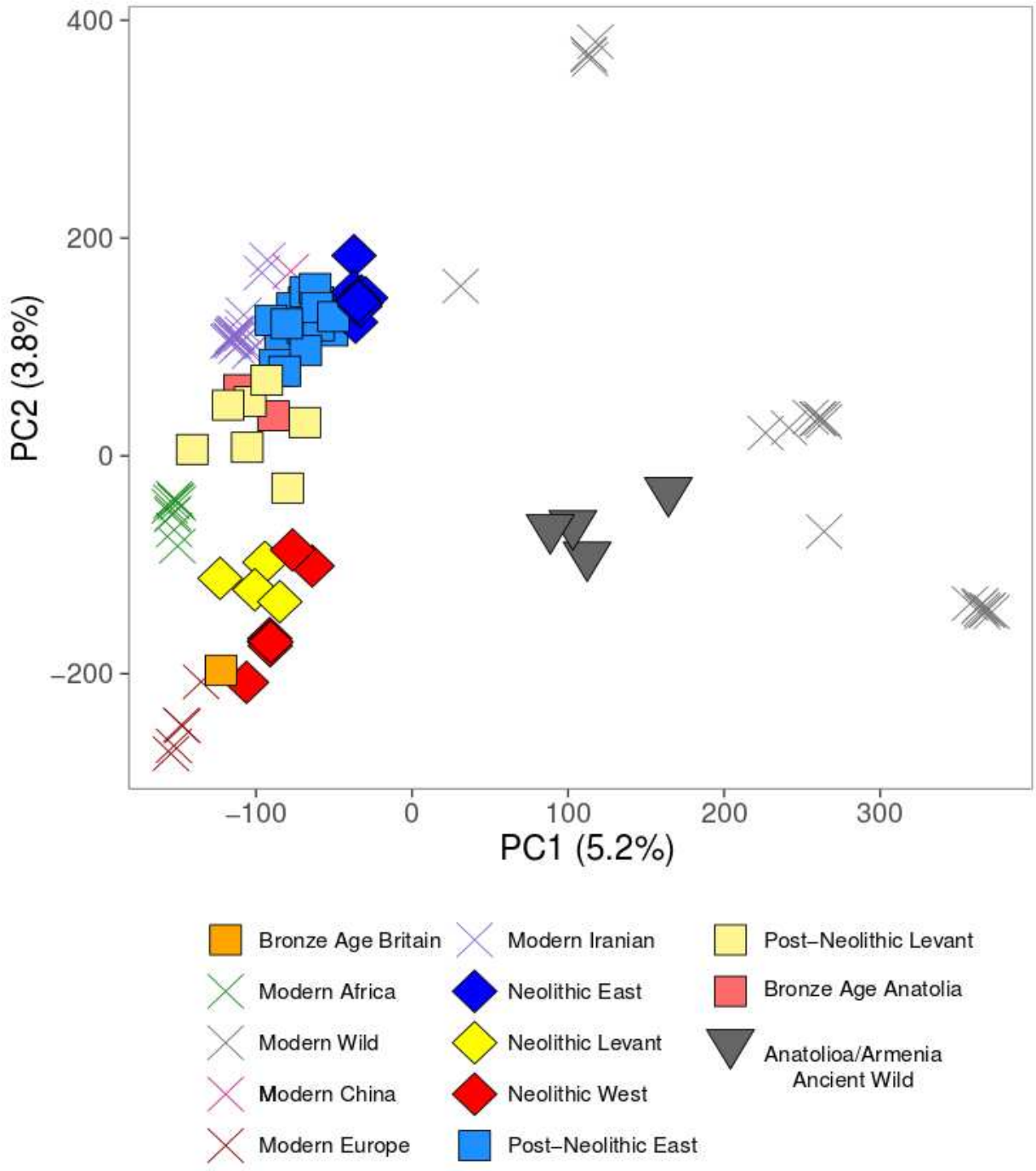

Fig. S7.
LASER projection PCA of modern and ancient wild and domestic goat samples, using pruned dataset. Values in parenthesis represent the percentage of variance explained by a given PC, as estimated by LASER. PC1 differentiates wild from domestic goat, PC2 eastern (Iranian, Chinese) from western (European) domestic goat.

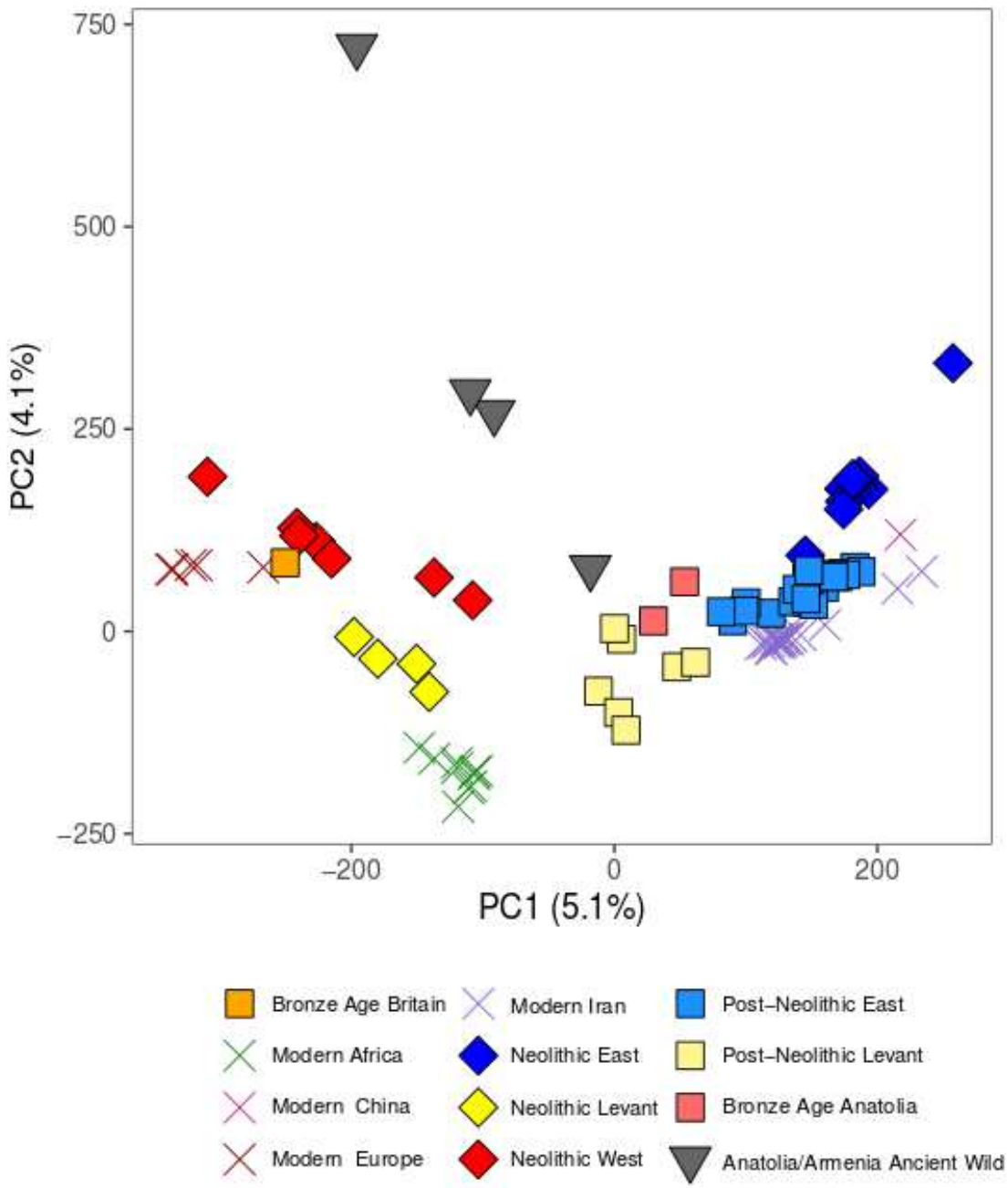

Fig. S8.
LASER projection PCA of all ancient samples and modern domestic goat, using pruned dataset. Values in parenthesis represent the percentage of variance explained by a given PC, as estimated by LASER. PC1 differentiates eastern (Iranian, Chinese) from western (European) domestic goat, while African goat and wild ancients fall on the extremes of PC2.

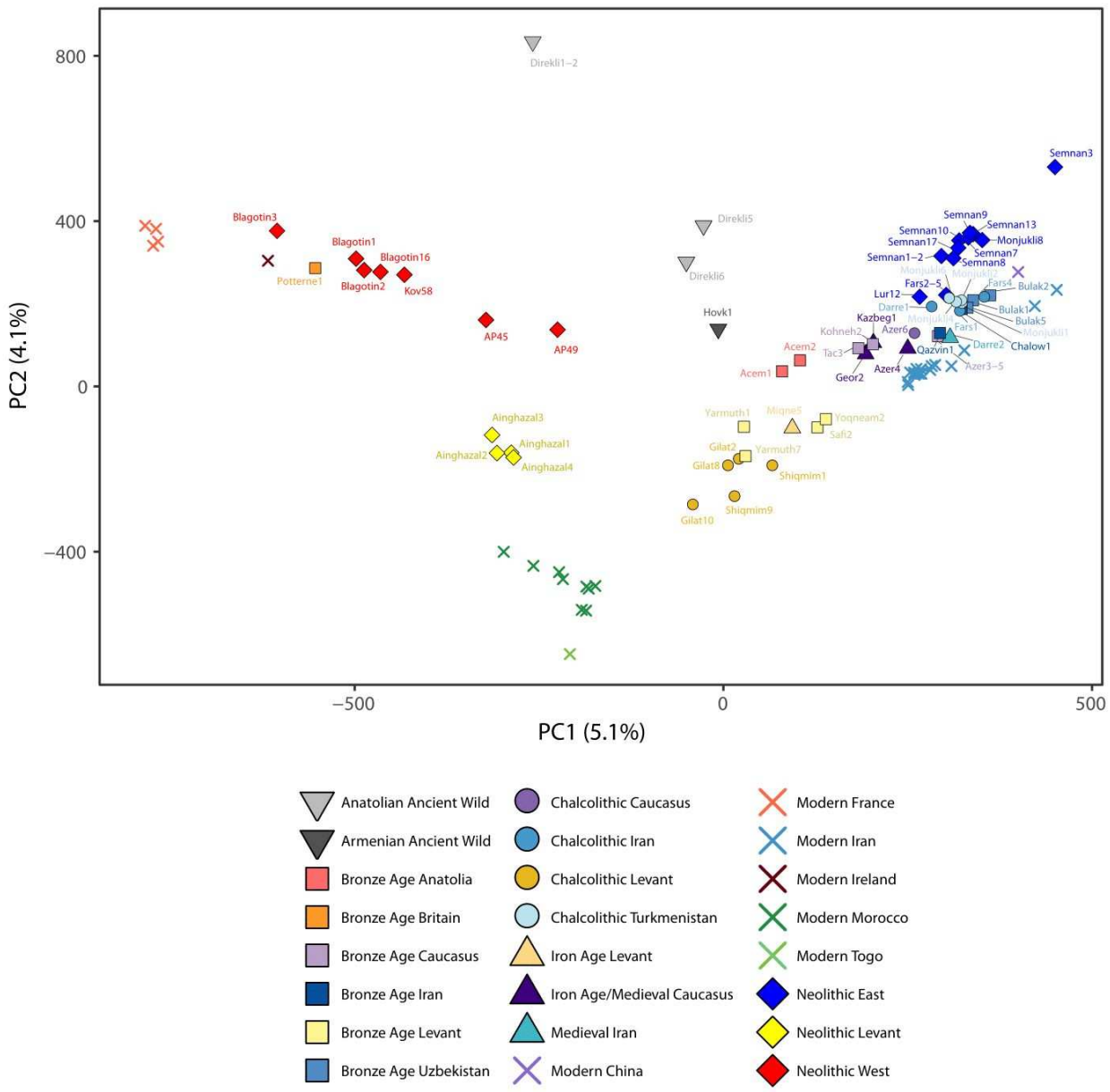

Fig. S9.

LASER projection PCA of all ancient samples and modern domestic goat, using granular subgroups and sample labels. Values in parenthesis represent the percentage of variance explained by a given PC, as estimated by LASER. Graph area has been increased and symbol size decreased to accommodate individual labels.

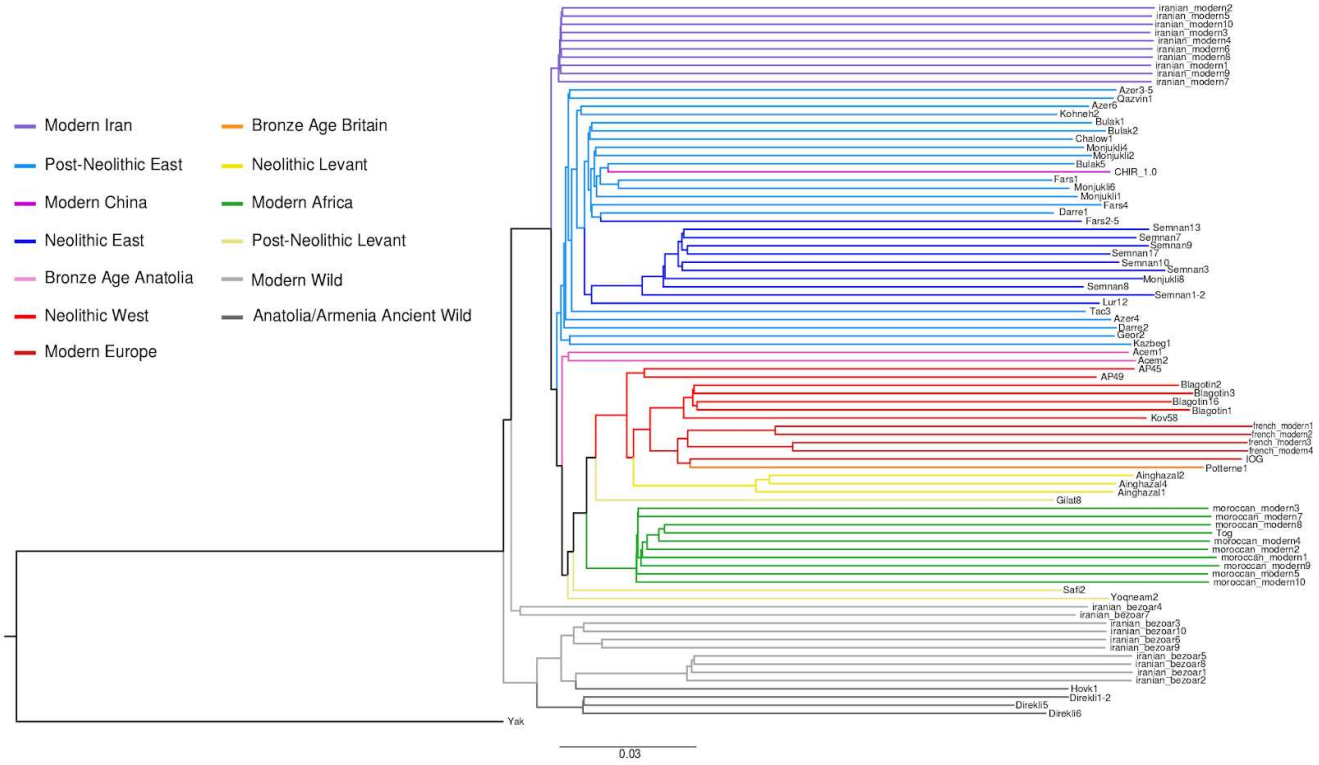

Fig. S10.

Neighbour-Joining tree of ancient and modern domestic and wild goat IBS matrix, using genomes >0.01X coverage. Wild goat, both ancient and modern, group to the exclusion of domestics. The central divide of ancient and modern domestic samples with between eastern, and western/Levantine goat. Modern Iranians appear admixed (fig. S18-S19), and here fall as an outgroup to domestics.

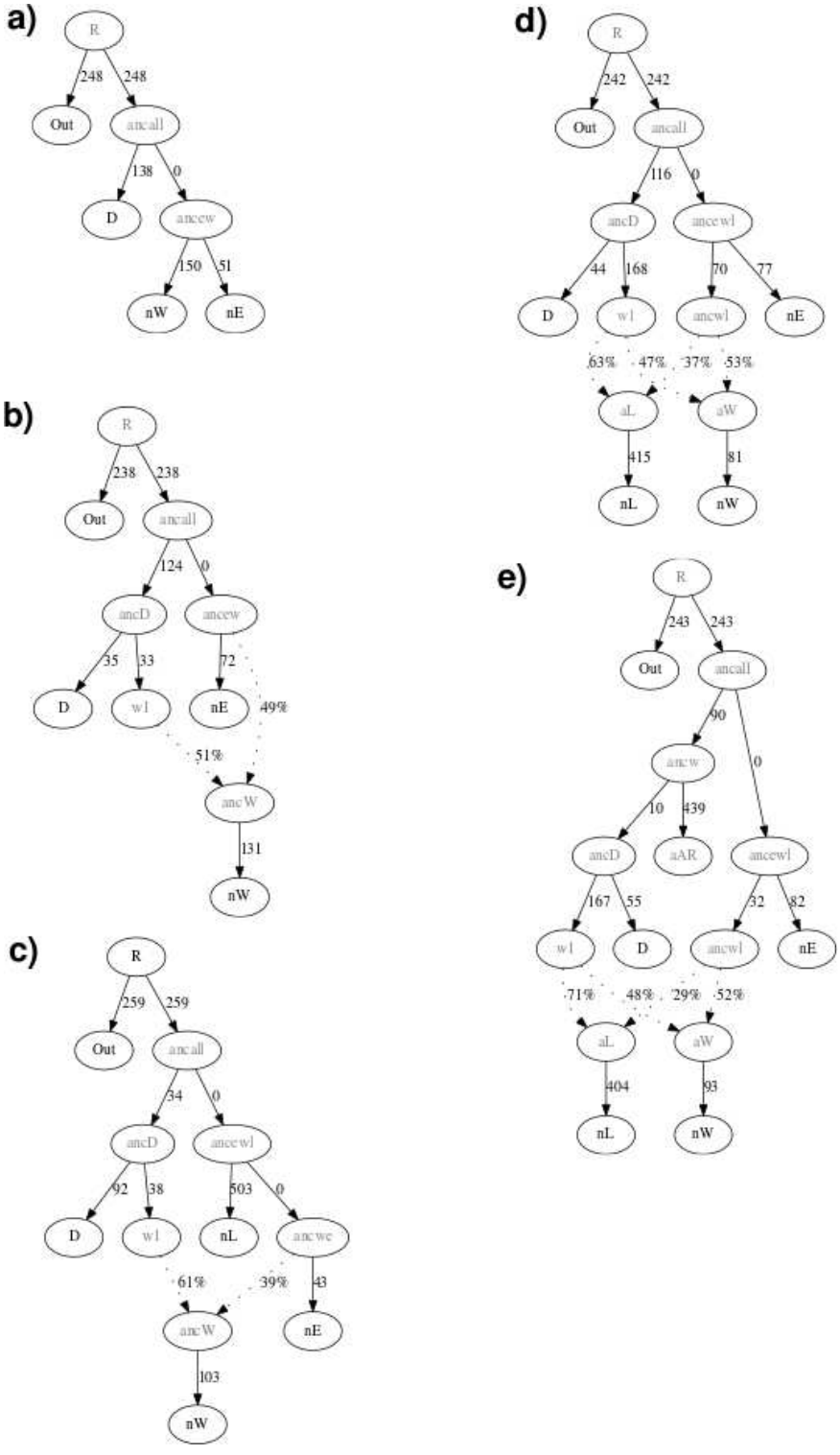
a)
R
248
248
Out
ancall
138
0
D
ancew
150
51
nW
nE
b)
R
238
238
Out
ancall
124
0
ancD
ancew
35
33
72
D
wl
nE
49%
51%
ancW
131
nW
c)
R
259
259
Out
ancall
34
0
ancD
ancewl
92
38
503
0
D
wl
nL
ancwe
61%
39%
43
ancW
nE
103
nW
d)
R
242
242
Out
ancall
116
0
ancD
ancewl
44
168
70
77
D
wl
ancwl
nE
63%
47%
37%
53%
aL
aW
415
81
nL
nW
e)
R
243
243
Out
ancall
90
0
ancw
10
439
ancD
aAR
ancewl
167
55
32
82
wl
D
ancwl
nE
71%
48%
29%
52%
aL
aW
404
93
nL
nW

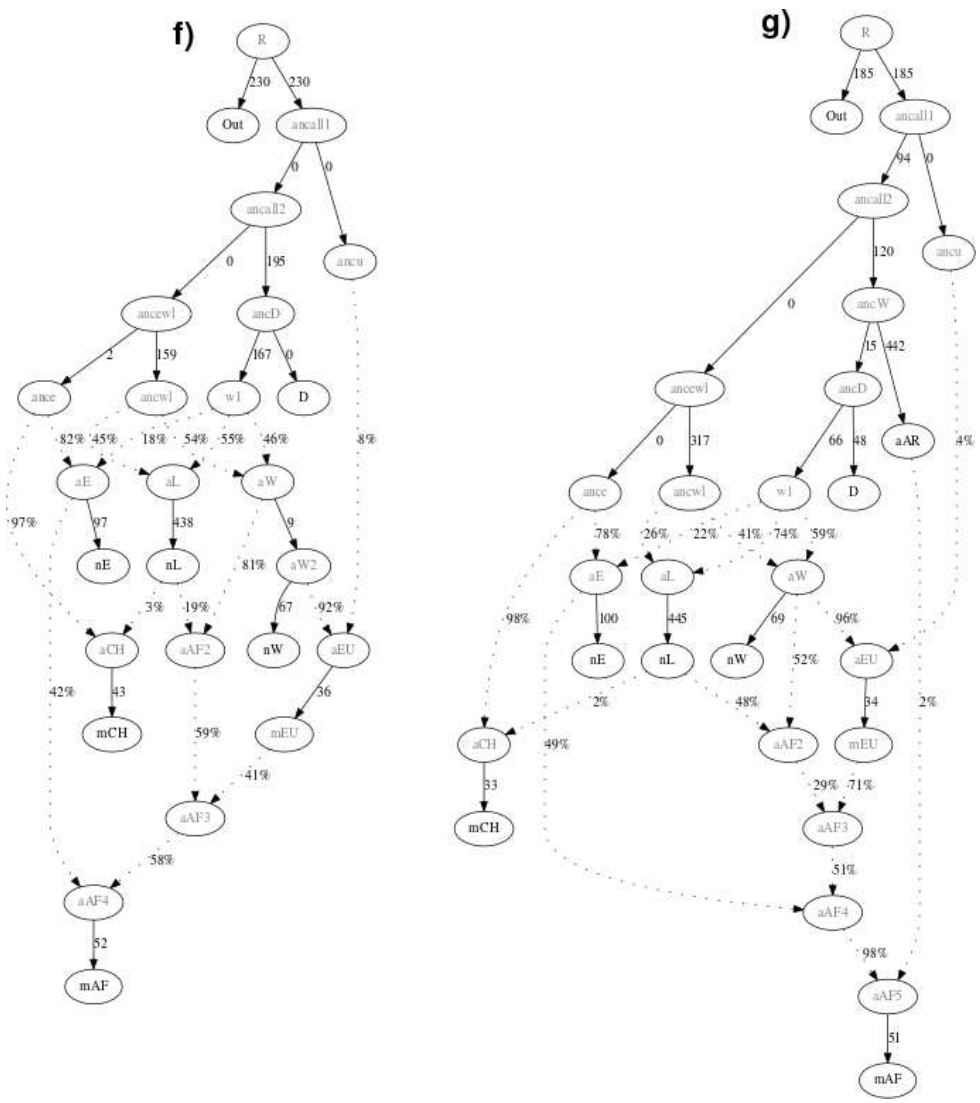

Fig. S11.

Admixture graph models for ancient and modern domestic goats. a) Base graph used, which was rejected. b) A modified version of the previous graph, allowing admixture from a wild population related to Ancient Anatolian Wilds into the ancestors of western Neolithics, which was not rejected. c) Neolithic Levant modelled as the outgroup of eastern and western Neolithic goat, but the graph is rejected. d) A model in which Neolithic Levant and Neolithic West share ancestry, and both subsequently admix with a wild population, is not rejected. e) Addition of the Ancient Armenian Wild genome to the root of the wild clade, which is not rejected. f) Model d, with the addition of modern African, Chinese, and European genomes, fits the data. Modern populations are modelled as a mixture of ancestries. g) The previous model with the addition of the ancient Armenian wild goat. This model results in three outlier f_4 statistics (ranging 3-3.3). Intermediate, theoretical populations are denoted in grey. Edge drift values = Fst x 1000. nW=Neolithic West, nE=Neolithic East, nL=Neolithic Levant, D=Ancient Anatolian Wild (Direkli), aAR=Ancient Armenian Wild (Hovk1), mEU=Modern Europe, mCH=Modern China, mAF=Modern Africa.

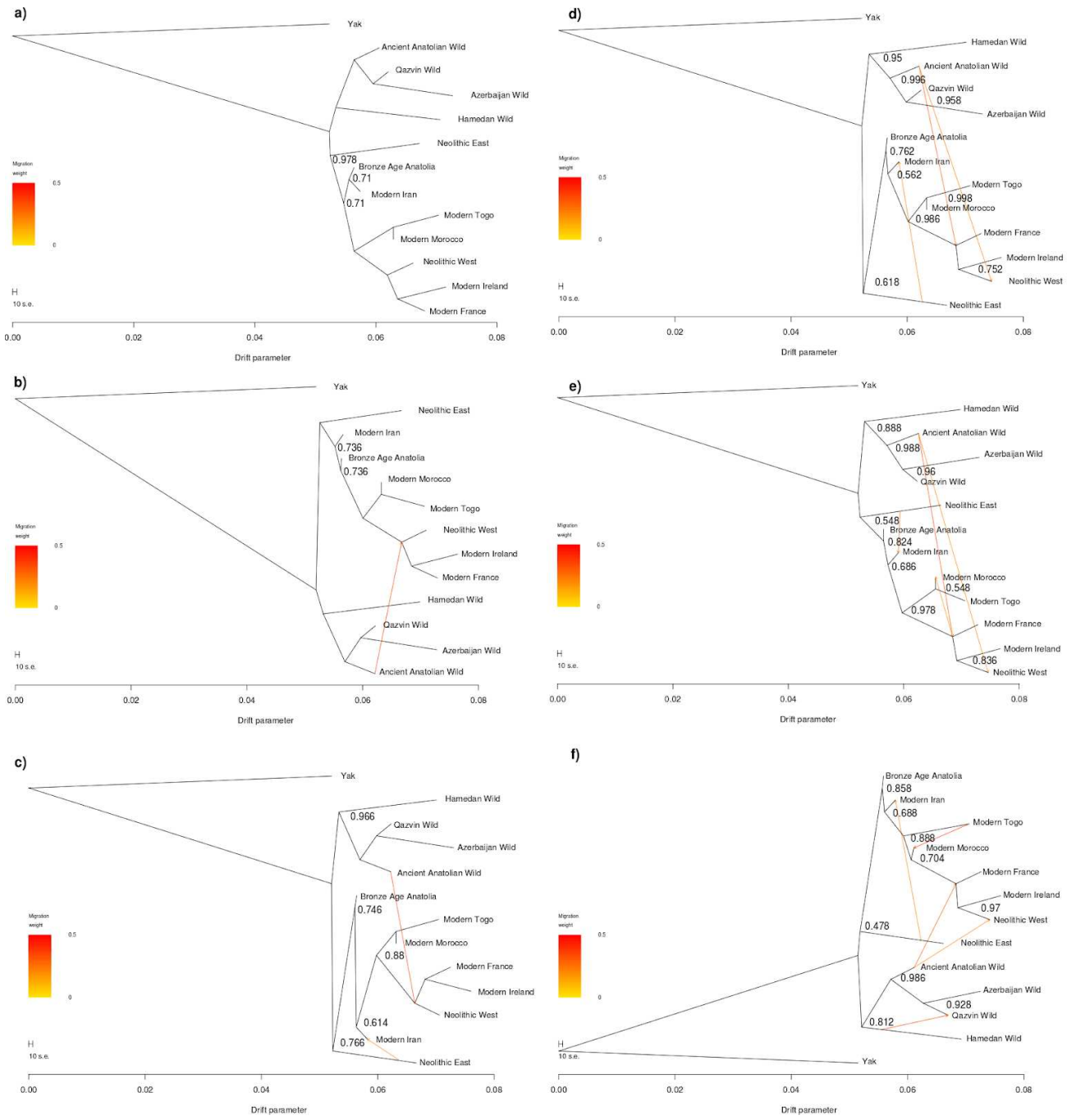

Fig. S12.

Treemix analysis of high coverage (>8X) samples. Bootstrap support (500 iterations) for branches is displayed with the bootstrap score was less than 1. Migration edges were varied from 0 to 5, shown in a) no migration edge, b) one migration edge, c) two migration edges, d) three migration edges, e) four migration edges, f) five migration edges. Wild goat are modelled as an outgroup to all domestics, with admixture from some wild populations into domestic branches.

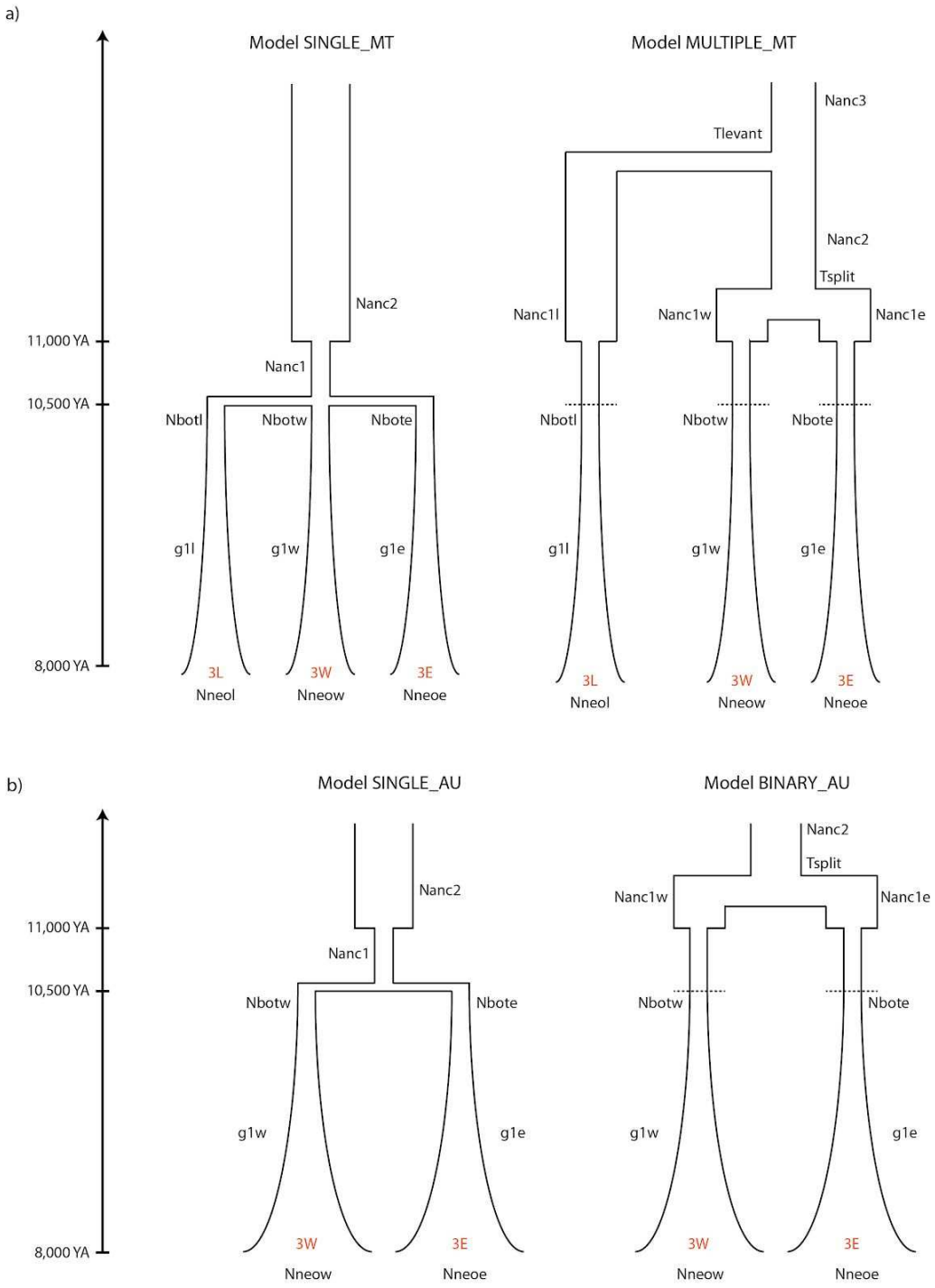

Fig. S13.

Demographic models tested with whole mitochondrial genomes (panel a) and whole genome sequences (panel b). YA: years ago. 3L: Neolithic Levant; 3W: Neolithic West and 3E: Neolithic East.

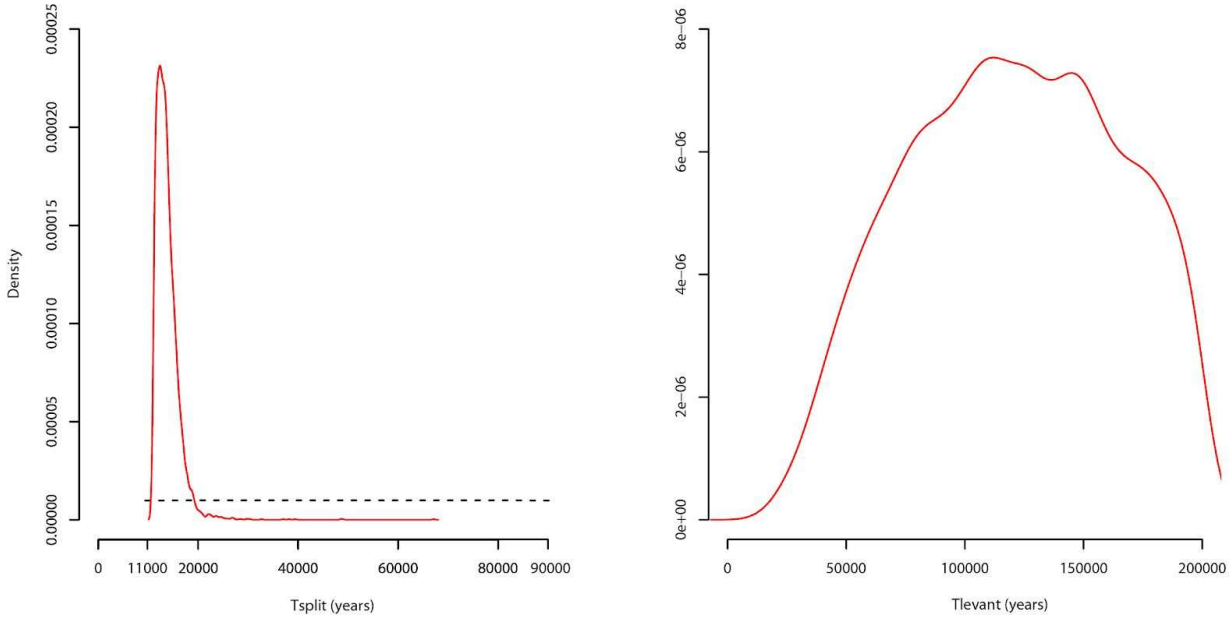

Fig. S14.

Posterior distribution of Tsplit and Tlevant estimated under model MULTIPLE_MT. Black dotted line: prior distribution; red line: posterior distribution calculated using a neuralnet algorithm.

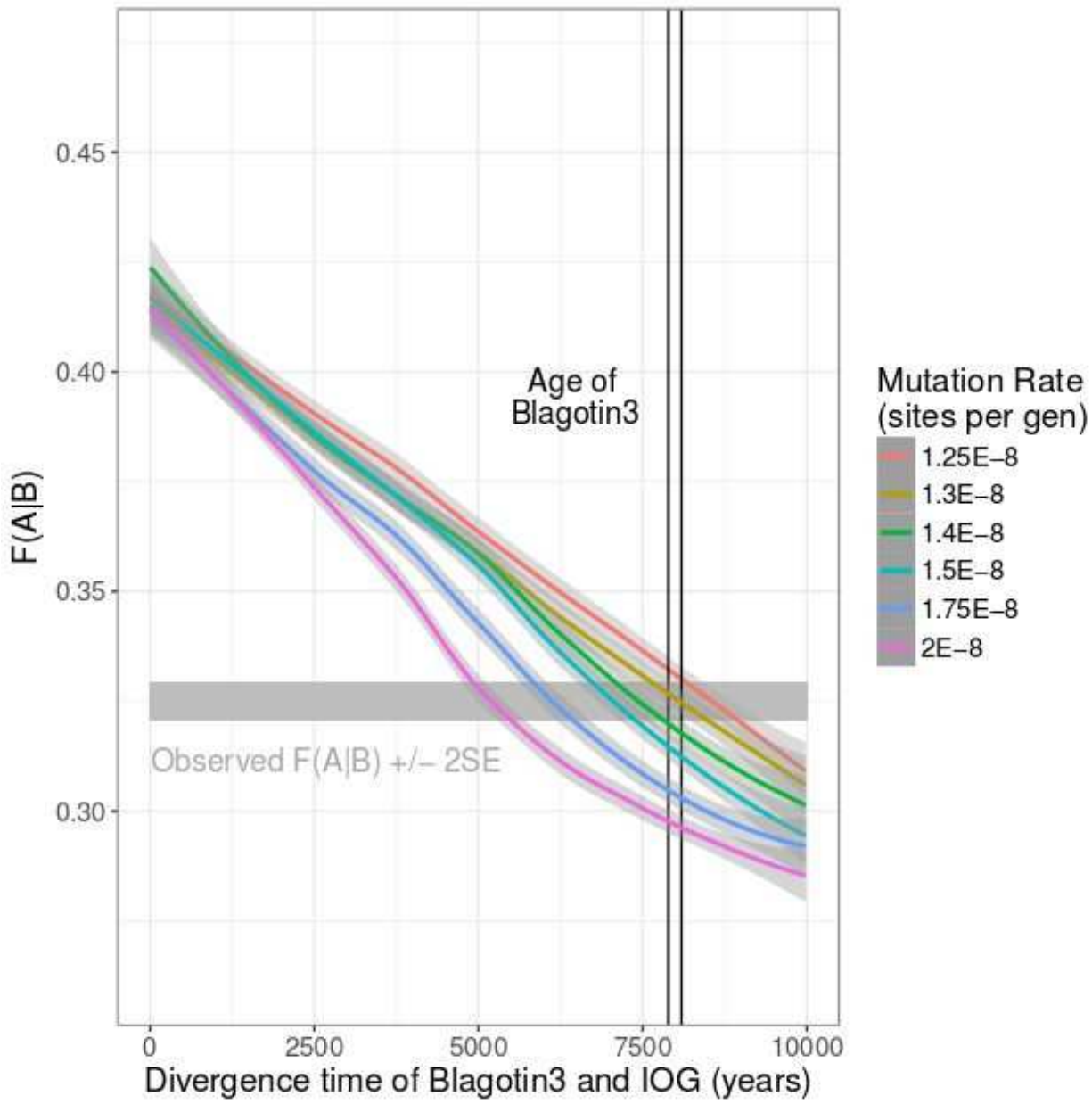

Fig. S15.

Estimation of the *Capra hircus* genome mutation rate, using Blagotin3 and IOG. Based on the observed F(A|B) value, 1.3E-8 sites per generation was chosen as the mutation rate for subsequent analyses.

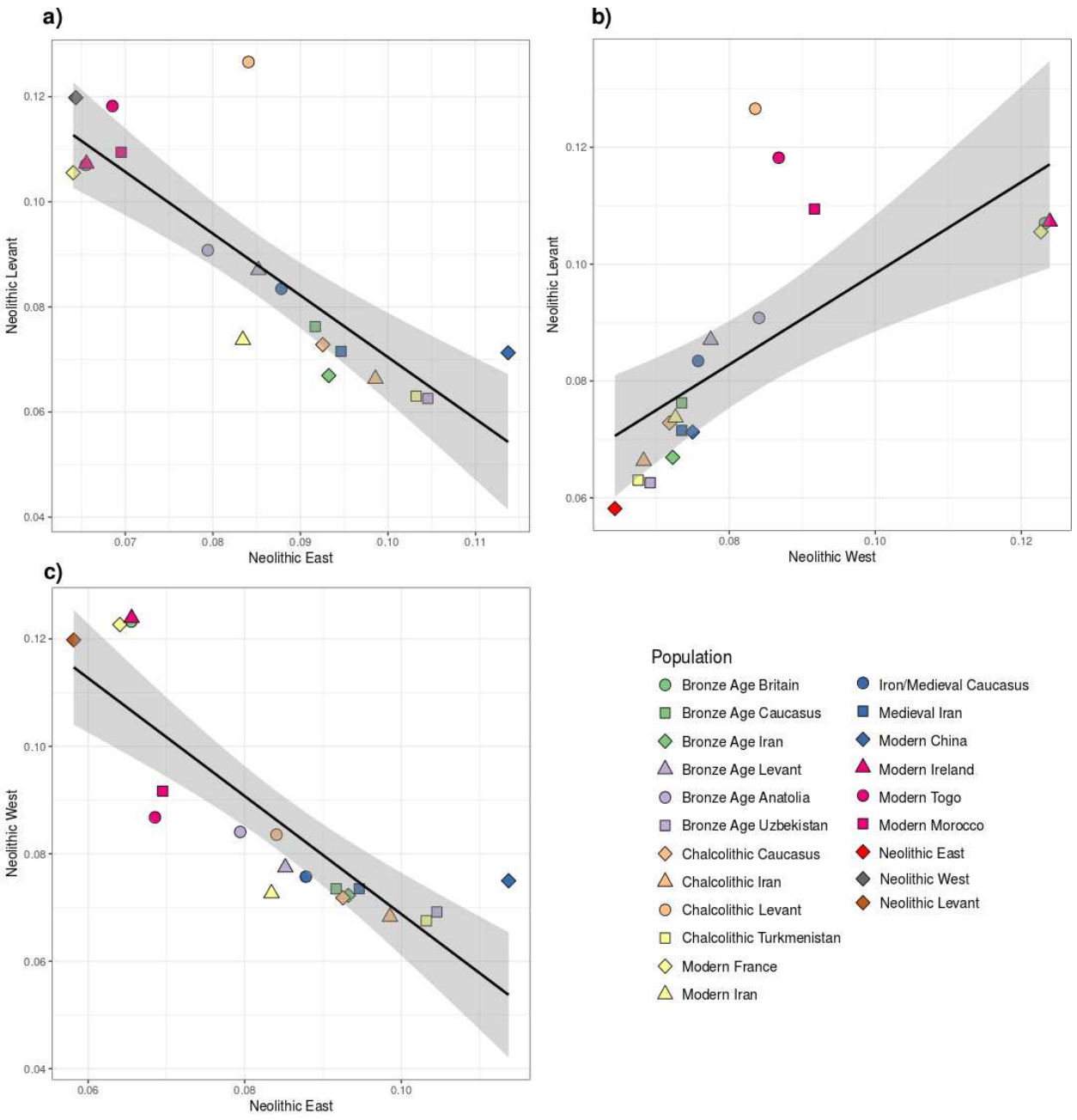

Fig. S16.

Pairwise shared drifts (f_3) plots, with linear regression and 95% confidence interval. Each domestic population shared drift with two Neolithic populations is plotted against one another: a) Neolithic Levant versus Neolithic East, b) Neolithic Levant versus Neolithic West, and c) Neolithic West versus Neolithic East. Outgroup used is Qazvin Bezoar. An excess of Levantine ancestry relative to western Neolithic ancestry is observed for African goats.

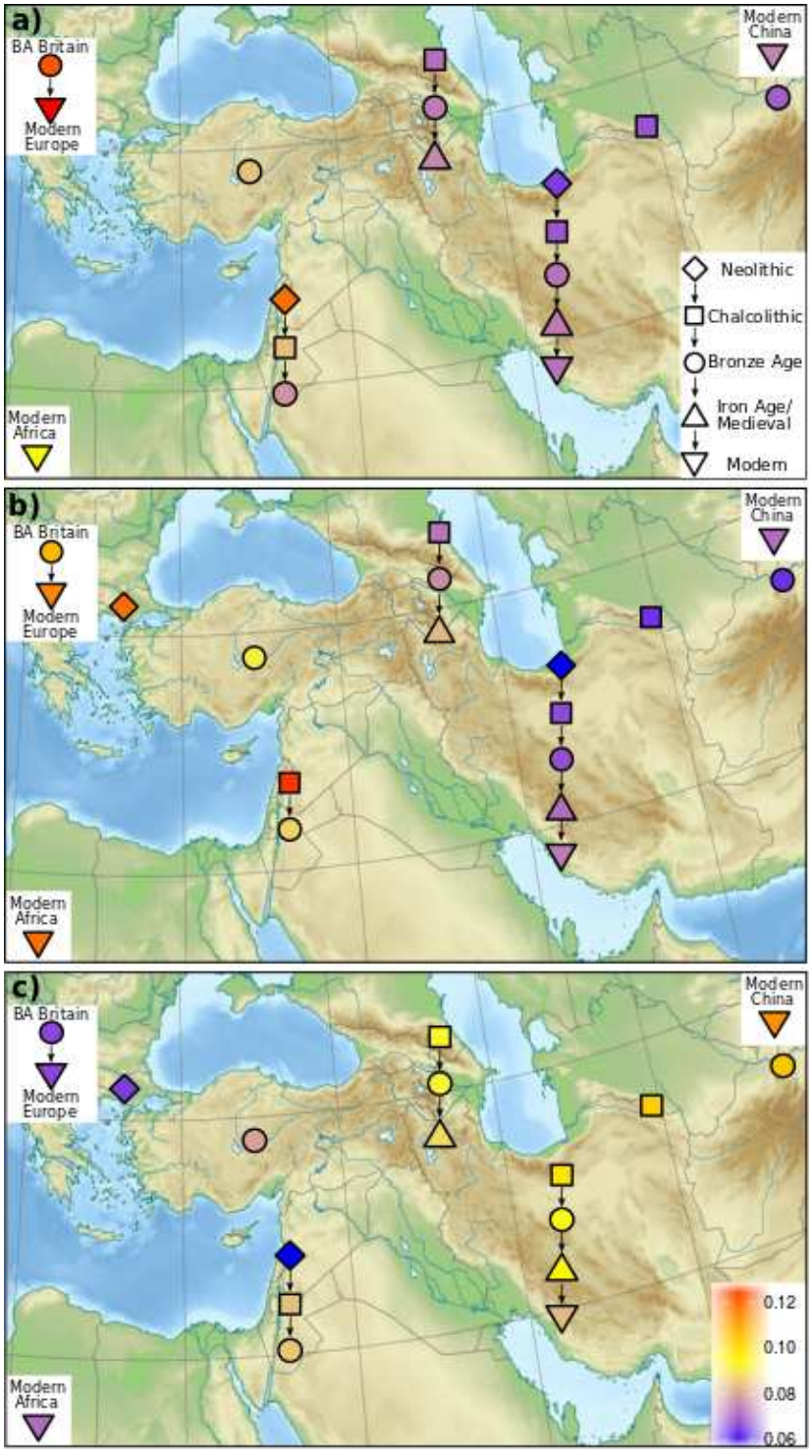

Fig. S17.

Plot of outgroup f_3 values of ancient and modern domestic goat, measuring the relative affinities with a) Neolithic West, b) Neolithic Levant, and c) Neolithic East. Qazvin Bezoar were selected as an outgroup due to the equal affinity to Neolithic East and Neolithic West, based on the *D* statistic Qazvin Bezoar(Neolithic East, Neolithic West), Z=-0.8.

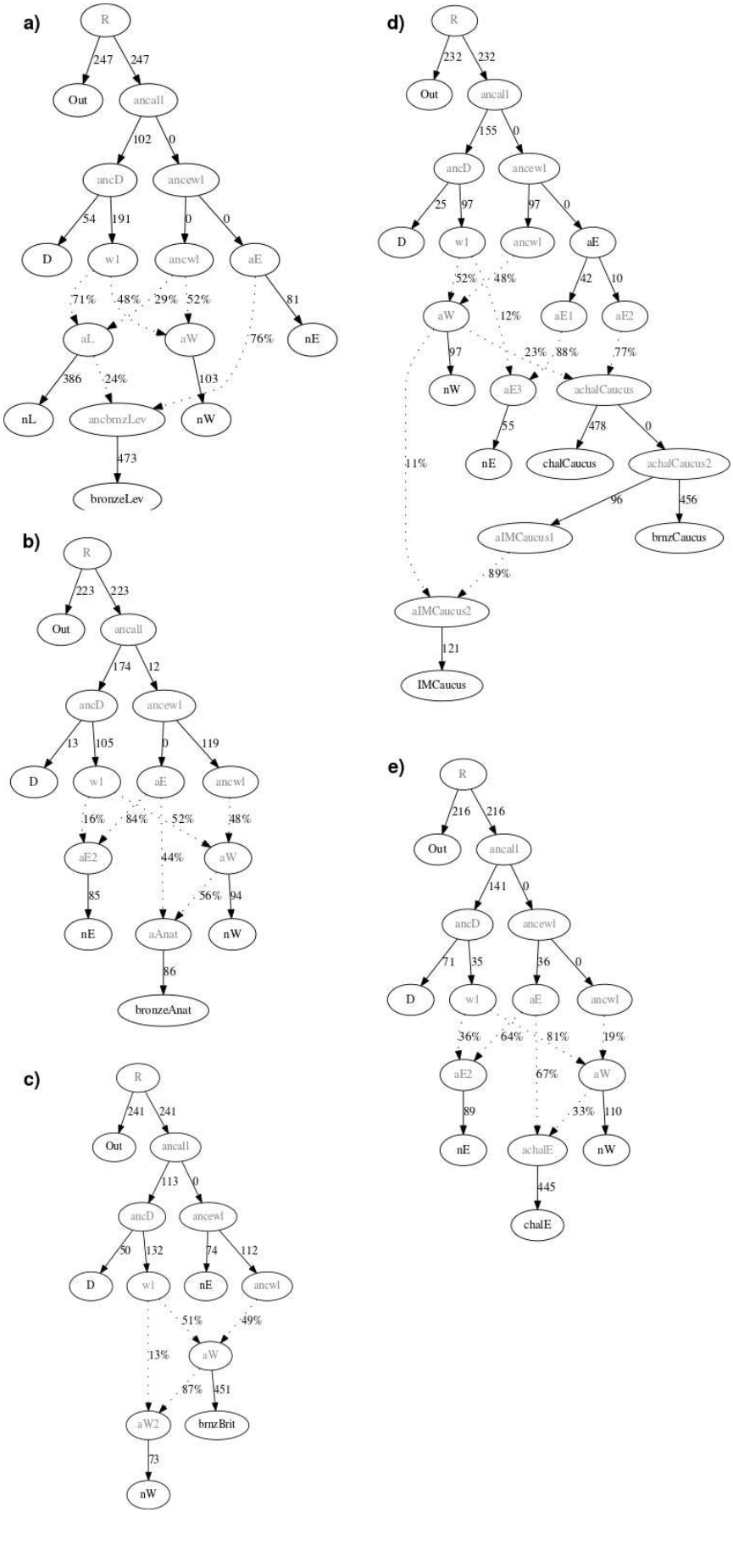
a)
R
247
247
Out
ancall
102
0
ancD
ancewl
54
191
0
0
D
w1
ancwl
aE
71%
48%
29%
52%
81
aL
aW
76%
nE
386
24%
103
nL
ancbrnzLev
nW
473
bronzeLev
b)
R
223
223
Out
ancall
174
12
ancD
ancew1
13
105
0
119
D
w1
aE
ancwl
16%
84%
52%
48%
aE2
44%
aW
85
56%
94
nE
aAnat
nW
86
bronzeAnat
c)
R
241
241
Out
ancall
113
0
ancD
ancewl
50
132
74
112
D
w1
nE
ancwl
51%
49%
13%
aW
87%
451
aW2
brnzBrit
73
nW
d)
R
232
232
Out
ancall
155
0
ancD
ancewl
25
97
97
0
D
w1
ancwl
aE
52%
48%
42
10
aW
12%
aE1
aE2
97
23%
88%
77%
nW
aE3
achalCaucus
55
478
0
11%
nE
chalCaucus
achalCaucus2
96
456
aIMCaucus1
brnzCaucus
89%
aIMCaucus2
121
IMCaucus
e)
R
216
216
Out
ancall
141
0
ancD
ancewl
71
35
36
0
D
w1
aE
ancwl
36%
64%
81%
19%
aE2
67%
aW
89
33%
110
nE
achalE
nW
445
chalE

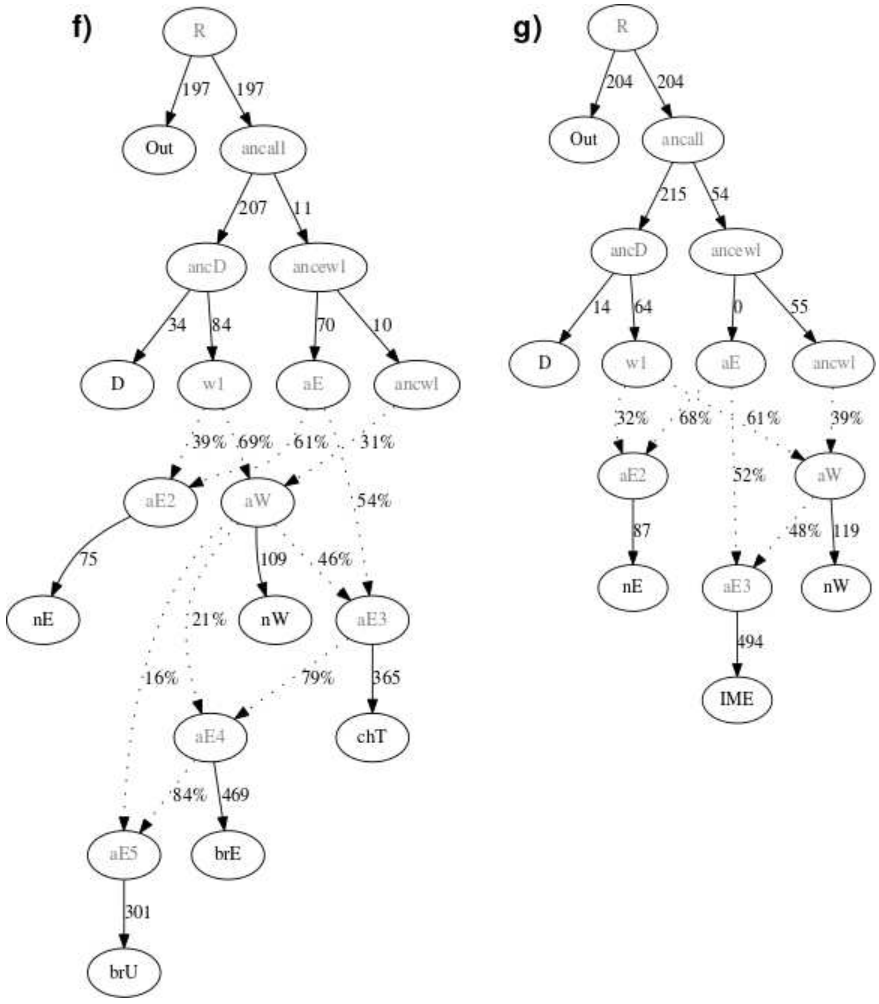

Fig. S18.

Admixture graph models for Post-Neolithic ancient domestic goats. a) Bronze Age Levant ancestry modelled as predominantly deriving from an Eastern Neolithic-like population, but with some contribution from a Neolithic Levant-related population. b) Bronze Age Anatolia modelled as roughly equal mixtures of populations related to both western and eastern Neolithics. c) Bronze Age Britain is modelled as a sister group to Neolithic West, which requires an additional wild input to fit. d), e), f), g) Post-Neolithic eastern populations relate to Neolithic East but require an input from a Neolithic West-like population, as well as additional wild ancestry in Neolithic East. Intermediate, theoretical populations are denoted in grey. Edge drift values = Fst x 1000. nW=Neolithic West, nE=Neolithic East, nL=Neolithic Levant, D=Ancient Anatolian Wild (Direkli), bronzeLev=Bronze Age Levant, bronzeAnat=Bronze Age Anatolia, brnzBrit=Bronze Age Britain, chalCaucus=Chalcolithic Caucacus, brnzCaucus=Bronze Age Caucasus, IMCaucus=Iron Age/Medieval Caucasus, chalE=Chalcolithic East, brE=Bronze Age Iran, chT=Chacolithic Turkmenistan,brU=Bronze Age Uzbekistan, IME=Iron Age/Medieval Iran

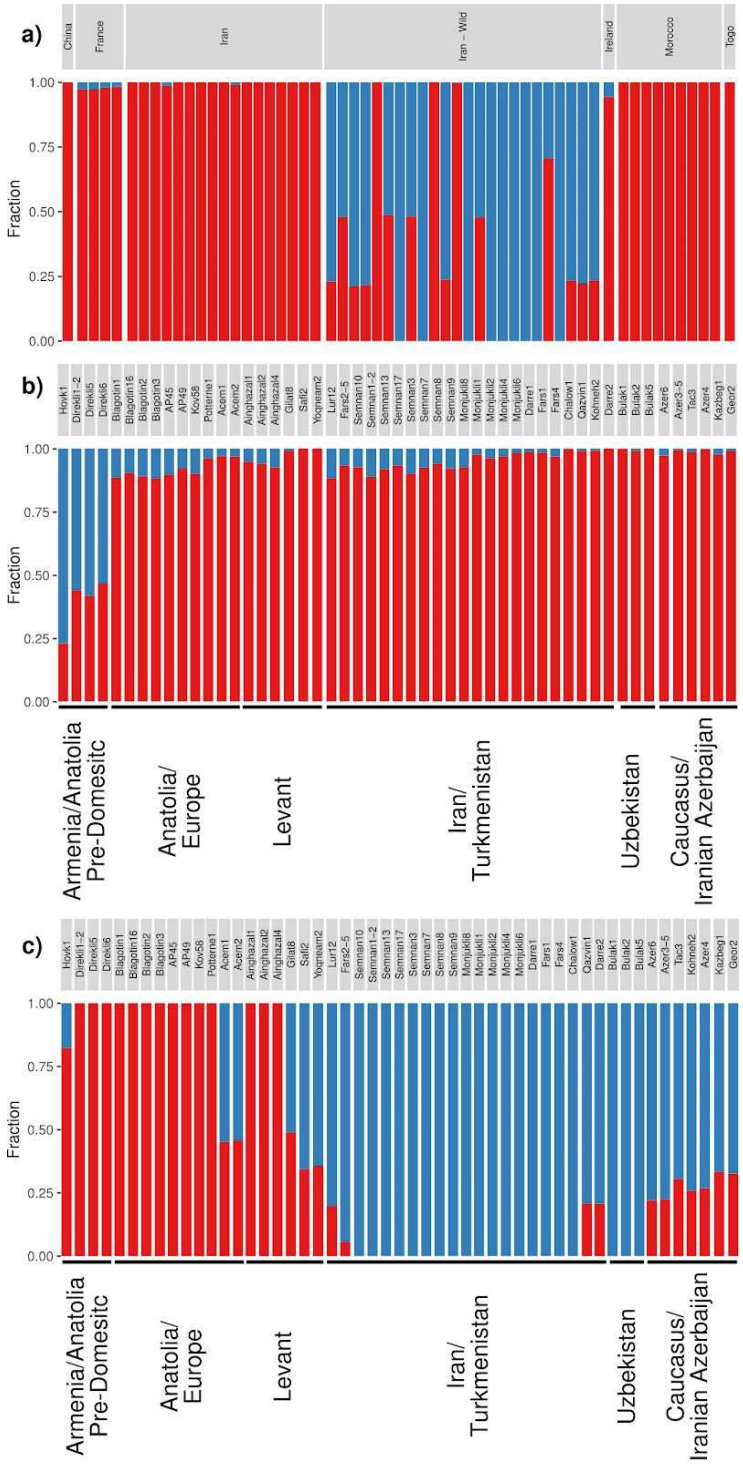

Fig. S19.

NGSadmix of a) modern and b) ancient wild and domestic goat, and c) ancient samples only. Ancestral allele frequencies and genome proportions of a) and b) were calculated together. Sample cutoff of 0.01X mean coverage. K=2. Samples within geographic region ordered by descending age.

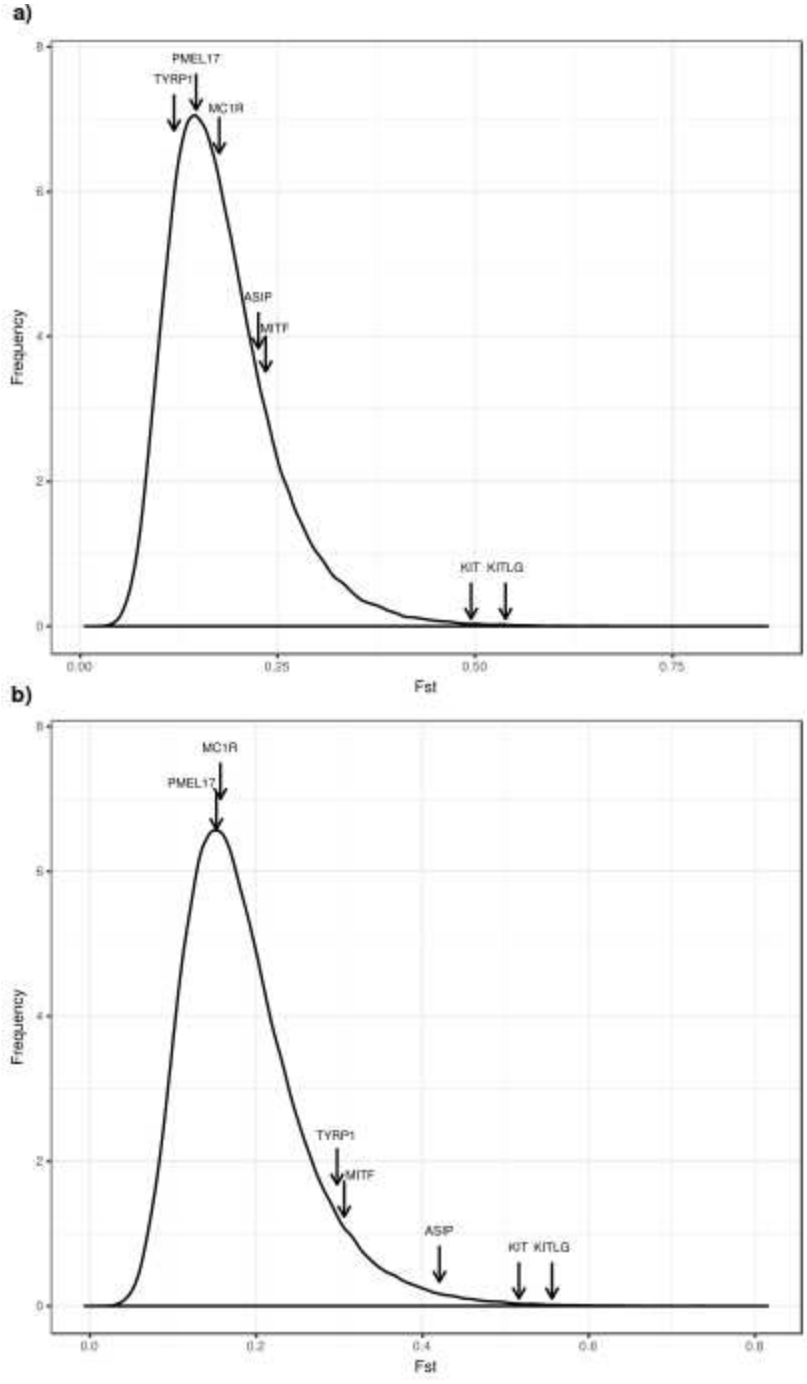

Fig. S20.

Distribution of Fst windows and pigmentation genes/outlier regions for a) Neolithic East versus Bezoar and b) Neolithic West versus Bezoar. *KIT* and *KITLG* fall on the outlier of the Fst distribution of both Neolithic East and Neolithic West.

Table S1

Sample Summary. Sample contexts marked with an asterisk indicate that the sample has been directly radiocarbon date (Table S3) - note discrepancy between contextual age of Darre2 and its radiocarbon age. mtDNA = Mitochondrial Haplogroup. Molecular Sex key: F = Female, M = Male, C.D. = Cannot Determine. Samples are ordered according to the site identifier numbers (Figure 1). Years are cal BC.

Sample	Site (Site Identifier)	Location	Context	Sex	mtDNA
Blagotin1	Blagotin-Poljna (1)	Trstenik, Serbia	Neolithic (ca. 6,100 BC)*	M	A
Blagotin2	Blagotin-Poljna (1)	Trstenik, Serbia	Neolithic (ca. 6,100 BC)*	F	A
Blagotin3	Blagotin-Poljna (1)	Trstenik, Serbia	Neolithic (ca. 6,100 BC)*	M	A
Blagotin16	Blagotin-Poljna (1)	Trstenik, Serbia	Neolithic (ca. 6,100 BC)	M	A
Uiv17	Uilvar (2)	Timişoara, Romania	Neolithic (5,250 - 5,050 BC)	F	A
Cav8	Čavdar (3)	Sofia District, Bulgaria	Neolithic (6,000 - 5,500 BC)	F	A
Ovc11	Ovčarovo-gorata (4)	Tărgovište, Bulgaria	Neolithic (5,700 - 5,500 BC)	F	A
Kov27	Kovačevo (5)	Blagoevgrad, Bulgaria	Neolithic (6,200 - 5,600 BC)	C.D.	A
Kov57	Kovačevo (5)	Blagoevgrad, Bulgaria	Neolithic (6,200 - 5,600 BC)	F	A
Kov60	Kovačevo (5)	Blagoevgrad, Bulgaria	Neolithic (6,200 - 5,600 BC)	F	A
AP38	Aşağı Pınar (6)	Kirklareli, Turkey	Neolithic*	F	C
AP44	Aşağı Pınar (6)	Kirklareli, Turkey	Neolithic (5,500 - 5,000 BC)	F	A
AP45	Aşağı Pınar (6)	Kirklareli, Turkey	Neolithic (5,300 - 5,000 BC)	F	A
AP46	Aşağı Pınar (6)	Kirklareli, Turkey	Neolithic*	F	C
AP49	Aşağı Pınar (6)	Kirklareli, Turkey	Neolithic (5,500 - 5,200 BC)	F	A
AP50	Aşağı Pınar (6)	Kirklareli, Turkey	Neolithic (5,300 - 5,000 BC)	F	A
Ulu38	Ulucak Höyük (7)	Izmir, Turkey	Neolithic (6,400 - 6,100 BC)	C.D.	A
Direkli1-2	Direkli Cave (8)	Taurus Mountains, Turkey	Epipaleolithic (ca. 9,500 BC)*	F	T
Direkli4	Direkli Cave (8)	Taurus Mountains, Turkey	Epipaleolithic (ca. 9,500 BC)*	M	F
Direkli5	Direkli Cave (8)	Taurus Mountains, Turkey	Epipaleolithic (ca. 9,500 BC)	M	T
Direkli6	Direkli Cave (8)	Taurus Mountains, Turkey	Epipaleolithic (ca. 9,500 BC)	M	T
Ghosh5	Abu Ghosh (9)	Judean Hills, Levant	Neolithic (ca. 8,000 BC)	F	F

Ainghazal1	Ain'Ghazal (10)	Amman, Jordan	Neolithic (ca. 8,000 BC)	M	F
Ainghazal2	Ain'Ghazal (10)	Amman, Jordan	Neolithic (ca. 8,000 BC)	F	F
Ainghazal3	Ain'Ghazal (10)	Amman, Jordan	Neolithic (ca. 8,000 BC)	F	F
Ainghazal4	Ain'Ghazal (10)	Amman, Jordan	Neolithic (ca. 8,000 BC)	M	F
Hovk1	Hovk-1 Cave (11)	Tavush, Armenia	Paleolithic*	F	F
Lur9	Kelek Asad Morad (12A)	Luristan, Iran	Neolithic (8,500 - 8,200 BC)	F	B
Lur12	Tepe Abdul Hosein (12B)	Luristan, Iran	Neolithic (ca. 7,000 BC)*	F	G
Semnan1-2	Sang-e Chakmaq (13)	Semnan, Iran	Neolithic (ca. 7,000 BC)*	F	B
Semnan3	Sang-e Chakmaq (13)	Semnan, Iran	Neolithic (ca. 6,000 BC)*	F	D
Semnan7	Sang-e Chakmaq (13)	Semnan, Iran	Neolithic (ca. 6,000 BC)	M	D
Semnan8	Sang-e Chakmaq (13)	Semnan, Iran	Neolithic (ca. 6,000 BC)	F	D
Semnan9	Sang-e Chakmaq (13)	Semnan, Iran	Neolithic (ca. 6,000 BC)	M	G
Semnan10	Sang-e Chakmaq (13)	Semnan, Iran	Neolithic (ca. 6,000 BC)	M	G
Semnan13	Sang-e Chakmaq (13)	Semnan, Iran	Neolithic (ca. 6,000 BC)	F	D
Semnan17	Sang-e Chakmaq (13)	Semnan, Iran	Neolithic (ca. 6,000 BC)	F	D
Fars1	Rahmat Abad (14)	Fars, Iran	Chalcolithic (ca. 4,600 BC)	M	A
Fars2-5	Rahmat Abad (14)	Fars, Iran	Neolithic (6,700 - 6,471 BC)*	M	B
Monjukli1	Monjukli Depe (15)	Meana-Čaača, Turkmenistan	Chalcolithic (5,100 - 4,500 BC)	F	A
Monjukli2	Monjukli Depe (15)	Meana-Čaača, Turkmenistan	Chalcolithic (5,100 - 4,500 BC)	F	D
Monjukli4	Monjukli Depe (15)	Meana-Čaača, Turkmenistan	Chalcolithic (5,100 - 4,500 BC)	F	A
Monjukli6	Monjukli Depe (15)	Meana-Čaača, Turkmenistan	Chalcolithic (5,100 - 4,500 BC)	M	D
Monjukli7	Monjukli Depe (15)	Meana-Čaača, Turkmenistan	Neolithic (6,400 - 5,900 BC)	F	D
Monjukli8	Monjukli Depe (15)	Meana-Čaača, Turkmenistan	Neolithic (6,400 - 5,900 BC)	M	D
Monjukli9	Monjukli Depe (15)	Meana-Čaača, Turkmenistan	Neolithic (6,400 - 5,900 BC)	M	G
Pie17	Pietrele (16)	Giurgiu, Romania	Chalcolithic (4,450 - 4,250 BC)	F	A
Dra34	Merdžumekja (17)	Drama, Bulgaria	Chalcolithic*	F	G
Kan19	Kanlıgeçit (18)	Kirklareli,Turkey	Bronze Age (2,700 - 2,200 BC)	C.D.	A
Kan23	Kanlıgeçit (18)	Kirklareli,Turkey	Bronze Age*	M	G

Kan25	Kanlıgeçit (18)	Kirklareli,Turkey	Bronze Age (2,700 - 2,200 BC)	C.D.	A
Acem1	Acemhöyük (19)	Aksaray Plain, Turkey	Bronze Age (ca. 2,500 BC)*	F	A
Acem2	Acemhöyük (19)	Aksaray Plain, Turkey	Bronze Age (ca. 1700 BC)	M	A
Tac1	Tachti Perda (20A)	Kakheti, Georgia	Bronze Age (1,400 - 1,000 BC)	F	A
Tac2	Tachti Perda (20A)	Kakheti, Georgia	Iron Age (1,000 - 700 BC)	F	A
Tac3	Tachti Perda (20A)	Kakheti, Georgia	Bronze Age (1,400 - 1,000 BC)	F	A
Geor2	Tamara Fort (20B)	Kazbegi, Georgia	Medieval (1,001 - 1,500 AD)	M	A
Kazbeg1	Tamara Fort (20B)	Kazbegi, Georgia	Medieval (901 - 1,000 AD)	F	A
Kohneh2	Kohneh Tepesi (21)	Azerbaijan, Iran	Bronze Age (3,300 - 3,000 BC)	F	A
Azer3-5	Tepe Hasanlu (22A)	Western Azerbaijan, Iran	Bronze Age (2,200-2,100 BC)	F	A
Azer4	Tepe Hasanlu (22A)	Western Azerbaijan, Iran	Iron Age (550 - 330 BC)	M	A
Azer6	Soha Chai Tepe (22B)	Zanjan, Iran	Chalcolithic (ca. 4,200 BC)	F	A
Qazvin1	Tepe Chizar (23)	Qazvin, Iran	Bronze Age (2,400 - 1,900 BC)	F	A
Darre1	Darre-ye Bolāghi (24A)	Fars, Iran	Chalcolithic (5,000 - 4,000 BC)	F	A
Darre2	Darre-ye Bolāghi (24A)	Fars, Iran	Chalcolithic (5,000 - 4,000 BC)*	F	A
Fars4	Mianrud (14/24C)	Fars, Iran	Chalcolithic (5,550 - 4,200 BC)*	F	A
Chalow1	Chalow (25)	Khorasan, Iran	Bronze Age (2,300 - 2,000 BC)	M	D
Bulak1	Tilla Bulak (26)	Surkhandarja, Uzbekistan	Bronze Age (2,000 - 1,700 BC)	F	A
Bulak2	Tilla Bulak (26)	Surkhandarja, Uzbekistan	Bronze Age (2,000 - 1,700 BC)	M	A
Bulak3	Tilla Bulak (26)	Surkhandarja, Uzbekistan	Bronze Age (2,000 - 1,700 BC)	F	A
Bulak4	Tilla Bulak (26)	Surkhandarja, Uzbekistan	Bronze Age (2,000 - 1,700 BC)	M	B
Bulak5	Tilla Bulak (26)	Surkhandarja, Uzbekistan	Bronze Age (2,000 - 1,700 BC)	F	D
Shiqmim1	Shiqmim (27A)	Northern Negev, Levant	Chalcolithic (4,300 - 3,700 BC)	F	D
Shiqmim9	Shiqmim (27A)	Northern Negev, Levant	Chalcolithic (4,300 - 3,700 BC)	M	D
Gilat2	Gilat (27B)	Northern Negev, Levant	Chalcolithic (4,500 - 4,200 BC)	M	A

Gilat8	Gilat (27B)	Northern Negev, Levant	Chalcolithic (4,500 - 4,200 BC)	M	D
Gilat10	Gilat (27B)	Northern Negev, Levant	Chalcolithic (4,500 - 4,200 BC)	F	A
Yarmut1	Tel Yarmuth (28A)	Bet Shemesh, Levant	Bronze Age (2,700 - 2,500 BC)	M	A
Yarmut7	Tel Yarmuth (28A)	Bet Shemesh, Levant	Bronze Age (2,650 - 2,200 BC)	F	A
Yoqneam2	Tel Yoqne'am (28B)	Haifa, Levant	Bronze Age (1,650 - 1,540 BC)	F	A
Safi2	Tel es-Safi/Gath (28C)	Ashkelon, Levant	Bronze Age (2,570 - 2,900 BC)	F	A
Miqne5	Tel Miqne-Ekron (28D)	Shephelah, Levant	Iron Age (ca. 700 BC)	M	A
Potterne1	Potterne (29)	Wiltshire, UK	Bronze Age (2,040 - 990 BC)	F	A

Table S2
Sample Groupings for PCA and ANGSD analyses. Samples are ordered as in Table S1, according to their site number.

Sample	Grouping for PCA	Grouping for autosomal analysis
Blagotin1	Neolithic West	Neolithic West
Blagotin2	Neolithic West	Neolithic West
Blagotin3	Neolithic West	Neolithic West
Blagotin16	Neolithic West	Neolithic West
Uiv17	-	-
Cav8	-	-
Ovc11	-	-
Kov27	-	-
Kov57	Neolithic West	Neolithic West
Kov60	-	-
AP38	Neolithic West	-
AP44	Neolithic West	-
AP45	Neolithic West	Neolithic West
AP46	Neolithic West	-
AP49	Neolithic West	Neolithic West
AP50	Neolithic West	-
Ulu38	-	-
Direkli1-2	Predomestic Bezoar	Predomestic Anatolia
Direkli4	-	-
Direkli5	Predomestic Bezoar	Predomestic Anatolia
Direkli6	Predomestic Bezoar	Predomestic Anatolia
Ghosh5	-	-
Ainghazal1	Neolithic Levant	Neolithic Levant
Ainghazal2	Neolithic Levant	Neolithic Levant
Ainghazal3	Neolithic Levant	-
Ainghazal4	Neolithic Levant	Neolithic Levant
Hovk1	Predomestic Bezoar	Predomestic Anatolia
Lur9	-	-
Lur12	Neolithic East	Neolithic East

Semnan1-2	Neolithic Iran	Neolithic East
Semnan3	Neolithic Iran	Neolithic East
Semnan7	Neolithic Iran	Neolithic East
Semnan8	Neolithic Iran	Neolithic East
Semnan9	Neolithic Iran	Neolithic East
Semnan10	Neolithic Iran	Neolithic East
Semnan13	Neolithic Iran	Neolithic East
Semnan17	Neolithic Iran	Neolithic East
Fars1	Post-Neolithic East	Chalcolithic Iran
Fars2-5	Neolithic East	Neolithic East
Monjukli1	Post-Neolithic East	Chalcolithic Turkmenistan
Monjukli2	Post-Neolithic East	Chalcolithic Turkmenistan
Monjukli4	Post-Neolithic East	Chalcolithic Turkmenistan
Monjukli6	Post-Neolithic East	Chalcolithic Turkmenistan
Monjukli7	Neolithic East	-
Monjukli8	Neolithic East	Neolithic East
Monjukli9	Neolithic East	-
Pie17	-	-
Dra34	-	-
Kan19	-	-
Kan23	-	-
Kan25	-	-
Acem1	Bronze Age Anatolia	Bronze Age Anatolia
Acem2	Bronze Age Anatolia	Bronze Age Anatolia
Tac1	Post-Neolithic East	-
Tac2	Post-Neolithic East	-
Tac3	Post-Neolithic East	Bronze Age Caucasus
Kazbeg1	Post-Neolithic East	Iron Age/Medieval Caucasus
Geor2	Post-Neolithic East	Iron Age/Medieval Caucasus
Kohneh2	Post-Neolithic East	Bronze Age Caucasus
Azer3-5	Post-Neolithic East	Bronze Age Caucasus
Azer4	Post-Neolithic East	Iron Age/Medieval Caucasus
Azer6	Post-Neolithic East	Chalcolithic Caucasus
Qazvin1	Post-Neolithic East	Bronze Age Iran

Darre1	Post-Neolithic East	Chalcolithic Iran
Darre2	Post-Neolithic East	Medieval Iran
Fars4	Post-Neolithic East	Chalcolithic Iran
Chalow1	Post-Neolithic East	Bronze Age Iran
Bulak1	Post-Neolithic East	Bronze Age Uzbekistan
Bulak2	Post-Neolithic East	Bronze Age Uzbekistan
Bulak3	-	-
Bulak4	-	-
Bulak5	Post-Neolithic East	Bronze Age Uzbekistan
Shiqmim1	Post-Neolithic Levant	Chalcolithic Levant
Shiqmim9	Post-Neolithic Levant	Chalcolithic Levant
Gilat2	Post-Neolithic Levant	-
Gilat8	Post-Neolithic Levant	Chalcolithic Levant
Gilat10	Post-Neolithic Levant	-
Yarmut1	Post-Neolithic Levant	Bronze Age Levant
Yarmut7	Post-Neolithic Levant	Bronze Age Levant
Yoqneam2	Post-Neolithic Levant	Bronze Age Levant
Safi2	Post-Neolithic Levant	Bronze Age Levant
Miqne5	Post-Neolithic Levant	-
Potterne1	Bronze Age Britain	Bronze Age Britain

Table S3

Radiocarbon Dating Information. 2 sigma calibration was performed using Oxcal 4.3 (*26*, *27*) and IntCal 13 (*28*).

Codex name	C14 Code	Context	Conventional Age (BP)	Calibrated C14 date (95.4% Probability)
Semnan1-2	UBA-33144	Neolithic	8157 +/- 74	7454-6850 cal BC
Semnan3	UBA-33145	Neolithic	7214 +/- 53	6214-6004 cal BC
Blagotin1	UBA-30289	Neolithic	7391 +/- 56	6398-6098 cal BC
Blagotin2	UBA-30290	Neolithic	7361 +/- 62	6379-6078 cal BC
Blagotin3	UBA-30292	Neolithic	7135 +/- 53	6096-5892 cal BC
Fars4	UBA-34976	Chalcolithic	6311 +/- 42	5460-5211 cal BC
AP38	KIA-42163	Neolithic	6390 +/- 30	5468-5316 cal BC
AP46	KIA-42164	Neolithic	6210 +/- 30	5293-5057 cal BC
Hovk1	UBA-31978	Paleolithic	>47074	NA
Dra34	ERL-12297	Chalcolithic	5636 +/- 49	4580-4354 cal BC
Kan23	KIA-42159	Bronze Age	4020 +/- 40	2833-2465 cal BC
Acem1	UBA-30288	Bronze Age	3782 +/- 41	2346-2040 cal BC
Direkli4	Beta-432464	Late Epipaleolithic	12130 +/- 40	12191-11882 cal BC
Direkli1-2	Beta-425280	Late Epipaleolithic	11370 +/- 40	11351-11166 cal BC
Lur12	Beta-470334	Neolithic	8810 +/- 30	8171-7745 cal BC
Fars2-5	Beta-470335	Neolithic	7980 +/- 30	7047-6772 cal BC
Darre2	UBA-34977	Chalcolithic	337 +/- 30	1473-1641 cal AD

Table S4

Sequencing statistics for whole genome samples. Samples are ordered as in Table S1, according to their site number.

Sample Name	Raw Read Count	Filtered Read count (>30bp)	Aligned Reads	Total reads after rmdup	Aligned reads after rmdup	q30 Aligned reads	Endogenous Content	Coverage (q30)
Blagotin1	1374961979	1216553609	1027304768	725051664	535802823	368273417	73.90	6.99
Blagotin2	1015818158	912908506	685826030	552273147	325190671	214314969	58.88	4.02
Blagotin3	785079584	1154899365	5216937865	930254368	820784420	618138762	88.23	11.47
Blagotin16	731037823	629697308	482748215	439295991	292346898	202242150	66.55	3.51
Kov57	62554831	58600604	5833945	57233074	4466415	3284888	7.80	0.07
AP45	57607602	48701302	2724863	47069521	1093082	695529	2.32	0.02
AP49	55105031	48449690	2170311	47692824	1413445	965079	2.96	0.02
Direkli1-2	1495484385	1352546196	941037602	1163399242	751890648	575128810	64.63	11.55
Direkli5	235416747	189541015	23245207	184814055	18518247	13083848	10.02	0.27
Direkli6	800438918	702517029	273524868	606627244	177635083	97371651	29.28	1.93
Ghosh5	20088538	19681029	12497	19680372	11840	7964	0.06	0.0001
Ainghazal1	83187399	75269854	3198903	74662520	2591569	1655535	3.47	0.03
Ainghazal2	128756310	119316119	5189545	118358959	4232385	3050323	3.58	0.06
Ainghazal3	74822625	72860762	258705	72839487	237430	155923	0.33	0.003
Ainghazal4	63597170	58367881	581645	58321821	535585	380297	0.92	0.01
Hovk1	493158399	479794460	216201216	450104781	186511537	133767664	41.44	3.08
Lur9	28327887	27426734	14520	27424848	12634	6863	0.05	0.0001
Lur12	622799577	606327375	90171769	589678393	73522787	49649146	12.47	1.05
Semnan1-2	512101554	1291151802	1216069964	1177640529	441646936	307561107	37.50	6.85
Semnan3	1290320470	1200758638	1053612961	943384035	792665122	624844041	84.02	14.89
Semnan7	264055600	235981957	70620635	211030082	128698407	181257506	60.99	3.28
Semnan8	145452599	131528398	27853991	121541550	17901036	12044508	14.73	0.21
Semnan9	363158752	344779210	271580143	252094796	178931891	134297213	70.98	3.05
Semnan10	526572133	482652509	195110498	398958390	111421418	76498235	27.93	1.43
Semnan13	385192146	370035589	215225143	290004604	135194158	100635730	46.62	2.54
Semnan17	85716449	82439264	15423383	75075910	8060029	5536825	10.74	0.12
Fars1	99020181	91837535	1548425	91768937	1479827	1034923	1.61	0.02
Fars2-5	90558575	88511665	2290892	88352205	2131432	1594541	2.41	0.03
Monjukli1	136651989	134153896	17216066	131030587	14092757	10310059	10.76	0.24
Monjukli2	104714174	103396156	13168495	101263399	11035738	8285525	10.90	0.21
Monjukli4	152229139	149118748	61381879	130057199	42320330	26112882	32.54	0.6
Monjukli6	23893097	23044817	2103345	22801351	1859879	1331463	8.16	0.03
Monjukli8	703151022	693598812	218375612	621245514	145172327	108285172	23.37	2.57
Acem1	535429853	479546615	390919313	398281063	309653761	223852082	77.75	4.76
Acem2	619205809	593031928	550580477	524275148	483899634	386712744	92.30	8.67

Tac3	57168101	49613035	17565101	40038836	7990902	5436690	19.96	0.13
Geor2	95217083	91863838	77607028	80692443	67514099	55121287	83.67	1.5
Kazbeg1	238441921	229262502	212461394	208682478	191881370	154299869	91.95	3.84
Kohneh2	14556493610	14639765752	3527754	33598312	3193277	2288871	9.50	0.04
Azer3-5	443123933	423297739	327085891	373433039	277381877	215865631	74.28	4.66
Azer4	232495520	224771105	193580054	173573899	142382848	110460711	82.03	2.57
Azer6	76508162	74024096	24448642	67035604	17460150	12825718	26.05	0.28
Qazvin1	348762506	336691099	169724178	257342838	184052376	140793855	71.52	3.16
Darre1	29565706	28494367	3162626	28125220	2793479	1997846	9.93	0.04
Darre2	261028786	250473871	219847784	230083532	199457445	161767556	86.69	3.93
Fars4	297308440	292702230	67002909	285797590	60098269	46280618	21.03	1.05
Bulak1	85489637	82832962	60012053	73493716	50672807	37602935	68.95	0.87
Bulak2	341223653	324211812	233519547	268169941	178162940	132665825	66.44	2.67
Bulak3	85110322	82036020	47896157	73277455	39137592	29187922	53.41	0.61
Bulak5	84666432	82853966	26122691	75571511	18840236	13700560	24.93	0.27
Chalow1	31355259	30944769	3284797	30548747	2888775	2033240	9.46	0.05
Shiqmim1	77911468	75040580	261432	75002748	223600	127811	0.30	0.0003
Shiqmim9	34543992	32852520	63403	32843295	54178	34456	0.16	0.0006
Gilat2	24581161	21607163	121796	21600257	114890	74236	0.53	0.012
Gilat8	102535491	97354551	1606816	97093658	1345923	805562	1.39	0.02
Gilat10	27002137	25701503	78520	25688876	65893	38180	0.26	0.0006
Yarmut1	39436031	38023365	134278	38015875	126788	88570	0.33	0.0013
Yarmut7	39308249	36288841	78084	36285009	74252	49504	0.20	0.008
Yoqneam2	246811430	240328651	151357469	220728269	131757087	100785472	59.69	2.2
Safi2	60911590	59866759	3305158	59491905	2930304	1949107	4.93	0.04
Miqne5	22442210	20880056	45657	20878262	43863	30629	0.21	0.0005
Potterne1	235320071	230025893	202851037	211757594	184582738	150603738	87.17	3.67

Table S5
lcMLkin results for top 30 pi_HAT comparisons.

Ind1	Ind2	k0_hat	k1_hat	k2_hat	pi_HAT	nbSNP
Direkli1	Direkli2	0.002	0.055	0.943	0.971	7700
Azer3	Azer5	0.001	0.098	0.902	0.95	5569
Semnan1	Semnan2	0.004	0.104	0.892	0.944	7601
Bulak1	Bulak3	0.036	0.052	0.912	0.938	2300
AP49	Blagotin16	0.48	0.236	0.284	0.402	167
Fars1	Fars4	0.407	0.398	0.195	0.394	134
Azer3	Darre1	0.22	0.778	0.002	0.391	212
AP45	Blagotin1	0.605	0.055	0.34	0.368	135
Darre2	Kohneh2	0.387	0.548	0.065	0.339	300
Fars5	Geor2	0.344	0.653	0.003	0.329	166
Direkli5	Kov58	0.571	0.234	0.195	0.312	107
Fars1	Yoqneam2	0.548	0.298	0.154	0.303	158
Azer4	Fars5	0.443	0.548	0.01	0.283	221
Monjukli1	Tac3	0.56	0.322	0.119	0.28	203
Ainghazal1	Blagotin3	0.682	0.093	0.225	0.271	260
Direkli1	Direkli6	0.518	0.435	0.047	0.265	5482
Semnan17	Semnan9	0.618	0.259	0.122	0.252	861
Semnan7	Semnan9	0.579	0.35	0.072	0.247	8248
Monjukli8	Semnan8	0.629	0.256	0.115	0.243	1354
Fars1	Qazvin1	0.74	0.045	0.215	0.238	173
Fars5	Semnan13	0.531	0.463	0.005	0.237	201
Chalow1	Lur12	0.741	0.055	0.204	0.231	228
Semnan13	Semnan7	0.587	0.365	0.048	0.231	7450
Semnan17	Semnan8	0.563	0.42	0.016	0.227	177
AP45	Blagotin2	0.56	0.428	0.013	0.226	128
Direkli2	Direkli6	0.607	0.336	0.057	0.225	6785
Blagotin16	Blagotin1	0.636	0.282	0.082	0.223	8705
Bulak2	Chalow1	0.748	0.065	0.187	0.22	365
Blagotin2	Blagotin3	0.61	0.342	0.048	0.219	8990
Blagotin1	Blagotin3	0.626	0.311	0.063	0.218	9461

Table S6

Mitochondrial alignment statistics for all samples, and read counts for mitochondrial-only samples. Samples are ordered as in Table S1, according to their site number.

Sample Name	Raw Read Count	Filtered Read count (>30bp)	>q30 Aligned reads	Coverage	Called Sites	%age called	mtDNA
Blagotin1	-	-	156487	544.63	16643	100.00	A
Blagotin2	-	-	109741	253.67	16643	100.00	A
Blagotin3	-	-	280193	885.45	16643	100.00	A
Blagotin16	-	-	101595	296.4	16643	100.00	A
Uiv17	2322143	2160471	268	0.95	1319	7.93	A
Cav8	1950148	1805472	146	0.58	7668	46.1	A
Ovc11	2146471	1996697	2521	8.63	15392	92.48	A
Kov27	2677699	2509963	802	3.12	9840	59.12	A
Kov57	3343260	3169499	1695	5.86	14259	85.68	A
Kov60	3241805	3013787	1884	6.97	15335	92.14	A
AP38	3534095	3019548	2258	7.61	15606	93.77	C
AP44	4165328	3806850	1078	3.57	10353	62.21	A
AP45	2289122	2033528	1874	6.47	14762	88.70	A
AP46	4532848	4175633	2834	9.77	16264	97.72	C
AP49	5315007	4799636	3744	12.69	16321	98.07	A
AP50	1849766	1709269	4262	14.31	16437	98.76	A
Ulu38	1743758	1612570	139	0.46	5849	35.1	A
Direkli1-2	-	-	263108	998.17	16436	98.76	T
Direkli4	213614388	187947946	42267	142.69	16481	99.03	F
Direkli5	-	-	38545	120.94	16327	98.10	T
Direkli6	-	-	147902	523.8	16405	98.57	T
Ghosh5	71302178	70329490	1970	6.25	13020	78.23	F
Ainghazal1	14251531	13532330	1930	5.46	12484	75.01	F
Ainghazal2	23443628	22984015	4464	12.78	15492	93.08	F
Ainghazal3	19347204	18976966	1363	4.25	10518	63.20	F
Ainghazal4	4413908	3983747	20575	65.44	16266	97.73	F
Hovk1	-	-	106522	519.39	16564	99.53	F
Lur9	4076792	3841739	653	1.69	16643	100.00	B
Lur12	-	-	127542	480	16643	100.00	G
Semnan1-2	-	-	211679	533.55	16595	99.71	B
Semnan3	-	-	328688	887.12	16643	100.00	D
Semnan7	-	-	103257	204.62	16643	100.00	D
Semnan8	-	-	26486	76.45	16643	100.00	D

Semnan9	-	-	103357	394.12	16643	100.00	G
Semnan10	-	-	122939	369.08	16643	100.00	G
Semnan13	-	-	27173	109.05	16643	100.00	D
Semnan17	-	-	35406	149.93	16643	100.00	D
Fars1	787006	724742	18142	40.38	16334	98.14	A
Fars2-5	7737720	7595927	190296	284.47	16643	100.00	B
Monjukli1	-	-	11337	96.78	16634	99.95	A
Monjukli2	-	-	22198	90.55	16643	100.00	D
Monjukli4	-	-	24260	123.04	16643	100.00	A
Monjukli6	494880	484544	31473	123.04	16643	100.00	D
Monjukli7	1436980	1372200	8835	31.87	16596	99.72	D
Monjukli8	-	-	97168	411.74	16643	100.00	D
Monjukli9	1276894	1232219	9637	33.02	16489	99.07	G
Pie17	3609599	3315507	2175	6.98	14815	89.02	A
Dra34	3962976	3762093	1594	5.44	13942	83.77	G
Kan19	5512329	5324761	2524	8.55	15133	90.93	A
Kan23	5371322	4640116	3297	10.56	16132	96.93	G
Kan25	5661187	5395828	2737	8.97	15222	91.46	A
Acem1	-	-	121434	411.03	16643	100.00	A
Acem2	-	-	214607	849.8	16643	100.00	A
Tac1	4805905	4499253	3389	11.45	16150	97.04	A
Tac2	4353357	4024959	2713	12.39	16641	99.99	A
Tac3	1791228	1668795	6193	25.27	16564	99.53	A
Geor2	-	-	35923	108	16535	99.35	A
Kazbeg1	-	-	48701	256.38	16641	99.99	A
Kohneh2	1347714	1266365	9516	29.56	16228	97.51	A
Azer3-5	-	-	136757	487.2	16643	100.00	A
Azer4	-	-	80707	309.59	16643	100.00	A
Azer6	94508	93159	9876	44	16632	99.93	A
Qazvin1	-	-	89984	448.01	16643	100.00	A
Darre1	801170	777629	26121	42.51	16332	98.13	A
Darre2	-	-	75967	365.56	16643	100.00	A
Fars4	-	-	30679	109.24	16643	100.00	A
Bulak1	-	-	56375	220.47	16643	100.00	A
Bulak2	-	-	67627	284.97	16643	100.00	A
Bulak3			50383	180.39	16643	100.00	A
Bulak4	456947	447106	17250	60.58	16591	99.69	B
Bulak5	-	-	31277	113.99	16643	100.00	D
Chalow1	2794368	2771283	69257	341.05	16643	100.00	D

Shiqmim1	44001686	43434209	4151	7	13292	79.87	D
Shiqmim9	1920566	1839287	247	0.85	1139	6.84	D
Gilat2	1779611	1617254	7066	16.58	15564	93.52	A
Gilat8	6635559	6474630	34690	133.77	16557	99.48	D
Gilat10	5784648	5582429	639	2.05	5636	33.86	A
Yarmut1	3524909	3392110	13436	40.41	16236	97.55	A
Yarmut7	1591537	1456896	3976	11.1	15282	91.82	A
Yoqneam2	-	-	92996	472.98	16643	100.00	A
Safi2	1886858	1858363	36440	134.14	16628	99.91	A
Miqne5	2352930	2165308	5389	12.22	15322	92.06	A
Potterne1	-	-	36623	217.21	16643	100.00	A

Table S7
Mitochondrial sequences used in study. Sequences used for mitochondrial realignment are indicated in bold text.

Name used	Accession No.	Haplogroup	Name used	Accession No.	Haplogroup
A1_01	KR059146.1	A1	A_45	KR059189.1	A
A1a_02	KR059147.1	A1a	A_46	KR059190.1	A
A1a_03	KR059148.1	A1a	A_47	KR059191.1	A
A1a_04	KR059149.1	A1a	A_48	KR059192.1	A
A1a_05	KR059150.1	A1a	A_49	KR059193.1	A
A1a_06	KR059151.1	A1a	A_50	KR059194.1	A
A2_07	KR059152.1	A2	A_51	KR059195.1	A
A2_08	KR059153.1	A2	A_52	KR059196.1	A
A2_09	KR059154.1	A2	A_53	KR059197.1	A
A2a_10	KR059155.1	A2a	A_54	KR059198.1	A
A2a_11	KR059156.1	A2a	A_55	KR059199.1	A
A2a1_12	KR059157.1	A2a1	A_56	KR059200.1	A
A2a1_13	KR059158.1	A2a1	A_57	KR059201.1	A
A2a1_14	KR059159.1	A2a1	A_58	KR059202.1	A
A2a1_15	KR059160.1	A2a1	A_59	KR059203.1	A
A2a1_16	KR059161.1	A2a1	A_60	KR059204.1	A
A2a1_17	KR059162.1	A2a1	A_61	KR059205.1	A
A2a1_18	KR059163.1	A2a1	A_62	KR059206.1	A
A2a1_19	KR059164.1	A2a1	A_63	KR059207.1	A
A3_20	KR059165.1	A3	A_64	KR059208.1	A
A3_21	KR059166.1	A3	A_65	KR059209.1	A
A3_22	KR059167.1	A3	D_bezoar_66	KR059210.1	D
A3_23	KR059168.1	A3	**D1_67**	KR059211.1	D1
A3_24	KR059169.1	A3	D1_68	KR059212.1	D1
A4_25	KR059170.1	A4	**G_69**	KR059213.1	G
A4_26	KR059171.1	A4	G_70	KR059214.1	G
A4_27	KR059172.1	A4	G_71	KR059215.1	G
A4_28	KR059173.1	A4	G_72	KR059216.1	G
A5_29	KR059174.1	A5	G_73	KR059217.1	G
A5_30	KR059175.1	A5	G_74	KR059218.1	G

A5_31	KR059176.1	A5	B_bezoar_75	KR059219.1	B
A5_32	KR059177.1	A5	B1_78	KR059220.1	B1
A6_33	KR059178.1	A6	C_bezoar_79	KR059221.1	C
A6_34	KR059179.1	A6	C1_bezoar_80	KR059222.1	C1
A7_36	KR059180.1	A7	**C1a_81**	KR059223.1	C1a
A7_37	KR059181.1	A7	C1a_82	KR059224.1	C1a
A7_38	KR059182.1	A7	C1a_83	KR059225.1	C1a
A_39	KR059183.1	A	**F_bezoar_84**	KR059226.1	F
A_40	KR059184.1	A	Goat Reference	NC_005044.2	D1
A_41	KR059185.1	A	Bezoar Reference	NC_028161.1	G
A_42	KR059186.1	A	**West Caucasus Tur**	NC_020683.1	Outgroup
A_43	KR059187.1	A	Nubian Ibex	NC_020624.1	Outgroup
A_44	KR059188.1	A	Markhor	NC_020622.1	Outgroup

Table S8

BEAST estimation of clock rates - using four partitions, two partitions, and four partitions with "Tur-like" sequences.

Partitions	Mean	Median	Standard Deviation	95% HPD	ESS
Four Partitions					
clockRate.D_loop	8.32E-07	8.27E-07	1.02E-07	[6.4522E-7, 1.0392E-6]	4855
clockRate.tRNA+rRNA+remainder	2.52E-08	2.51E-08	2.98E-09	[1.9473E-8, 3.1007E-8]	9971
clockRate.C3	1.13E-07	1.12E-07	9.40E-09	[9.4415E-8, 1.3111E-7]	5545
clockRate.C1-2	1.84E-08	1.83E-08	1.95E-09	[1.4649E-8, 2.2274E-8]	8628
Partitions	**Mean**	**Median**	**Standard Deviation**	**95% HPD**	**ESS**
Two Partitions					
clockRate.D_loop	8.35E-07	8.29E-07	1.01E-07	[6.4359E-7, 1.0344E-6]	5943
clockRate.Non-D_loop	5.57E-08	5.55E-08	4.59E-09	[4.6446E-8, 6.4438E-8]	5285
Partitions	**Mean**	**Median**	**Standard Deviation**	**95% HPD**	**ESS**
Four Partitions, Tur					
clockRate.D_loop	8.28E-07	8.22E-07	9.61E-08	[6.4907E-7, 1.0222E-6]	5766
clockRate.tRNA+rRNA+remainder	2.70E-08	2.68E-08	2.82E-09	[2.1602E-8, 3.2578E-8]	8690
clockRate.C3	1.18E-07	1.18E-07	9.39E-09	[1.0052E-7, 1.371E-7]	5162
clockRate.C1-2	1.88E-08	1.88E-08	1.82E-09	[1.5284E-8, 2.2388E-8]	7454

Table S9

BEAST estimation of node age - using *Capra hircus/aegagrus* only, and additionally *Capra falconeri* and *Capra caucasica*.

Tree Node	Median Age (years ago)	Age 95% HPD (years ago)
***Capra hircus/aegagrus* only**		
F|CBGDA	250,213	209,130-297,574
C|BGDA	73,616	60,756-88,122
B|GDA	46,678	38,471-55,603
G|DA	36,207	29,923-43,393
D|A	27,770	22,580-33,542
C internal split	8,964	7,783-10,577
B internal split	13,155	10,505-16,468
G internal split	11,041	8,118-14,672
D internal split	9,760	8,386-11,630
A internal split	11,993	10,031-14,510
Capra hircus, aegagrus, falconeri, caucasica		
T|MFCBGDA	315,976	268,736-368,761
M|FCBGDA	297,042	250,619-346,741
T|Direkli1-2	167,548	137,231-201,478

Table S10

Mitochondrial DNA genetic diversity. π: nucleotide diversity.

Population	Acronym	Sample size	No. of usable sites	π per site(10-4)
Neolithic West	3W	7	14315.5	1.63
Chalcolithic and Bronze Age West	2W	12	13883.2	24.57
Iron Age, Medieval and Modern West	1W	15	15428.4	11.32
Neolithic East	3E	13	15404.2	22.4
Chalcolithic, and Bronze Age East	2E	19	15316.4	11.97
Iron Age, Medieval and Modern East	1E	12	15426.3	14.25
Neolithic Levant	3L	3	12717.7	15.2
Chalcolithic, and Bronze Age Levant	2L	7	13942.1	8.44
Iron Age, Medieval and Modern Levant	1L	5	14911.0	5.43

[a]Both the number of usable sites and π were calculated as average per population.

Table S11

Hudson's pairwise Fst based on whole mitochondrial genomes. For populations acronyms see Table S10.

	3W	**2W**	**1W**	**3E**	**2E**	**1E**	**3L**	**2L**	**1L**
3W	-	0.00	0.00	0.16	0.00	0.00	0.97	0.11	0.18
2W	0.00	-	0.09	0.15	0.14	0.04	0.87	0.00	0.00
1W	0.00	0.09	-	0.26	0.03	0.00	0.93	0.00	0.00
3E	0.16	0.15	0.26	-	0.20	0.19	0.88	0.05	0.14
2E	0.00	0.14	0.03	0.20	-	0.08	0.93	0.00	0.00
1E	0.00	0.04	0.00	0.19	0.08	-	0.92	0.00	0.00
3L	0.97	0.87	0.93	0.88	0.93	0.92	-	0.94	0.95
2L	0.11	0.00	0.00	0.05	0.00	0.00	0.94	-	0.00
1L	0.18	0.00	0.00	0.14	0.00	0.00	0.95	0.00	-

Table S12
AMOVA grouping.

Samples - Neolithic	Samples - Chalcolithic/Bronze Age	Samples - Iron Age/Medieval/Modern	Samples - Iron Age/Medieval/Modern (Cont)	Structure - Neolithic
Neolithic East Iran	**Bronze Age Uzbekistan**	**Iron Age-Modern Iran/Caucasus**	**Modern Central Europe**	**Group 1**
Semnan1-2	Bulak1	Azer4	A1a_02	Neolithic SE Europe
Semnan10	Bulak2	Darre2	A1a_05	Neolithic West Anatolia
Semnan13	Bulak4	Geor2	A3_22	Neolithic Serbia
Semnan17	Bulak5	Kazbeg1	A4_26	**Group 2**
Semnan3	**Chalcolithic Turkmenistan**	Tac2	A4_27	Neolithic East Iran
Semnan7	Monjukli1	A_45	A5_29	Neolithic West Iran
Semnan8	Monjukli2	A_47	A7_36	Neolithic Turkmenistan
Semnan9	Monjukli4	A_48	A7_37	**Group 3**
Neolithic Levant	Monjukli6	A_62	A_43	Neolithic Levant
Ainghazal1	**Chalcolithic/Bronze Age Caucasus**	A_63	A_50	
Ainghazal2	Azer3-5	A_64	A_54	**Structure - Chalcolithic/Bronze Age**
Ainghazal4	Azer6	G_69	C1a_81	**Group 1**
Neolithic South East Europe	Kohneh2	G_72	C1a_82	Chalcolithic/Bronze Age SE Europe
Kov57	Tac1	G_73	**Modern Mediterranean**	Chalcolithic/Bronze Age Anatolia
Kov60	Tac3	G_74	A1_01	**Group 2**
Ovc11	**Chalcolithic/Bronze Age Iran**	**Iron-Modern Levant**	A1a_03	Bronze Age Uzbekistan
Neolithic Serbia	Chalow1	Miqne5	A1a_04	Chalcolithic Turkmenistan
Blagotin1	Darre1	A2_08	A2a_11	Chalcolithic/Bronze Age Caucasus
Blagotin16	Fars1	A2a1_15	A2a1_17	Chalcolithic/Bronze Age Iran
Blagotin2	Fars4	A5_30	A2a1_18	**Group 3**
Blagotin3	Qazvin1	A_39	A2a1_19	Chalcolithic/Bronze Age Levant
Neolithic Turkmenistan	**Chalcolithic/Bronze Age SE Europe**	**Modern East/Central Asia**	A3_20	
Monjukli7	Dra34	A35	A3_21	**Structure - Iron Age/Medieval/Modern**
Monjukli8	Pie17	D1_67	A3_23	**Group 1**
Monjukli9	**Chalcolithic/Bronze Age**	D1_68	A3_24	Modern East/Central Asia

	Anatolia			
Neolithic West Anatolia	Acem1	B1_78	A4_25	Iron Age-Modern Iran/Caucasus
AP38	Acem2	**Modern Turkey**	A4_28	**Group 2**
AP45	Kan19	A1a_06	A5_31	Iron-Modern Levant
AP46	Kan23	A2_07	A5_32	**Group 3**
AP49	Kan25	A2a1_13	A7_38	Modern Central Europe
AP50	**Chalcolithic/Bronze Age Levant**	A2a1_16	A_41	Modern Mediterranean
Neolithic West Iran	Gilat10	A6_33	A_46	**Group 4**
Fars2-5	Gilat2	A6_34	A_49	Modern Turkey
Lur12	Gilat8	A_42	A_51	
	Safi2	A_55	A_52	
	Shiqmim1	A_56	A_53	
	Shiqmim9	A_57	A_61	
	Yarmut1	A_58	A_65	
	Yarmut7	A_59	C1a_83	
	Yoqneam2	A_60		
		G_70		
		G_71		

Table S13
Arlequin AMOVA results.

	d.f.	Sum of squares	Variance Components	Percentage of variation	Fixation Indices	P value
Neolithic						
Among groups	2	675.938	49.58747 Va	80.57	0.806	0.028+-0.006
Among populations	3	37.089	0.16038 Vb	0.26	0.013	0.413+-0.017
Within populations	17	200.625	11.80147 Vc	19.17	0.808	0.000+-0.000
Chalcolithic and Bronze Age						
Among groups	2	35.64	-0.08976 Va	-0.65	-0.006	0.359+-0.013
Among populations	5	86.978	1.08891 Vb	7.87	0.078	0.235+-0.015
Within populations	19	372.193	12.83424 Vc	92.78	0.072	0.082+-0.008
Iron Age, Medieval and Modern						
Among groups	3	102.017	-0.57519 Va	-2.62	-0.026	0.463+-0.018
Among populations	2	85.113	1.86819 Vb	8.5	0.083	0.047+-0.009
Within populations	71	1468.22	20.67915 Vc	94.12	0.059	0.009+-0.003

Table S14
List of samples included in the demographic modelling for both mtDNA and autosomal data.

Sample name	Population	mtDNA missing data	mtDNA modelling	Autosomal modelling
Kov57	3W	2104	yes	no
Kov60	3W	1079	yes	no
Blagotin16	3W	0	yes	yes
Blagotin1	3W	0	yes	yes
Blagotin2	3W	0	yes	yes
Blagotin3	3W	0	yes	yes
Ovc11	3W	930	yes	no
Semnan10	3E	0	yes	no
Semnan1-2	3E	0	yes	yes
Semnan13	3E	0	yes	yes
Semnan17	3E	0	yes	no
Semnan3	3E	0	yes	yes
Semnan7	3E	0	yes	yes
Semnan8	3E	0	yes	no
Semnan9	3E	0	yes	yes
Monjukli7	3E	45	yes	no
Monjukli8	3E	0	yes	no
Monjukli9	3E	116	yes	no
Lur12	3E	0	yes	no
Fars2-5	3E	0	yes	no
Ainghazal1	3L	3598	yes	no
Ainghazal2	3L	743	yes	no
Ainghazal4	3L	63	yes	no

Table S15

Mitochondrial DNA summary statistics for samples included in the demographic modelling. π: nucleotide diversity.

Population	Acronym	Sample size	No. of usable sites[a]	π per site(10-4)[a]
Neolithic West	3W	7	14315.5	1.63
Neolithic East	3E	13	15404.2	22.4
Neolithic Levant	3L	3	12717.7	15.2

[a]Both the number of usable sites and π were calculated as average per population.

Table S16

Pairwise Hudson's Fst based on whole mitochondrial genomes for samples included in the demographic modelling. For population acronyms see Table S10.

Population	**3W**	**3E**	**3L**
3W	/	0.16	0.97
3E	0.16	/	0.88
3L	0.97	0.88	/

Table S17

Prior distributions for all parameters of model SINGLE_MT and MULTIPLE_MT. [a] Time points are expressed in generations considering already that our Neolithic samples are placed at 8,000 years ago.

Model SINGLE_MT		**Model MULTIPLE_MT**	
Nneol	Uniform (10-50,000)	Nneol	Uniform (10-50,000)
Nneow	Uniform (10-50,000)	Nneow	Uniform (10-50,000)
Nneoe	Uniform (10-50,000)	Nneoe	Uniform (10-50,000)
Nbotl	Uniform (10-5,000)	Nbotl	Uniform (10-5,000)
Nbotw	Uniform (10-5,000)	Nbotw	Uniform (10-5,000)
Nbote	Uniform (10-5,000)	Nbote	Uniform (10-5,000)
Nanc1	Uniform (10-50,000)	Nanc1l	Uniform (1000-50,000)
Nanc2	Uniform (1000-50,000)	Nanc1w	Uniform (1000-50,000)
		Nanc1e	Uniform (1000-50,000)
Rules applied:		Nanc2	Uniform (1000-50,000)
Nbotl, Nbotw and Nbote < Nanc1		Nanc3	Uniform (1000-50,000)
Nanc1< Nanc2		Tsplit	Uniform (4400-36,000)[a]
Nbot < Nneo for each population		Tlevant	Uniform (Tsplit-80,000)[a]
		Rules applied:	
		Nbotl, Nbotw and Nbote < Nanc1	
		Nanc1w and Nanc1e < Nanc2	
		Nbot < Nneo for each population	
		Nanc2 < Nanc3	
		Nanc1l < Nanc3	

Table S18

Model posterior probabilities calculated by a weighted multinomial logistic regression using whole mitochondrial genomes.

Number of simulations retained	Model SINGLE_MT	Model MULTIPLE_MT
25,000	0.20	0.80
50,000	0.19	0.81

Table S19.
Parameter estimation under the most supported model. Prior distributions and estimates of both Tsplit and Tlevant have been converted in years using a generation time of 2.5 years and they already took into account that the Neolithic samples are placed at 8,000 years ago.

Model MULTIPLE_MT	Prior	0.025[a]	Median	Mode	0.975[a]
Tsplit	Uniform (11,000-90,000)	11,132	13,309	12,083	18,421
Tlevant	Uniform (Tsplit-200,000)	38,482	121,674	138,370	195,210

[a]Upper and lower limits of the 95% credible interval.

Table S20
Number of SNPs used in qpGraph analysis.

Graph Figure	Number of SNPs
S14a	134566
S14b	134566
S14c	12023
S14d	12023
S14e	9009
S14f	16040
S14g	11740
S15a	9908
S15b	146711
S15c	94585
S15d	28432
S15e	86099
S15f	65597
S15g	113979

Table S21

f_4 ratio estimation of Anatolian Ancient Wild ancestry, divided into two groups (Direkli1-2 and Direkli5+Direkli6), in Neolithic Levant and Neolithic West.

Test	f_4 ratio	SE	Z
f_4(Yak, Direkli5+Dirkeli6; Neolithic West, Neolithic Iran) / f_4(Yak, Direkli5+Dirkeli6; Direkli1-2, Neolithic Iran)	0.500783	0.016381	30.571
f_4(Yak, Direkli5+Dirkeli6; Neolithic Levant, Neolithic Iran) / f_4(Yak, Direkli5+Dirkeli6; Direkli1-2, Neolithic Iran)	0.556317	0.06707	8.295

Table S22

Prior distributions for all parameters of model SINGLE_AU and BINARY_AU. [a]Time points are expressed in generations considering already that our Neolithic samples are placed at 8,000 years ago.

Model SINGLE_AU		**Model BINARY_AU**	
Nneow	Uniform (10-50,000)	Nneow	Uniform (10-50,000)
Nneoe	Uniform (10-50,000)	Nneoe	Uniform (10-50,000)
Nbotw	Uniform (10-5,000)	Nbotw	Uniform (10-5,000)
Nbote	Uniform (10-5,000)	Nbote	Uniform (10-5,000)
Nanc1	Uniform (10-50,000)	Nanc1w	Uniform (1000-50,000)
Nanc2	Uniform (1000-50,000)	Nanc1e	Uniform (1000-50,000)
		Nanc2	Uniform (1000-50,000)
Rules applied:		Tsplit	Uniform (4400-36,000)[a]
Nbotw and Nbote < Nanc1			
Nanc1< Nanc2		**Rules applied:**	
Nbot < Nneo for each population		Nbot < Nanc1 for each population	
		Nanc1w and Nanc1e < Nanc2	
		Nbot < Nneo for each population	

Table S23

Model posterior probabilities calculated by a weighted multinomial logistic regression using whole genome sequences .

Number of simulations retained	Model SINGLE_AU	Model BINARY_AU
25,000	0.00	1.00
50,000	0.26	0.74

Table S24

Genetic diversity based on whole genome sequences. π: nucleotide diversity.

Population	Acronym	Sample size	π per site
Neolithic West	3W	4	0.15
Chalcolithic and Bronze Age West	2W	2	0.17
Neolithic East	3E	5	0.16
Chalcolithic, and Bronze Age East	2E	2	0.17
Iron Age, Medieval and Modern East	1E	3	0.17

Table S25

Hudson's pairwise Fst based on whole genome sequences. For populations acronyms see Table S10.

	1E	**2E**	**2W**	**3E**	**3W**
1E	-	0.00	0.01	0.07	0.12
2E	0.00	-	0.02	0.08	0.13
2W	0.01	0.02	-	0.09	0.10
3E	0.07	0.08	0.09	-	0.17
3W	0.12	0.13	0.10	0.17	-

Table S26
Modern samples included in analyses.

EBI Sample Accession	Grouping (Country)	Coverage (q30)	Study Name	NGSadmix subsample	Selection subsample
SAMEA2417033	Modern Europe (France)	13.75	french_modern2	Yes	-
SAMEA2417034	Modern Europe (France)	13.47	french_modern3	Yes	-
SAMEA2417035	Modern Europe (France)	14.52	french_modern1	Yes	-
SAMEA2417036	Modern Europe (France)	14.19	french_modern3	Yes	-
SAMEA2065435	Modern Iran	13.24	iranian_modern11	No	-
SAMEA2065428	Modern Iran	13.24	iranian_modern13	No	-
SAMEA1968884	Modern Iran	13.06	iranian_modern6	Yes	-
SAMEA2065432	Modern Iran	12.27	iranian_modern14	Yes	-
SAMEA2065425	Modern Iran	12.32	iranian_modern15	No	-
SAMEA2065429	Modern Iran	13.75	iranian_modern16	No	-
SAMEA2065423	Modern Iran	13.89	iranian_modern1	No	-
SAMEA2065430	Modern Iran	12.87	iranian_modern17	No	-
SAMEA2065434	Modern Iran	12.99	iranian_modern18	No	-
SAMEA2065587	Modern Iran	12.26	iranian_modern12	Yes	-
SAMEA2065427	Modern Iran	13.67	iranian_modern19	No	-
SAMEA2065431	Modern Iran	12.07	iranian_modern2	No	-
SAMEA2065433	Modern Iran	13.41	iranian_modern7	No	-
SAMEA2065424	Modern Iran	12.92	iranian_modern3	No	-
SAMEA1966659	Modern Iran	13.3	iranian_modern20	No	-
SAMEA2065422	Modern Iran	13.12	iranian_modern4	Yes	-
SAMEA2065436	Modern Iran	13	iranian_modern10	Yes	-
SAMEA2065438	Modern Iran	11.53	iranian_modern8	No	-
SAMEA2065437	Modern Iran	11.24	iranian_modern9	No	-
SAMEA2065426	Modern Iran	11.62	iranian_modern5	No	-
SAMEA2065224	Azerbaijan Wild	11.26	iranian_bezoar6	No	Yes
SAMEA2065212	Azerbaijan Wild	11.67	iranian_bezoar8	No	Yes
SAMEA2065216	Azerbaijan Wild	6.81	iranian_bezoar11	No	Yes
SAMEA2065220	Azerbaijan Wild	12.42	iranian_bezoar3	No	Yes
SAMEA2065217	Azerbaijan Wild	6.69	iranian_bezoar13	Yes	Yes
SAMEA2065214	Azerbaijan Wild	7.54	iranian_bezoar14	No	Yes

SAMEA2065213	Azerbaijan Wild	11.52	iranian_bezoar15	No	Yes
SAMEA2065215	Azerbaijan Wild	12.12	iranian_bezoar16	Yes	Yes
SAMEA2065218	Azerbaijan Wild	12.93	iranian_bezoar17	No	Yes
SAMEA2188056	Azerbaijan Wild	12.73	iranian_bezoar19	No	Yes
SAMEA2065421	Qazvin Wild	6.87	iranian_bezoar4	Yes	Yes
SAMEA1966535	Qazvin Wild	12.79	iranian_bezoar2	No	Yes
SAMEA2065226	Qazvin Wild	11.72	iranian_bezoar10	No	Yes
SAMEA2395407	Qazvin Wild	14.96	iranian_bezoar1	No	Yes
SAMEA2395406	Qazvin Wild	13.55	iranian_bezoar20	Yes	Yes
SAMEA2395408	Qazvin Wild	14.61	iranian_bezoar21	No	Yes
SAMEA2065222	Hamedan Wild	5.63	iranian_bezoar5	No	No
SAMEA2065221	Hamedan Wild	6.13	iranian_bezoar7	No	No
SAMEA2065225	Hamedan Wild	6.85	iranian_bezoar9	Yes	No
SAMEA2065223	Hamedan Wild	5.34	iranian_bezoar12	No	No
SAMEA2065227	Hamedan Wild	10.07	iranian_bezoar18	No	No
SAMN00857836	Modern China	20.86	CHIR_1.0	No	-
SAMEA2012964	Modern Africa (Morocco)	12.71	moroccan1	No	-
SAMEA2012826	Modern Africa (Morocco)	15.43	moroccan4	No	-
SAMEA2012908	Modern Africa (Morocco)	12.61	moroccan5	Yes	-
SAMEA2012707	Modern Africa (Morocco)	13.84	moroccan2	Yes	-
SAMEA2013048	Modern Africa (Morocco)	15.08	moroccan6	No	-
SAMEA2013062	Modern Africa (Morocco)	15.82	moroccan7	No	-
SAMEA2012822	Modern Africa (Morocco)	13.51	moroccan8	No	-
SAMEA2012705	Modern Africa (Morocco)	13.59	moroccan3	Yes	-
SAMEA2012903	Modern Africa (Morocco)	12.93	moroccan9	Yes	-
ERS2429990	Modern Africa (Togo)	36.48	Tog	Yes	-
ERS2429989	Modern Europe (Ireland - Old Irish Goat)	41.93	IOG	Yes	-
SAMN02720826	Outgroup	25.81	Sheep	-	-
SAMN00744358	Outgroup	20.83	Yak	-	-

Table S27

f_3 outgroup analysis using Qazvin Bezoar as outgroup. Shared drift is calculated between Source 1 and a fixed Source 2. When a Modern population is used a Source 2, Modern Africa and Modern Europe groupings are split into their country subgroupings.

Source1	Source2	Target	f3	stderr	Z	SNPs
Modern Ireland	Neolithic West	Qazvin Bezoar	0.123889	0.001229	100.791	420364
Bronze Age Britain	Neolithic West	Qazvin Bezoar	0.12322	0.001401	87.959	284601
Modern France	Neolithic West	Qazvin Bezoar	0.122664	0.000999	122.772	459754
Neolithic Levant	Neolithic West	Qazvin Bezoar	0.11981	0.003041	39.402	32434
Modern Morocco	Neolithic West	Qazvin Bezoar	0.091661	0.000852	107.53	530484
Modern Togo	Neolithic West	Qazvin Bezoar	0.086778	0.001024	84.721	425583
Bronze Age Turkey	Neolithic West	Qazvin Bezoar	0.084072	0.000941	89.322	441676
Chalcolithic Levant	Neolithic West	Qazvin Bezoar	0.083559	0.00705	11.852	5354
Bronze Age Levant	Neolithic West	Qazvin Bezoar	0.077457	0.001157	66.917	319829
Iron/Medieval Caucasus	Neolithic West	Qazvin Bezoar	0.075741	0.000902	83.989	414630
Modern China	Neolithic West	Qazvin Bezoar	0.074984	0.001002	74.851	427613
Medieval Iran	Neolithic West	Qazvin Bezoar	0.073504	0.001109	66.307	334797
Bronze Age Caucasus	Neolithic West	Qazvin Bezoar	0.073493	0.001087	67.636	356921
Modern Iranian	Neolithic West	Qazvin Bezoar	0.072636	0.000762	95.299	631996
Bronze Age Iran	Neolithic West	Qazvin Bezoar	0.072265	0.001062	68.027	291818
Chalcolithic Caucasus	Neolithic West	Qazvin Bezoar	0.071819	0.001719	41.791	88064
Bronze Age Uzbekistan	Neolithic West	Qazvin Bezoar	0.069172	0.001075	64.356	346849
Chalcolithic Iran	Neolithic West	Qazvin Bezoar	0.06828	0.001193	57.222	246500
Chalcolithic Turkmenistan	Neolithic West	Qazvin Bezoar	0.067531	0.001166	57.914	240018
Neolithic East	Neolithic West	Qazvin Bezoar	0.064342	0.000855	75.289	461853
Modern Europe	Neolithic Levant	Qazvin Bezoar	0.128978	0.001092	118.136	301428
Modern Africa	Neolithic Levant	Qazvin Bezoar	0.094711	0.000967	97.894	342051
Modern China	Neolithic East	Qazvin Bezoar	0.113707	0.001172	97.019	433543
Bronze Age Uzbekistan	Neolithic East	Qazvin Bezoar	0.104535	0.001121	93.222	353610
Chalcolithic Turkmenistan	Neolithic East	Qazvin Bezoar	0.103202	0.001252	82.411	245262
Chalcolithic Iran	Neolithic East	Qazvin Bezoar	0.098555	0.001294	76.179	252478
Medieval Iran	Neolithic East	Qazvin Bezoar	0.09463	0.001156	81.856	344465
Bronze Age Iran	Neolithic East	Qazvin Bezoar	0.093232	0.001182	78.902	299586
Chalcolithic Caucasus	Neolithic East	Qazvin Bezoar	0.092549	0.001664	55.611	90606

Bronze Age Caucasus	Neolithic East	Qazvin Bezoar	0.091684	0.001043	87.921	366718
Iron/Medieval Caucasus	Neolithic East	Qazvin Bezoar	0.087821	0.000933	94.173	424515
Bronze Age Levant	Neolithic East	Qazvin Bezoar	0.085193	0.001068	79.789	329800
Chalcolithic Levant	Neolithic East	Qazvin Bezoar	0.084061	0.005949	14.129	5531
Modern Iranian	Neolithic East	Qazvin Bezoar	0.083417	0.000811	102.919	624969
Bronze Age Turkey	Neolithic East	Qazvin Bezoar	0.079426	0.000899	88.323	453359
Modern Morocco	Neolithic East	Qazvin Bezoar	0.069522	0.000762	91.232	544904
Modern Togo	Neolithic East	Qazvin Bezoar	0.068529	0.000896	76.472	440651
Modern Ireland	Neolithic East	Qazvin Bezoar	0.065552	0.000977	67.125	441239
Bronze Age Britain	Neolithic East	Qazvin Bezoar	0.065507	0.001124	58.261	297381
Neolithic West	Neolithic East	Qazvin Bezoar	0.064342	0.000855	75.289	461853
Modern France	Neolithic East	Qazvin Bezoar	0.064052	0.000804	79.64	486147
Neolithic Levant	Neolithic East	Qazvin Bezoar	0.058158	0.00245	23.739	34106
Modern Europe	Neolithic East	Qazvin Bezoar	0.065523	0.000871	75.254	323774
Modern Africa	Neolithic East	Qazvin Bezoar	0.071164	0.000855	83.213	354502
Chalcolithic Levant	Neolithic Levant	Qazvin Bezoar	0.126596	0.032227	3.928	419
Neolithic West	Neolithic Levant	Qazvin Bezoar	0.11981	0.003041	39.402	32434
Modern Togo	Neolithic Levant	Qazvin Bezoar	0.1182	0.00355	33.294	30293
Modern Morocco	Neolithic Levant	Qazvin Bezoar	0.109433	0.002556	42.816	40605
Modern Ireland	Neolithic Levant	Qazvin Bezoar	0.107262	0.003319	32.313	30391
Bronze Age Britain	Neolithic Levant	Qazvin Bezoar	0.10702	0.004677	22.882	19720
Modern France	Neolithic Levant	Qazvin Bezoar	0.105528	0.002822	37.393	34765
Bronze Age Turkey	Neolithic Levant	Qazvin Bezoar	0.090797	0.002743	33.101	32075
Bronze Age Levant	Neolithic Levant	Qazvin Bezoar	0.087019	0.004206	20.689	22706
Iron/Medieval Caucasus	Neolithic Levant	Qazvin Bezoar	0.083435	0.00298	27.994	29697
Bronze Age Caucasus	Neolithic Levant	Qazvin Bezoar	0.076253	0.003911	19.496	25485
Modern Iranian	Neolithic Levant	Qazvin Bezoar	0.073716	0.002063	35.727	49563
Chalcolithic Caucasus	Neolithic Levant	Qazvin Bezoar	0.072823	0.007153	10.181	6403
Medieval Iran	Neolithic Levant	Qazvin Bezoar	0.071535	0.004039	17.709	23823
Modern China	Neolithic Levant	Qazvin Bezoar	0.071273	0.003154	22.595	30382
Bronze Age Iran	Neolithic Levant	Qazvin Bezoar	0.066933	0.004106	16.303	20921
Chalcolithic Iran	Neolithic Levant	Qazvin Bezoar	0.066313	0.00454	14.605	18248
Chalcolithic Turkmenistan	Neolithic Levant	Qazvin Bezoar	0.063019	0.004062	15.516	17584
Bronze Age Uzbekistan	Neolithic Levant	Qazvin Bezoar	0.062576	0.003432	18.232	25099
Neolithic East	Neolithic Levant	Qazvin Bezoar	0.058158	0.00245	23.739	34106

Modern Europe	Neolithic Levant	Qazvin Bezoar	0.115816	0.003293	35.173	23941
Modern Africa	Neolithic Levant	Qazvin Bezoar	0.119699	0.003157	37.914	27171
Modern Morocco	Modern Togo	Qazvin Bezoar	0.144041	0.001088	132.409	510855
Chalcolithic Levant	Modern Togo	Qazvin Bezoar	0.12116	0.008448	14.342	4990
Neolithic Levant	Modern Togo	Qazvin Bezoar	0.1182	0.00355	33.294	30293
Bronze Age Levant	Modern Togo	Qazvin Bezoar	0.098929	0.001416	69.86	298064
Modern France	Modern Togo	Qazvin Bezoar	0.097623	0.001011	96.582	450563
Bronze Age Anatolia	Modern Togo	Qazvin Bezoar	0.095176	0.001078	88.261	419139
Modern Iran	Modern Togo	Qazvin Bezoar	0.092206	0.000885	104.195	620742
Bronze Age Britain	Modern Togo	Qazvin Bezoar	0.091532	0.001488	61.495	268690
Iron/Medieval Caucasus	Modern Togo	Qazvin Bezoar	0.087091	0.001021	85.264	389919
Neolithic West	Modern Togo	Qazvin Bezoar	0.086778	0.001024	84.721	425583
Bronze Age Caucasus	Modern Togo	Qazvin Bezoar	0.086055	0.001284	67.032	333504
Medieval Iran	Modern Togo	Qazvin Bezoar	0.085288	0.001273	66.994	312776
Bronze Age Iran	Modern Togo	Qazvin Bezoar	0.084209	0.001452	57.985	272304
Chalcolithic Caucasus	Modern Togo	Qazvin Bezoar	0.080821	0.002111	38.285	81991
Bronze Age Uzbekistan	Modern Togo	Qazvin Bezoar	0.076849	0.001143	67.249	324543
Modern China	Modern Togo	Qazvin Bezoar	0.075755	0.001069	70.898	402362
Chalcolithic Turkmenistan	Modern Togo	Qazvin Bezoar	0.074277	0.001339	55.479	223800
Chalcolithic Iran	Modern Togo	Qazvin Bezoar	0.07378	0.001341	55.029	229939
Neolithic East	Modern Togo	Qazvin Bezoar	0.068529	0.000896	76.472	440651
Bronze Age Britain	Modern Ireland	Qazvin Bezoar	0.150809	0.001893	79.677	266578
Modern France	Modern Ireland	Qazvin Bezoar	0.138768	0.001187	116.907	443741
Neolithic West	Modern Ireland	Qazvin Bezoar	0.123889	0.001229	100.791	420364
Neolithic Levant	Modern Ireland	Qazvin Bezoar	0.107262	0.003319	32.313	30391
Modern Morocco	Modern Ireland	Qazvin Bezoar	0.099728	0.000976	102.14	518808
Modern Togo	Modern Ireland	Qazvin Bezoar	0.094471	0.001186	79.63	401130
Bronze Age Anatolia	Modern Ireland	Qazvin Bezoar	0.08612	0.001088	79.125	420195
Modern Iran	Modern Ireland	Qazvin Bezoar	0.080006	0.000873	91.63	623720
Bronze Age Levant	Modern Ireland	Qazvin Bezoar	0.079755	0.001301	61.318	299267
Chalcolithic Levant	Modern Ireland	Qazvin Bezoar	0.079371	0.007879	10.073	4986
Iron/Medieval Caucasus	Modern Ireland	Qazvin Bezoar	0.079116	0.001061	74.57	390763
Bronze Age Iran	Modern Ireland	Qazvin Bezoar	0.07656	0.001333	57.419	272895
Chalcolithic Caucasus	Modern Ireland	Qazvin Bezoar	0.076216	0.002129	35.802	82144
Medieval Iran	Modern Ireland	Qazvin Bezoar	0.075895	0.001288	58.946	313289

Bronze Age Caucasus	Modern Ireland	Qazvin Bezoar	0.075429	0.001205	62.586	334050
Modern China	Modern Ireland	Qazvin Bezoar	0.070485	0.001147	61.439	402922
Bronze Age Uzbekistan	Modern Ireland	Qazvin Bezoar	0.069884	0.001211	57.693	324916
Chalcolithic Turkmenistan	Modern Ireland	Qazvin Bezoar	0.069551	0.001327	52.424	224113
Chalcolithic Iran	Modern Ireland	Qazvin Bezoar	0.069106	0.001373	50.347	230022
Neolithic East	Modern Ireland	Qazvin Bezoar	0.065552	0.000977	67.125	441239

Table S28

Fst Outlier Regions and Overlapping Genes. Entries discontinued in NCBI are excluded. The nearest gene to an outlier region is show when no annotated genes are found. When multiple genes are found in a region, the gene(s) overlapping with the highest Fst 50kb window, or the nearest gene to that window, is marked in bold. If multiple genes overlap the highest Fst window, both are marked in bold.

Population	Chromosome	Region Start	Region End	Genes in region	Nearest Gene
Neolithic West	1	133120000	133210000	SRPRB, **LOC102172205, LOC102172488**	-
	1	143980000	144100000	**PRMT2**	-
	5	18060000	18180000	None	**KITLG**, DUSP6
	6	68180000	68340000	**KIT**	-
	17	20730000	20850000	**LOC102170258 (WBP11)**	-
	28	22170000	22390000	SIRT1, **HERC4**, MYPN	-
	29	28660000	28750000	KIRREL3	-
Neolithic East	2	78830000	78940000	**STAT1, STAT4**	-
	2	127950000	128050000	**IL22RA1, MYOM3**	-
	3	51280000	51460000	**GBP6**, LOC106501943	-
	3	102850000	102950000	**MACF1**, **KIAA0754**	-
	4	73500000	73590000	None	IGFBP3
	4	92400000	92600000	MKLN1	-
	5	18020000	18180000	None	**KITLG**, DUSP6
	6	68220000	68400000	KIT	-
	6	86460000	86580000	**EPGN**, EREG	-
	8	38500000	38600000	**RCL1**, AK3	-
	8	38620000	38770000	CDC37L1, **SPATA6L**, PPAPDC2	-
	9	11560000	11690000	None	RSPO3
	10	38440000	38530000	None	RPS29
	26	14970000	15110000	**LOC102185708 (CYP2C19)**, LOC102185056 (CYP2C9)	-

Table S29

Nonsynonymous variants in outlier regions. The allele identified as being low frequency (<0.2) in bezoar but fixed in an ancient Neolithic high coverage is indicated in bold.

Chromosome	Position	Gene	Reference	Ancestral	Derived	Derived Frequency - East	Derived Frequency - West	Ancestral Residue	Derived Residue
1	133157078	LOC102172205	C	C	**T**	0.65	0.00	A	T
1	133167772	LOC102172205	G	**G**	A	0.00	0.00	N	K
2	78845804	STAT1	T	**T**	G	0.09	0.30	N	T
2	127995419	MYOM3	G	A	**G**	1.00	0.00	K	R
5	17673144	KITLG	T	T	**A**	1.00	0.43	T	S
6	68332366	KIT	T	T	**A**	0.00	0.75	Y	N
26	15057235	LOC102185708 (CYP2C19)	G	**G**	C	0.00	1.00	T	R
28	22205610	SIRT1	C	A	**C**	0.10	0.81	Q	D
28	22205761	SIRT1	T	T	**G**	0.11	0.75	S	A

Table S30
Fst values for pigmentation genes.

Gene	Chromosome	Start	End	Highest Fst window - East	Mean Fst - East	Highest Fst window - West	Mean Fst - West
PMEL17	5	55829082	55845319	0.163902	0.146615	0.16488	0.15210
TYRP1	8	30671334	30687862	0.144336	0.118669	0.324814	0.29731
ASIP	13	61693104	61698483	0.273657	0.225399	0.493624	0.42040
MC1R	18	14208837	14212670	0.196922	0.175957	0.168685	0.15691
MITF	22	31427864	31659079	0.283904	0.234776	0.466363	0.30581

Table S31. *D* statistic test. ABBA/BABA test statistics, calculated in the for (H1, H2, H3, Outgroup), using *Bos grunniens* as the outgroup.

Table S32. Outlier Fst windows. Highest Fst window within each outlier regions of selection analysis.